

**DEVELOPMENT OF GREEN CHROMATOGRAPHIC
TECHNIQUES AND STIMULI-RESPONSIVE MATERIALS
BASED ON CO₂-SWITCHABLE CHEMISTRY**

by

Xilong Yuan

A thesis submitted to the Department of Chemistry

In conformity with the requirements for

the degree of Doctor of Philosophy

Queen's University

Kingston, Ontario, Canada

(November 2017)

Copyright © Xilong Yuan, 2017

Abstract

Developing alternatives to organic solvents and salts in chromatographic separation is highly desired. In this thesis, original studies were performed to demonstrate the feasibility of using CO₂-modified aqueous solvents as an environmentally friendly mobile phase.

Porous polymer monoliths were considered as a straightforward approach for the preparation of capillary columns with various functionality. A copolymer column containing dimethylaminoethyl methacrylate (DMAEMA) was investigated for the effect of CO₂ on separation. Although a slight decrease of retention time of aromatic compounds was initially observed using acetic acid-modified solvent, the chromatographic separation using CO₂-modified solvent was not reproducible, presumably resulting from the difficulty of reliably introducing gaseous CO₂ into the nano LC system. Because different pH and temperature conditions can be easily applied, the pH and thermo-responsive behaviour of the copolymer column was also investigated. It showed the capability of pH and temperature for manipulating retention time and selectivity for various compounds. Because of the presence of ionizable groups, the column was also demonstrated for ion exchange separation of proteins.

Following the initial work, a conventional HPLC system was used instead. A custom CO₂ delivery system (1 bar CO₂) was assembled to provide CO₂-modified aqueous solvent with pH 3.9 ~ 6.5. A significant hydrophobicity switch of the stationary phase was observed by a reduction in retention time, when using CO₂-modified solvents for the diethylaminoethyl (DEAE) and polyethylenimine (PEI) functionalized columns. In

particular, the polyethylenimine column can be used to perform separation of organic molecules using 100% water without any organic solvent added. Another study was also conducted utilizing primary, secondary and tertiary amine functionalized silica particles (3.5 μm). A pH-/CO₂-dependent ion exchange separation was demonstrated considering the protonation / deprotonation of both stationary phase and analytes. Carboxylic acid compounds were effectively separated using only carbonated water as the mobile phase.

Despite the development of green chromatographic separations, this thesis also demonstrated the pH-/CO₂-responsive surface wettability / adhesion of a polymer monolith surface grafted with functional polymers. Preliminary results indicate significant potential for applications such as drug screening and cell culture by introducing stimuli-responsive domains in droplet microarrays.

Co-Authorship

The work discussed in this thesis was conducted and presented by the author in the Department of Chemistry at Queen's University under the supervision of Dr. Richard Oleschuk. I hereby certify that all work described in this thesis is the original work of the author. Any published ideas and/or productions from the work of others are fully acknowledged in accordance with the required referencing practices. Any and all contributions from collaborators are noted below.

In Chapter 3, Eun Gi Kim finished part of the data collection of chromatographic separations. Connor Sanders performed the pH measurement of carbonated solvents in HPLC. In Chapter 4, Kunqiang Jiang and Bruce Richter contributed to the packing of silica particles in chromatographic columns. Kyle Boniface and Connor Sanders participated in the preparation and characterization of functionalized silica particles. Calvin Palmer participated in part of the chromatographic tests. In Chapter 5, Prashant Agrawal completed the preparation of the polymer sample and collected fifty percent of the raw data about water contact angle and hysteresis.

Part of the thesis work has been published or submitted:

Yuan, X.; Kim, E. G.; Sanders, C. A.; Richter, B. E.; Cunningham, M. F.; Jessop, P. G.; Oleschuk, R. D. *Green Chemistry* 2017, 19, 1757-1765.

Yuan, X., Richter, B. E., Jiang, K., Boniface, K. J., Cormier, A., Sanders, C. A., Palmer, C., Jessop, P. G., Cunningham, M. F., Oleschuk, R. D. *Green Chemistry* 2017, Manuscript Accepted.

Acknowledgements

I would like to express my sincere gratitude to my supervisor, Dr. Richard Oleschuk, for his kind support and guidance throughout my thesis. Your patience, encouragement and dedication have made my PhD studies a very exciting and rewarding experience. Dr. Philip Jessop is truly appreciated for his kind support and guidance for my research. Dr. Michael Cunningham, Dr. Guojun Liu and Dr. Bruce Richter are acknowledged for their enlightening consultations in research projects. I was also very thankful to work with a few undergraduate students who have helped contribute towards my thesis research, including Eun Gi Kim, Connor Sanders and Calvin Palmer. I would like to acknowledge NSERC (Natural Sciences and Engineering Research Council of Canada), Agilent Technologies, and Queen's University for providing the funding, equipment and technical assistance to support my research.

The switchable surface team members, Kyle Boniface, Hanbin Liu, Alex Cormier, Kunqiang Jiang, are acknowledged for their generous support. Specially, I would like to thank the past and present 'O' Lab fellows, especially Yueqiao Fu, Zhenpo Xu, Kyle Bachus, Prashant Agrawal, David Simon and Matthias Hermann. Life with you all is filled with insightful discussions, refreshing lunch breaks, leisure evenings and much more. My close friends in Kingston and around, especially Yang Chen and Xiaowei Wu are acknowledged, who have been the most uplifting and supportive people. My parents, Jianying Du and Ying Yuan, my sister Jinli Yuan, have been backing me up with love and sympathy. Without their support, I wouldn't be where I am today.

Table of Contents

Abstract	ii
Co-Authorship	iv
Acknowledgements	v
List of Figures	x
List of Tables	xvi
List of Abbreviations	xvii
Chapter 1 Introduction	1
1.1 Background	1
1.1.1 Green chemistry and its principles	1
1.1.2 Green analytical chemistry	2
1.1.3 Green chromatography	5
1.2 CO ₂ -switchable chemistry	10
1.2.1 Carbon dioxide	10
1.2.2 CO ₂ -switchable groups	14
1.2.3 CO ₂ -switchable technologies	16
1.3 Principles of liquid chromatography	21
1.3.1 Modes of separation	21
1.3.2 Functional groups of columns	24
1.3.3 Effect of pH on retention	25
1.3.3.1 Effect of pH in RPC	25
1.3.3.2 Effect of pH in IEC	28
1.3.4 Column supports	30
1.3.4.1 Porous polymer monolith	30
1.3.4.2 Silica spheres	33
1.3.5 Chromatographic parameters ^{79, 113, 114}	34
1.4 Project outline	36
1.5 References	39
Chapter 2 Chromatographic characteristics of a DMAEMA-co-EDMA polymeric monolithic column	46
2.1 Introduction	46
2.2 Experimental	48
2.2.1 Materials	48

2.2.2 Preparation of polymer monolith columns.....	49
2.2.3 Chromatographic conditions	51
2.2.4 Mobile phase preparation.....	53
2.3 Results and Discussion.....	54
2.3.1 Column preparation and characterization	54
2.3.2 CO ₂ -switchability of the column.....	60
2.3.3 Effect of pH on retention time	64
2.3.4 Effect of temperature on the chromatography.....	68
2.3.5 Ion exchange separation using the copolymer monolith.....	71
2.4 Conclusive remarks.....	73
2.5 References.....	75
Chapter 3 CO ₂ -switchable separation with commercial columns.....	77
3.1 Introduction.....	77
3.2 Theory	79
3.3 Experimental	81
3.3.1 Instrumentation.....	81
3.3.2 The CO ₂ Delivery System.....	82
3.3.3 Chromatographic Columns	85
3.3.4 Sample Preparation	85
3.3.5 ΔG° Determination	87
3.3.6 Zeta Potential Measurement.....	88
3.4 Results and discussion	89
3.4.1 CO ₂ Partial Pressure and pH.....	89
3.4.2 Diethylaminoethyl Column (DEAE)	90
3.4.3 Polyethylenimine Column (PEI).....	95
3.4.4 Carboxymethyl Column (CM)	99
3.5 Conclusions.....	102
3.6 References.....	104
Chapter 4 Carbonated water for the separation of carboxylic acid compounds.....	107
4.1 Introduction.....	107
4.2 Experimental	110
4.2.1 Materials and instruments	110
4.2.2 Functionalization of silica spheres	111
4.2.3 Characterization of prepared silica spheres.....	111

4.2.4 CO ₂ delivery system.....	112
4.2.5 Mobile phase solutions.....	113
4.2.6 Chromatographic conditions	114
4.3 Results and discussion	115
4.3.1 Silica sphere characterization.....	115
4.3.2 Zeta potential of amine-functionalized silica	118
4.3.3 Ion exchange equilibria.....	119
4.3.4 Effect of pH.....	121
4.4 Separation of carboxylic compounds	125
4.4.1 Effect of CO ₂	125
4.5 1°, 2°, 3° amines	126
4.5.1 Effect of pH.....	126
4.5.2 Effect of CO ₂	127
4.6 Conclusions.....	130
4.7 References.....	132
Chapter 5 Towards the development of pH/CO ₂ -switchable polymer monolith surfaces with tunable surface wettability and adhesion	135
5.1 Literature review	135
5.1.1 Superhydrophobic surfaces	135
5.1.2 Measurements of Surfaces with Superwettability.....	135
5.1.3 Different superhydrophobic states	136
5.1.4 Fabrication of superhydrophobic and superhydrophilic surfaces.....	138
5.1.5 Stimuli-responsive surfaces with switchable wettability and adhesion	140
5.1.6 Superhydrophilic-Superhydrophobic Micropatterns / Microarrays	143
5.2 Overview	146
5.3 Experimental.....	148
5.3.1 Materials and instruments	148
5.3.2 Preparation of generic polymer monolith substrate	149
5.3.3 Photografting.....	150
5.3.4 Material characterization.....	151
5.3.5 Contact angle measurement	151
5.3.6 Droplets with different pH	151
5.4 Results and discussions	152
5.4.1 Material characterization.....	152

5.4.2 Characterization of surface wettability	153
5.4.2.1 Effect of generic polymer.....	154
5.4.2.2 Effect of top and bottom slides	154
5.4.2.3 Effect of photografting monomer.....	156
5.4.3 Characterization of surface adhesion by hysteresis.....	158
5.4.4 Surface wetting with different pH droplets	159
5.5 Conclusions.....	163
5.6 References.....	165
Chapter 6 Conclusions and recommendations	167

List of Figures

Figure 1.1 “Greenness” of different chromatographic scenarios. Reprinted from reference ¹³ with permission from Elsevier.	8
Figure 1.2 A distribution plot of carbonic acid (hydrated CO ₂ and H ₂ CO ₃) and the subsequent dissociated species based upon pH. Reproduced using data from reference. ⁵⁸	13
Figure 1.3 pH of carbonated water versus the partial pressure of carbon dioxide above the solution (23 °C). Reproduced from reference ⁶⁰ by permission of The Royal Society of Chemistry.	13
Figure 1.4 Schematic of protein adsorption and release using CO ₂ -switchable surface with polymer brushes. Reproduced from reference ⁷⁷ with permission of The Royal Society of Chemistry.....	18
Figure 1.5 Schematic of CO ₂ -switchable drying agent using silica particles grafted with PDMAPMAM chains. Reproduced from reference ⁶⁵ with permission of The Royal Society of Chemistry.....	19
Figure 1.6 Schematic of the separation of α -Tocopherol from its homologues and recovery of the extractant. Reprinted with permission from reference. ⁷⁸ Copyright © (2014) American Chemical Society.....	20
Figure 1.7 CO ₂ induced “switching” of surface properties for amine functionalized stationary phase particles. Tertiary amine bonded phase before (left) and after (right) exposure to CO ₂ . The tertiary amine (left) presents a hydrophobic, neutral state while the tertiary amine phase (right) represents a hydrophilic and protonated state of the groups. Reproduced from reference ⁶⁰ by permission of The Royal Society of Chemistry.	21
Figure 1.8 Hypothetical illustration of the RPC separation of an acidic compound HA from a basic compound B as a function of pH. (a) Ionization of HA and B as a function of mobile phase pH and effect on k. (b) separation as a function of mobile phase pH. Reprinted from reference ⁷⁹ with permission. Copyright © 2010 by John Wiley & Sons, Inc.....	27
Figure 1.9 Effect of mobile-phase pH on RPC retention as a function of solute type. Sample: 1, salicylic acid; 2, phenobarbitone; 3, phenacetin; 4, nicotine; 5, methylamphetamine (shaded peak). Conditions for separations: 300 × 4.0-mm C18 column (10.0 μ m particles); 40% methanol-phosphate buffer; ambient temperature; 2.0 mL/min. Reprinted from reference ⁸⁰ with permission. Copyright © (1975) Elsevier.....	28

Figure 1.10 Retention data for inorganic anions in the pH range 4.3-6.0. A quaternary amine anion exchanger was used with 5.0 mM phthalate (pK_a 5.5) as eluent. Reprinted from reference ⁸¹ with permission. Copyright © (1984) Elsevier.	30
Figure 2.1 Scanning electron microscope images of unsatisfactory polymer monolithic columns. The inner diameter of the columns is 75 μm	55
Figure 2.2 Scanning electron microscope images of poly(DMAEMA-co-EDMA) monolithic column with different volume ratios of monomer/crosslinker: (A1) 20:80 (A2) 30:70 (A3) 40:60; corresponding to the composition of polymerization mixture A1 - A3 in Table 2.1.....	56
Figure 2.3 Scanning electron microscope images of poly(DMAEMA-co-EDMA) monolithic column with different volume ratios of 2-propanol and 1,4-butanediol: B1) 60:30; B2) 62:28; B3) 64:26; B4) 66:24; corresponding to the column B1-B4 in Table 2.2.....	57
Figure 2.4 Scanning electron microscope images (magnified) of poly(DMAEMA-co-EDMA) monolithic column with different ratios of 2-propanol and 1,4-butanediol: B1) 60:30; B2) 62:28; B3) 64:26; B4) 66:24; corresponding to the column B1-B4 in Table 2.2.....	58
Figure 2.5 Backpressure of the poly(DMAEMA-co-EDMA) monolithic columns made from different solvents represented by the volume weighted solvent polarity. Column dimension: 10.0 cm \times 100 μm I.D. Solvent: 95.0% acetonitrile at 1.0 $\mu\text{L min}^{-1}$	59
Figure 2.6 ATR-IR spectroscopy of DMAEMA and the poly(DMAEMA-co-EDMA) monolithic material.	60
Figure 2.7 Chromatograms of benzene, naphthalene and anthracene (in the order of elution) separated (A) without modifier and (B) with 0.10% acetic acid in the mobile phases. Conditions: poly(DMAEMA-co-EDMA) monolithic column, 100 μm I.D., 15.0 cm; mobile phase is a gradient of water and acetonitrile, 0-1 min, 80% water; 1-10 min, 80% - 50% water; 10-15 min, 50% water; flow rate 1.0 $\mu\text{L min}^{-1}$, injection volume 2.0 μL , UV detection 254 nm.	62
Figure 2.8 Representative chromatograms showing the irreproducibility of using CO_2 -modified solvent with repeated injections on nano LC. Conditions: poly(DMAEMA-co-EDMA) monolithic column, 100 μm I.D., 15.0 cm; mobile phase: 0-1 min, 80% carbonated water; 1-10 min, 80% - 50% carbonated water; 10-15 min, 50% carbonated water; flow rate 1.0 $\mu\text{L min}^{-1}$; injection volume 2.0 μL ; sample: naphthalene; UV detection 254 nm.....	63
Figure 2.9 Chromatograms of 1) 4-butylaniline, 2) phenanthrene, and 3) ketoprofen separated using poly(DMAEMA-co-EDMA) column using acidic (pH 3.4), neutral (pH 7.0) and basic (pH 10.4) solutions. Conditions: poly(DMAEMA-co-EDMA) monolithic column, 100 μm I.D., 15.0 cm; mobile phase, 0-1 min, 80% water; 1-10 min, 80% - 50% water; 10-15 min, 50% water; flow rate 1.0 $\mu\text{L min}^{-1}$, injection volume 2.0 μL , UV detection 254 nm. The concentration of	

phenanthrene in the top panel chromatogram is higher because stock solution of phenanthrene was spiked in the mixture to increase the intensity of peak 2.	67
Figure 2.10 Retention scheme of the basic (4-butylaniline), neutral (phenanthrene), and acidic (ketoprofen) analytes on the poly(DMAEMA-co-EDMA) monolithic column, showing the protonation of stationary phase and dissociation of the analytes.	68
Figure 2.11 Chromatograms of 1) 4-butylaniline, 2) phenanthrene, and 3) ketoprofen separated using poly(DMAEMA-co-EDMA) column at 25 °C and 65 °C. Conditions: poly(DMAEMA-co-EDMA) monolithic column, 100 µm I.D., 15.0 cm; mobile phase, 0-1 min, 80% water; 1-10 min, 80% - 50% water; 10-15 min, 50% water; flow rate 1.0 µL min ⁻¹ , injection volume 2.0 µL, UV detection 254 nm.	70
Figure 2.12 Schematic of the thermo-responsive change of the poly(DMAEMA-co-EDMA) monolithic column between a collapsed form at low temperature and an extended form at higher temperature.	71
Figure 2.13 Chromatograms of 1) myoglobin, 2) transferrin, 3) bovine serum albumin separated at various temperatures. Conditions: poly(DMAEMA-co-EDMA) monolithic column, 200 µm I.D., 15.0 cm; mobile phase A: Tris-HCl buffer at pH 7.6, mobile phase B, same as A except with 1 M NaCl; Gradient: 0-2 min, 100% water; 2-17 min, 100% A ~ 100% B; flow rate 4.0 µL min ⁻¹ , injection volume 2.0 µL, UV detection 214 nm.	72
Figure 3.1 CO ₂ induced “switching” the surface properties of amine functionalized stationary phase particles. Tertiary amine bonded phase before (left) and after (right) exposure to CO ₂ . The neutral tertiary amine presents a hydrophobic state favourable for retention (↑ retention factor, k) while the protonated tertiary amine phase favours elution (↓ k).	81
Figure 3.2 Gas delivery system coupled with HPLC, including a two-stage regulator, a rotameter, and a gas dispersion tube. (Gaseous CO ₂ flow rate, 20 mL/min; HPLC degasser bypassed; < 50% CO ₂ -saturated solvent B utilized). N ₂ bubbling was used to remove the dissolved ambient CO ₂ in Reservoir A and maintain pH 7.0.	84
Figure 3.3 System backpressure plots for 0%, 25%, 50%, and 100% CO ₂ -saturated solvents. Conditions: Agilent Bio-monolith DEAE column; mobile phase: 80/20 (v/v%) H ₂ O/acetonitrile; flow rate: 1.0 mL/min.	84
Figure 3.4 The measured pH of CO ₂ dissolved in water produced post-pump by mixing different ratios of CO ₂ -saturated water (1 bar) and N ₂ bubbled water; calculated pH of CO ₂ dissolved water at different CO ₂ partial pressure. The plot identifies the pH range accessible with a water / CO ₂ -modified solvent system.	90

Figure 3.5 Plots of retention factors with varying percentages of CO ₂ -saturated solvent measuring naphthalene, anthracene, 3- <i>tert</i> -butylphenol, 3-phenylphenol, 4-butylaniline, and diphenylamine. Conditions: Agilent Bio-monomolith DEAE column; Solvent A: 80% water/20% acetonitrile; Solvent B: identical to A except saturated with CO ₂ at 1 bar; flow rate: 1.0 mL/min; UV 254 nm.	91
Figure 3.6 Chromatograms produced using different CO ₂ -modified solvents (%B) for a) a mixture of naphthalene, 3- <i>tert</i> -butylphenol, 3-phenyl phenol and b) a mixture of 4-butylaniline, diphenylamine and anthracene. Conditions: Eprogen PEI column; solvent A: water, solvent B: CO ₂ -saturated water; isocratic; flow rate: 1.0 mL/min; UV 254 nm.	96
Figure 3.7 Comparison of an acetonitrile/H ₂ O and a CO ₂ -saturated water mobile phase based separation using the PEI column.....	99
Figure 3.8 Chromatograms produced using different CO ₂ -modified solvents (%B) for mixture of a) naphthalene, 3- <i>tert</i> -butylphenol, 3-phenylphenol; b) 4-butylaniline, diphenylamine, anthracene. Conditions: Eprogen CM column; solvent A: 95% H ₂ O/5% acetonitrile; solvent B: CO ₂ -saturated solvent A; isocratic; flow rate: 1.0 mL/min; UV 254 nm.	101
Figure 3.9 Plot of pH vs percentage of CO ₂ saturated water in HPLC as the mobile phase (solid line), percentage protonation of 4-butylaniline versus pH (dashed line).	102
Figure 4.1 Analyte structures and predicted <i>pK_a</i> values and <i>Log P</i> values.....	115
Figure 4.2 Representative scanning electron microscope images of silica spheres after the functionalization reaction at two different magnifications. The images are obtained from a FEI MLA 650 FEG Scanning Electron Microscopy.....	117
Figure 4.3 Solid-state NMR spectra and peak assignments. (a) ²⁹ Si NMR spectrum of tertiary amine functionalized silica. (b) ¹³ C NMR spectrum of primary amine functionalized silica. (c) ¹³ C NMR spectrum of secondary amine functionalized silica. (d) ¹³ C NMR spectrum of tertiary amine functionalized silica.	118
Figure 4.4 Zeta potential of bare silica (▽), primary (■), secondary (●) and tertiary (▲) amine functionalized silica spheres at various pH's. The size of the error bars is less than the size of the symbols (n ≥ 3).....	120
Figure 4.5 Retention time of naproxen (□), ibuprofen (○) and ketoprofen (△) at various mobile phase pH. Conditions: Tertiary amine functionalized column (2.1 mm × 50 mm), flow rate 0.40 mL min ⁻¹ , UV 254 nm. Aqueous solutions at various pH's were generated by mixing 0.01 M glycolic acid and 0.001 M NaOH. The error bars are smaller than the symbols (n ≥ 3).....	123

Figure 4.6 a) Overlaid figures containing the zeta potential of tertiary amine silica spheres vs pH (dotted line), and percentage fraction of deprotonated ibuprofen vs pH (dashed line). The blue shaded region shows the pH range that mixtures of water and carbonated water (1 bar) can access. The error bars are smaller than the symbols ($n \geq 3$). b) Schematic diagram showing the protonation of the stationary phase amine groups at lower pH (e.g. pH 3.0) and the dissociation of carboxylic acid compounds at higher pH (e.g. pH 7.0). 124

Figure 4.7 Chromatograms of ibuprofen (1), naproxen (2), and ketoprofen (3) on a tertiary amine column with various percentages of CO₂ saturated water (Solvent B) and non-carbonated water (Solvent A) as mobile phase. Conditions: tertiary amine-functionalized column (2.1 mm × 50 mm), flow rate 0.40 mL min⁻¹, UV 254 nm. 128

Figure 4.8 a) Retention time of ibuprofen on primary (□), secondary (○), and tertiary (△) amine columns at various pH's of the mobile phase. b) Chromatograms of ibuprofen (1), naproxen (2), and ketoprofen (3) on tertiary amine column and secondary amine column with 20% CO₂ saturated water as mobile phase. Conditions: secondary amine-functionalized column (2.1 mm × 50 mm), flow rate 0.40 mL min⁻¹, UV 254 nm. 129

Figure 5.1 Different states of superhydrophobic surfaces: a) Wenzel state, b) Cassie's superhydrophobic state, c) the "Lotus" state (a special case of Cassie's superhydrophobic state), d) the transitional superhydrophobic state between Wenzel's and Cassie's states, and e) the "Gecko" state of the PS nanotube surface. The gray shaded area represents the sealed air, whereas the other air pockets are continuous with the atmosphere (open state). Reproduced from reference⁵ with permission. Copyright © (2007) John Wiley and Sons Inc. 137

Figure 5.2 Schematic representation of the method for A) making superhydrophobic porous polymer films on a glass support and for B) creating superhydrophilic micropatterns by UV-initiated photografting. Reproduced from reference⁸ with permission. Copyright © (2011) John Wiley and Sons Inc. 140

Figure 5.3 A summary of typical smart molecules and moieties that are sensitive to external stimuli including temperature, light, pH, ion (salt), sugar, solvent, stress, and electricity, and can respond in the way of wettability change. Reprinted with permission from reference.³ Copyright © (2015) American Chemical Society. 143

Figure 5.4 A) Schematic of a superhydrophilic, nanoporous polymer layer grafted with superhydrophobic moieties. When an aqueous solution is rolled along the surface, the extreme wettability contrast of superhydrophilic spots on a superhydrophobic background leads to the spontaneous formation of a high-density array of separated microdroplets. B) Snapshot of water being rolled along a superhydrophilic-superhydrophobic patterned surface (1.0 mm diameter

circles, 100 μm barriers) to form droplets only in the superhydrophilic spots. Droplets formed in square and hexagonal superhydrophilic patterns. Reproduced from reference¹⁷ by permission of The Royal Society of Chemistry. 145

Figure 5.5 Zeta potential of non-grafted BMA-co-EDMA, DEAEMA and DIPAEMA grafted polymer at various pH conditions. 153

Figure 5.6 Water contact angles of DEAEMA grafted BMA-co-EDMA monolith surface (sample 1A, bottom slide), before and after treated with carbonated water. 157

Figure 5.7 Contact angle change of a droplet of pH 2.8 on different surfaces. 160

Figure 5.8 (A). Photographs of 1) aqueous solutions of bromocresol green (BCG, 5×10^{-5} M), 2) BCG solution treated with gaseous CO_2 for 10 seconds, 3) carbonated solution treated with N_2 for 1 minute, 4) Carbonated solution treated with N_2 for 2 minutes. Flow rate of CO_2 and N_2 are 100 mL min^{-1} , a gas dispersion tube (O.D. \times L $7.0 \text{ mm} \times 135 \text{ mm}$, porosity $4.0 - 8.0 \mu\text{m}$) was used. (B). Photographs of $10 \mu\text{L}$ droplets dispensed on a hydrophilic array. 1) Aqueous solutions of BCG (5×10^{-5} M), 2) BCG solution treated with gaseous CO_2 for 10 seconds, 3) carbonated solution exposed in air for 1 minute, 4) carbonated solution exposed in air for 2 minutes. 162

List of Tables

Table 1.1 The 12 principles of green chemistry and relevant principles for green analytical chemistry (in bold). Adapted from reference. ¹	3
Table 1.2 Types and structures of CO ₂ -switchable functional groups.....	15
Table 1.3 Functional groups for typical liquid chromatography modes and eluents.	25
Table 2.1 Compositions of the polymerization mixture for poly(DMAEMA-co-EDMA) monolithic column with varying ratios of monomer / crosslinker.	50
Table 2.2 Compositions of the polymerization mixture for poly(DMAEMA-co-EDMA) monolithic column with varying amounts of 2-propanol and 1,4-butanediol.....	50
Table 2.3 List of organic compounds used for the reversed phase chromatography with polymer monolithic column.	52
Table 2.4 List of proteins used for the ion exchange chromatography with the polymer monolithic column. Theoretical <i>pI</i> was calculated using ExPasy. ²³	53
Table 3.1 Column dimensions (obtained from manufacturer data sheets).....	86
Table 3.2 Analytes structure, <i>Log P</i> and <i>pK_a</i> values. ²⁹	87
Table 3.3 Zeta potential (mV) of stationary phase suspensions.	94
Table 3.4 Gibbs free energy difference ($\Delta\Delta G^\circ$, kJ mol ⁻¹) of chromatographic adsorption between the modified solvents and the modifier-free solvents. (*data was not acquired due to non-retention of 4-butylaniline)	94
Table 4.1 Elemental composition of bare silica and primary, secondary and tertiary amine functionalized silica spheres.....	116
Table 4.2 Chromatographic results on the tertiary amine column with 5%, 10%, 20% CO ₂ saturated water as the mobile phase.....	126
Table 4.3 Chromatographic result for a secondary amine column with 20% CO ₂ saturated water as the mobile phase.	130
Table 5.1 Composition of polymerization and photografting mixtures.	150
Table 5.2 Water contact angles of non-grafted and grafted polymer monoliths before and after treatment with CO ₂ (carbonated water).....	155
Table 5.3 Water contact angle hysteresis of non-grafted and photografted BMA-co-EDMA monolith before and after treatment with carbonated water.	159

List of Abbreviations

ACN	Acetonitrile
AIBN	2, 2'-Azobis (2-methylpropionitrile)
AMPS	2-Acrylamido-2-methyl-1-propanesulphonic acid
ARCA	Advancing and receding contact angle
ATR-IR	Attenuated total reflection infrared spectroscopy
BMA	n-Butyl methacrylate
CAH	Contact angle hysteresis
CFCs	Chlorofluorocarbons
CM	Carboxymethyl
DEAE	Diethylaminoethyl
DEAEMA	Diethylaminoethyl methacrylate
DESI	Desorption electrospray ionization
DIPAEMA	2-(Diisopropylamino)ethyl methacrylate
DMAEMA	Dimethylaminoethyl methacrylate
DMPAP	2, 2-Dimethyl-2-phenylacetophenone
EDMA	Ethylene glycol dimethacrylate
HCFCs	Hydrochlorofluorocarbons
HEMA	Hydroxyethyl methacrylate
HFCs	Hydrofluorocarbons
HILIC	Hydrophilic interaction chromatography
HOAc	Glacial acetic acid
HPLC	High-performance liquid chromatography
IEC	Ion exchange chromatography
IPAAm	N-isopropylacrylamide
LCST	Lower critical solution temperature
MeOH	Methanol

NAS	N-acryloxysuccinimide
NPC	Normal phase chromatography
PAA	Poly(acrylic acid)
PCBs	Polychlorinated biphenyls
PDEAEMA	Poly(diethylaminoethyl methacrylate)
PDMAEMA	Poly(dimethylaminoethyl methacrylate)
PDMAPMAm	Poly(dimethylaminopropyl methacrylamide)
PEI	Polyethylenimine
PNIPAAm	Poly(N-isopropylacrylamide)
PPM	Porous polymer monolith
RPC	Reversed phase chromatography
SA	Sliding angle
SAX	Strong anion exchange chromatography
SCX	Strong cation exchange chromatography
SEM	Scanning electron microscopy
SFC	Supercritical fluid chromatography
SHS	Switchable hydrophobicity solvent
SI-ATRP	Surface-initiated atom transfer radical polymerization
THF	Tetrahydrofuran
UHPLC	Ultra-high-performance liquid chromatography
VAL	4-Dimethyl-2-vinyl-2-oxazolin-5-one
VWSP	Volume weighted solvent polarity
WAX	Weak anion exchange chromatography
WCA	Water contact angle
WCX	Weak cation exchange chromatography
XPS	X-ray photoelectron spectroscopy
γ -MAPS	3-(Trimethoxysilyl) propyl methacrylate

Chapter 1 Introduction

1.1 Background

1.1.1 Green chemistry and its principles

Chemicals are present in every aspect of the natural environment and human life. Modern chemistry dates back to alchemy in the seventeenth and eighteen centuries, and it has been continuously advancing human life and economic prosperity ever since. Chemistry makes better materials, safer food, effective drugs and improved health. Despite the benefits chemistry has brought to us in the past, chemicals have adversely affected the environment, and human health. As an example, polychlorinated biphenyls (PCBs) were first synthesized in 1877 and used as dielectric and coolant fluids in electrical apparatus.¹ Soon after it was found that PCBs are neurotoxic and cause endocrine disruption and cancer in animals and humans. More than a hundred years later, PCB production was finally banned by the United States Congress and the *Stockholm Convention on Persistent Organic Pollutants*.²

Some chemical exposure directly risks human health, however other chemicals may impact the environment and indirectly pose a threat to human well-being. For example, chlorofluorocarbons (CFCs) have been suspected as responsible for the depletion of the ozone layer since the 1970s.³ Following the discovery of the Antarctic ozone hole in 1985, an international treaty, the *Montreal Protocol on Substances that Deplete the Ozone Layer* phased out the production of CFCs. Alternative compounds such as hydrochlorofluorocarbons (HCFCs) and hydrofluorocarbons (HFCs) were developed as a

replacement to CFCs, which are considered to cause minimal destruction to the ozone layer. As a result of those efforts, the ozone hole in Antarctica is slowly recovering.⁴ Looking back at those developments, we realize that we don't recognize problems until they adversely affect the environment or human health. Therefore, it becomes crucial to change our mind-set where we don't think of chemistry in terms of waste treatment but rather the prevention of waste generation. Undoubtedly, the chemical sciences and industry will be forced towards more sustainable development, aimed at minimizing the impact of chemical processes, while maintaining the quality and efficacy of the products.

The reasons for more sustainable development are obvious, however how can humankind improve chemical processes. Paul Anastas and John Warner have identified valuable guidelines that have come to be known as the 12 principles of green chemistry (Table 1.1).¹

1.1.2 Green analytical chemistry

Analytical measurements are essential to both the understanding of the quality and quantity of therapeutic materials, and identifying environmental contaminant concentrations. As a result, the measurements assist in making decisions for health care and environmental protection. However, ironically, analytical laboratories are listed as a major waste generator.⁵ Quality control and assurance laboratories associated with the pharmaceutical sector in particular consume large quantities of harmful organic solvents while producing and monitoring drugs for human health. Furthermore, environmental analysis laboratories that monitor, measure, and characterize environmental problems also both consume and generate significant volumes of harmful organic solvent.

Table 1.1 The 12 principles of green chemistry and relevant principles for green analytical chemistry (in bold). Adapted from reference.¹

1.	Prevent Waste: <i>It is better to prevent waste than to treat or clean up waste after it has been created.</i>
2.	Maximize Atom Economy: <i>Synthetic methods should be designed to maximize the incorporation of all materials used in the process into the final product.</i>
3.	Design Less Hazardous Chemical Syntheses: <i>Wherever practicable, synthetic methods should be designed to use and generate substances that possess little or no toxicity to human health and the environment.</i>
4.	Design Safer Chemicals and Products: <i>Chemical products should be designed to affect their desired function while minimizing their toxicity.</i>
5.	Use Safer Solvents/Reaction Conditions and Auxiliaries: <i>The use of auxiliary substances (e.g. solvents, separation agents, etc.) should be made unnecessary whenever possible and innocuous when used.</i>
6.	Increase Energy Efficiency: <i>Energy requirements of chemical processes should be recognized for their environmental and economical impacts and should be minimized. If possible, synthetic methods should be conducted at ambient temperature and pressure.</i>
7.	Use Renewable Feedstocks: <i>A raw material or feedstock should be renewable rather than depleting whenever technically and economically practicable.</i>
8.	Reduce Derivatives: <i>Unnecessary derivatization (use of protection/deprotection, temporary modification of physical/chemical processes) should be minimized or avoided if possible, because such steps require additional reagents and can generate waste.</i>
9.	Use Catalysis: <i>Catalytic reagents (as selective as possible) are superior to stoichiometric reagents.</i>
10.	Design for Degradation: <i>Chemical products should be designed so that at the end of their function they break down into innocuous degradation products and do not persist in the environment.</i>
11.	Analyze in Real-time to Prevent Pollution: <i>Analytical methodologies need to be further developed to allow for the real-time, in-process monitoring and control prior to the formation of hazardous substances.</i>
12.	Minimize Potential for Accidents: <i>Substances and the form of a substance used in a chemical process should be chosen to minimize the potential for chemical accidents, including releases, explosions, and fires.</i>

Several industrial and scientific pioneers have established the concept and principles governing green chemistry.⁶⁻¹⁰ Not surprisingly some of the principles for green chemistry are also closely related with green analytical chemistry (Table 1.1). Since the original comments and reviews on green analytical chemistry were published, more researchers have published articles on environmentally friendly analysis, using the

terminology “green analytical chemistry” or “green analysis. For instance, more than 3000 scientific papers were published containing the keyword “green analysis” according to a SciFinder search of the Chemical Abstract Database.^{11, 12}

The overarching goal of green analytical chemistry is to use analytical procedures that generate less hazardous waste, are safe to use, and are more benign to the environment.⁷⁻¹⁰ Various principles have been proposed to guide the development of green analytical techniques. The “3R” principles are commonly mentioned and they refer to efforts towards the ‘R’eduction of solvents consumed and waste generated, ‘R’eplacement of existing solvents with greener alternatives, and ‘R’ecycling via distillation or other approaches.¹³

A “profile of greenness” was proposed by Keith *et al.* in 2007 which provides evaluation criteria for analytical methodologies.⁸ The profile criteria were summarized using four key terms: PBT (persistent, bioaccumulative, and toxic), Hazardous, Corrosive, and Waste. The profile criteria that make a method “less green” are defined as follows.

A method is “less green” if

1. PBT - a chemical used in the method is listed as a PBT, as defined by the Environmental Protection Agency’s “*Toxic Release Inventory*” (TRI);
2. Hazardous - a chemical used in the method is listed on the TRI or on one of the *Resource Conservation and Recovery Act*’s D, F, P or U hazardous waste lists;
3. Corrosive - the pH during the analysis is < 2 or > 12;

4. Wastes - the amount of waste generated is > 50 g.

Different strategies and practice were adopted towards greening analytical methodologies, including modifying and improving established methods as well as more significant leaps that completely redesign an analytical approach. For example, *in situ* analysis may be conducted by integrating techniques consuming small amounts of organic solvents, such as liquid/solid phase microextraction^{14, 15} and/or supercritical fluid extraction.^{16, 17} Microwave, ultrasound, temperature and pressure may also assist in the extraction step of sample preparation to reduce the consumption of harmful solvents.^{16, 18, 19} Miniaturized analysis may be performed that benefits from the development of micro total analysis systems (μ TAS).²⁰⁻²⁴ For example, microchip liquid chromatography could significantly reduce solvent consumption associated with chromatography by utilizing small amounts of reagents.^{2, 25-29} In general, the “3R” principles for green analytical chemistry specifically guide the development of green sample preparation and green chromatographic techniques, because sample preparation and chromatographic separation are the most significant consumers of harmful organic solvents.

1.1.3 Green chromatography

Chemical separations account for about half of US industrial energy use and 10 - 15% of the nation’s total energy consumption.³⁰ Immense amounts of energy and harmful organic solvents are consumed in chemical separation processes. As an important separation technique, chromatographic separation is widely used in the purification and analysis of chemicals. Specifically, high-performance liquid chromatography (HPLC) and related chromatographic techniques are the most widely utilized analytical tools in

analytical separations. According to a recent survey performed regarding HPLC column use, columns with conventional column dimensions (2.0 - 7.8 mm I.D.) are still the workhorses in analytical laboratories.³¹ For example, a stationary-phase column of 4.6 mm internal diameter (I.D.) and 20 cm length is usually operated at a mobile-phase flow rate of about 1.0 - 1.5 mL min⁻¹. Under those conditions, more than one liter of effluent is generated for disposal in a day because a major portion of the effluent is harmful organic solvent.¹³ Although the 1 L of waste may seem to be trivial, the cumulative effect of analytical HPLC in analytical laboratories is substantial. A single pharmaceutical company may have well over 1000 HPLC instruments operating on a continuous basis.¹³

The goal of green chromatography is to lower the consumption of hazardous solvents and it has raised significant awareness and interest in both industry and academia.^{6, 12, 13, 32-35} Greener liquid chromatography can be achieved with various strategies. For example, faster chromatography is a straightforward route for green chromatography. With the same eluent flow rate, shorter analysis times can save significant amounts of solvent. Columns with smaller particles have been employed to acquire a comparable efficiency at shorter column lengths, resulting in the emergence of ultra-high-performance liquid chromatography (UHPLC). Smaller particles ($\leq 2 \mu\text{m}$) are utilized in UHPLC systems, compared with the conventional particles size ($\geq 3.5 \mu\text{m}$). As a result, a UHPLC system with a 2.1-mm I.D. column could enable 80% overall solvent savings compared to conventional HPLC. The combined advantages of speed and efficiency for UHPLC have made it a trending technology and a significant step towards greener chromatography.

Another strategy for green chromatography focuses on reducing the scale of the chromatographic experiment. The 4.6 mm I.D. is a standard dimension column that is typically operated at a flow rate of 1.0 mL min^{-1} . This standard column diameter is more of a historic relic resulting from technical limitations in the 1970s, rather than performance considerations. Smaller I.D. columns require much less solvent and generate reduced waste and microbore column (0.30 - 2.0 mm), capillary column (0.10 - 0.30 mm) and nano-bore column ($\leq 0.10 \text{ }\mu\text{m}$) are all commercially available. For example, merely $\approx 200 \text{ mL}$ solvent is consumed if a capillary/chip LC column is continuously operated for a year at a flow rate of 400 nL min^{-1} compared to a conventional LC, which consumes $\approx 500 \text{ L}$ operated at 1.0 mL min^{-1} . Nevertheless, some bottlenecks still prevent the wider adoption of smaller scale columns. High-pressure pumps and more robust connections / tubing are required. The adverse effects of extra-column volumes on separation efficiency are more problematic for smaller scale columns and the limit of detection for microflow LC is generally higher due to the incorporation of smaller flow path (*e.g.*, UV detector).

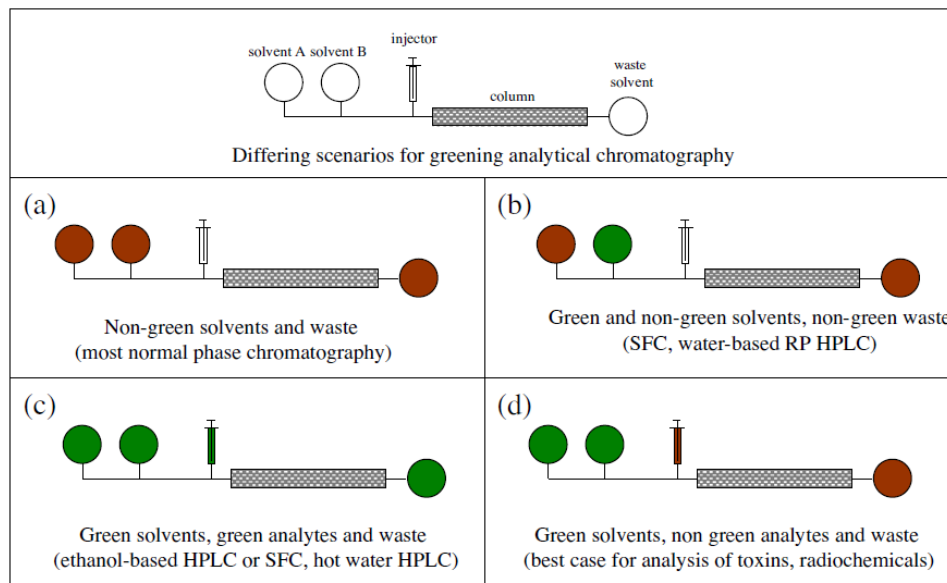


Figure 1.1 “Greenness” of different chromatographic scenarios. Reprinted from reference¹³ with permission from Elsevier.

In addition to solvent-reduction strategies, other green chromatography efforts focus on replacing toxic or flammable solvents with greener alternatives.¹² A variety of scenarios exist for greening chromatographic separations.¹³ As depicted in Figure 1.1 a, the worst scenario utilizes non-green solvents for both solvent A and B, with the waste generated also being non-green. Normal phase chromatography (NPC) is an example of this scenario, which uses toxic organic mobile phase components (*e.g.* hexanes, ethyl acetate, chloroform). The scenario shown in Figure 1.1 b represents the combination of a green solvent (*e.g.* water, ethanol, or carbon dioxide) with a non-green solvent. For example, reversed phase chromatography (RPC) utilizes both an organic phase and an aqueous phase. Scenario in Figure 1.1 c and d are greener because both solvent A and B are green solvents. Those technologies may generate no waste at all, as the effluent could be directly disposed of down a drain, assuming that the analytes are non-toxic.

In particular, replacement of acetonitrile with ethanol in reversed phase chromatography has been attempted due to its higher availability and less waste consumed for producing ethanol.³⁶⁻³⁸ For example, it was found that ethanol has the ability to separate eight alkylbenzene compounds with similar speed although the efficiency is not superior to acetonitrile. Nevertheless, acetonitrile is still a more popular solvent, because of the limitations of other solvents, such as UV cut-off, viscosity, cost, *etc.*

Supercritical fluid chromatography (SFC) represents one of the true success stories of green chromatography and extraction, where the replacement technology is both greener and undoubtedly better. Supercritical CO₂ has been extensively used as a solvent in pressurized and heated conditions (*e.g.* > 100 bar, > 40 °C) because supercritical CO₂ exhibits solvent properties similar to petrochemical-derived hydrocarbons. Therefore, it represents a greener replacement for commonly used normal phase chromatography solvents (*e.g.* hexanes). Alternatively, enhanced fluidity liquids based upon sub-critical CO₂ have also demonstrated improved efficiency and/or reduced cost.³⁹⁻⁴³

In the scenarios of Figure 1.1, we notice that the stationary phase (or column) has not been mentioned from the perspective of saving solvent. Strategically, it is also promising to develop novel stationary phase materials towards the goal of greener chromatography. In fact, with the development of nanotechnology, surface chemistry and polymer science, a growing number of stimuli-responsive chromatographic materials have been reported.^{44, 45} For example, thermo-responsive stationary phases on silica or polymer surfaces were demonstrated to separate organic molecules using various temperature

conditions.⁴⁶⁻⁵¹ Alternatively, pH and salt responsive surfaces are exploited for the separation of small molecules and biomolecules.⁵²⁻⁵⁴

Responsive stationary phases provide another dimension of control for chromatography. However, limitations still exist that have discouraged a wider adoption. For example, thermo-responsive approach is limited by the thermal conductivity of the chromatographic column and biomolecules can be susceptible to high temperature. Permanent salts are required in pH responsive conditions, and they are still difficult to remove following the separation.

1.2 CO₂-switchable chemistry

1.2.1 Carbon dioxide

In the past decades, the environmental effects of carbon dioxide (CO₂) have become of significant interest because CO₂ is a major greenhouse gas. Burning of carbon-based fuels continues to increase the concentration of CO₂ in the atmosphere, which is considered a major contributor to global warming. However, from the perspective of industrial and academic applications, CO₂ is a relatively benign reagent with great availability, low economic and environmental cost for use / disposal.

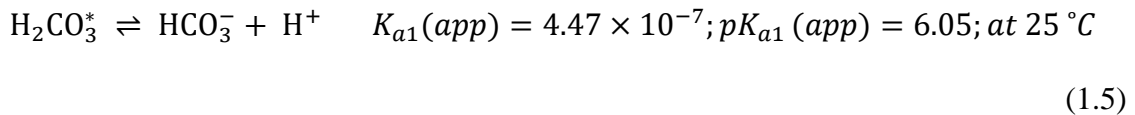
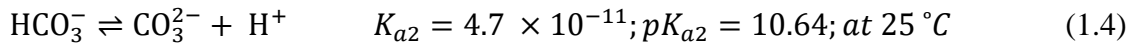
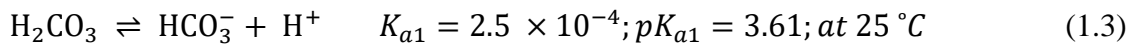
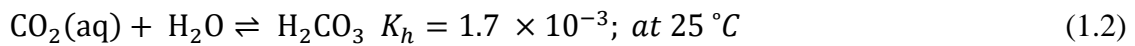
CO₂ is a colourless gas accounting for 0.040% of atmosphere gases by volume. CO₂ is mostly produced by the combustion of wood, carbohydrates and major carbon- and hydrocarbon-rich fossil fuels. It is also a by-product of many commercial processes: synthetic ammonia production, hydrogen production and chemical syntheses involving carbon monoxide.⁵⁵ In the chemical industry, carbon dioxide is mainly consumed as an ingredient in the production of urea and methanol.⁵⁵ CO₂ has been widely used as a less

expensive inert gas and welding gas compared to both argon and helium. Supercritical fluid chromatography, using a mixture of CO₂ and organic modifier, is considered a “green” technology that reduces organic solvent use by up to 90% for the decaffeination of coffee, separation of enantiomers in the pharmaceutical industry, *etc.*⁵⁶ The solvent turns to gas, when the pressure is released, often precipitating the solute from the gas phase for easy recovery. The low viscosity of the supercritical fluid also permits faster flow to increase productivity. SFC provides increased speed and resolution, relative to liquid chromatography, because of the higher diffusion coefficient of solutes in supercritical fluids. Carbon dioxide is the supercritical fluid of choice for chromatography because it is compatible with flame ionization and ultraviolet detectors, it has a low critical temperature and pressure, and it is nontoxic.

All the properties CO₂ possesses come from the nature of the chemical itself. Specifically, the relatively high solubility of CO₂ in water (at room temperature and 1 bar) and the acidity of carbonic acid provide us with an accessible path to “CO₂ switchable technologies”. Henry’s Law (Equation 1.1) describes how CO₂ dissolves in water, where the concentration of dissolved CO₂, c , is proportional to the CO₂ partial pressure p , and inversely proportional to the Henry’s Law constant, k_H , which is 29.4 L·atm mol⁻¹ at 298 K for CO₂ in water.⁵⁷ Therefore, at a given temperature, the concentration of dissolved CO₂ is determined by the partial pressure, p , of carbon dioxide above the solution.

When CO₂ is dissolved in water, it forms carbonic acid (H_2CO_3), and this hydration equilibrium is shown as Equation 1.2. Additionally, Equation 1.3 and 1.4 represent the dissociation of carbonic acid, therefore producing the bicarbonate ion, HCO₃⁻, and

dissociation of the bicarbonate ion into the carbonate ion CO_3^{2-} respectively. It should be noted, the first dissociation constant of carbonic acid (pK_{a1}) could be mistaken with the apparent dissociation constant $pK_{a1}(\text{app})$. The difference is that, this apparent dissociation constant for H_2CO_3 takes account of the concentration for both dissolved $\text{CO}_2(\text{aq})$ and H_2CO_3 . Therefore, H_2CO_3^* is used to represent the two species when writing the aqueous chemical equilibrium (Equation 1.5). The fraction of species depends on the pH of the carbonic solution, which is plotted in Figure 1.2 according to theoretical calculations.⁵⁸



Considering all of above chemical equilibrium as well as the auto-dissociation of water in a solution, the concentration of H^+ (pH) can be determined according to the temperature and $p\text{CO}_2$. For normal atmospheric conditions ($p\text{CO}_2 = 4.0 \times 10^{-4}$ atm), a slightly acid solution is present (pH 5.7). For a CO_2 pressure typical of that in soda drink bottles ($p\text{CO}_2 \sim 2.5$ atm), a relatively acidic medium is achieved (pH 3.7). For CO_2 saturated water ($p\text{CO}_2 = 1$ atm), pH of the solution is 4.0.⁵⁹ Therefore, purging water with CO_2 at 1 atm could produce an aqueous solution with pH ~ 4.0 . Recovery of the pH can be

simply realized by purging with N₂/Ar, or elevating the temperature of the solution. This versatile feature has prompted researchers to develop CO₂-switchable moieties in order to address a wide range of applications and technical challenges.

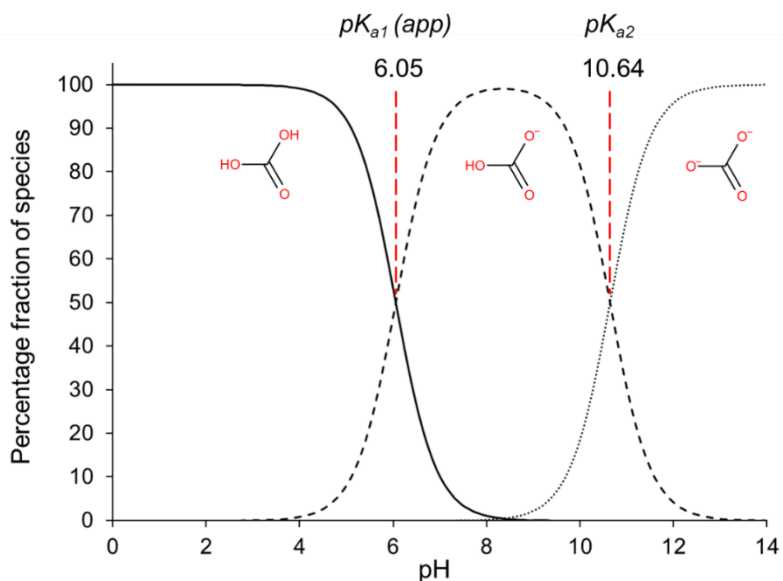


Figure 1.2 A distribution plot of carbonic acid (hydrated CO₂ and H₂CO₃) and the subsequent dissociated species based upon pH. Reproduced using data from reference.⁵⁸

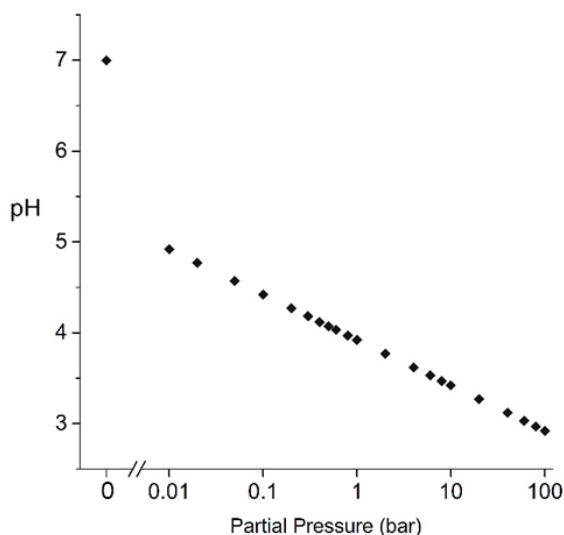


Figure 1.3 pH of carbonated water versus the partial pressure of carbon dioxide above the solution (23 °C). Reproduced from reference⁶⁰ by permission of The Royal Society of Chemistry.

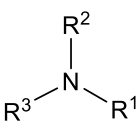
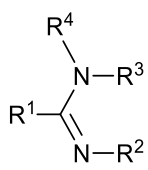
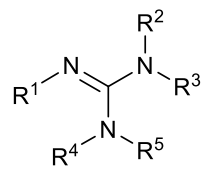
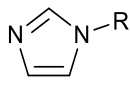
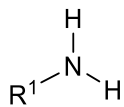
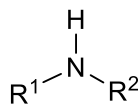
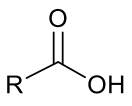
At a given temperature, the pH of an aqueous solution containing dissolved CO₂ is determined by the partial pressure (pCO_2) of carbon dioxide above the solution. According to the Henry's law constant of CO₂ and the dissociation constant of carbonic acid, the pH of CO₂ dissolved water at different partial pressure levels can be calculated and is shown in Figure 1.3.^{59, 61} The presence of CO₂ in water ($pCO_2 = 1$ bar) results in a solution with pH 3.9. Reducing the CO₂ partial pressure to 0.1 bar produces a solution with pH 4.4.

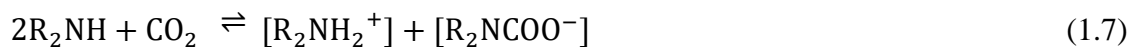
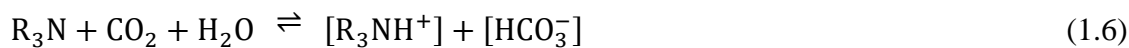
1.2.2 CO₂-switchable groups

In this thesis, the selection of functional groups for CO₂-switchable chromatography is based on the knowledge of CO₂-switchable groups. CO₂-switchable functional groups include those groups that switch from neutral to cationic, anionic, or carbamate salts, as shown in Table 1.2 in the presence or absence of CO₂.⁶² Basic groups are typically switched from a neutral form into a protonated form (bicarbonate salt) by the addition of CO₂ (Equation 1.6). Basicity of the functional group is evaluated by pK_{aH} of its conjugate acid, with a higher pK_{aH} indicating a stronger base. The stronger the base group is, the more easily CO₂ may switch it to a cationic form. Conversely, it requires more energy to reverse the reaction and convert the cations back to neutral forms.⁶² In general, amidine and guanidine are stronger bases than the amine group. Therefore, amine groups are usually more easily converted from the bicarbonate salt to a neutral form. Another important factor affecting the reversible switch is steric hindrance. If there is not a bulky substitutive group adjacent to the nitrogen (primary and secondary amine shown in Table 1.2), a carbamate salt is likely to form (Equation 1.7).⁶³⁻⁶⁵ It requires much more energy to reverse the formation of carbamate salt, therefore, those groups are less favourable for certain applications requiring a fast switch. Conversely, bulky secondary and bulky

primary amines are found to be CO₂-switchable by conversion into bicarbonate salts, because the bulky group inhibits the carbamate formation. In water, carboxylic acids are also found to be switchable groups in response to CO₂. The addition of CO₂ switches the anionic carboxylate to a hydrophobic, uncharged form, and the absence of CO₂ switches the molecular carboxylic acid to an anionic state (Equation 1.8).

Table 1.2 Types and structures of CO₂-switchable functional groups

Switch from neutral to cationic			
			
Amine	Amidine	Guanidine	Imidazole
Switch from neutral to carbamate salts			
			
Primary amine (non-bulky)	Secondary amine (non-bulky)		
Switch from neutral to anionic			
			
Carboxylic acid			





1.2.3 CO₂-switchable technologies

Because of the unique properties of CO₂, a variety of CO₂-switchable technologies (*e.g.* solvents, surfactants, and surfaces) have been developed.^{62, 64-68} Switchable materials are also referred as stimuli-responsive materials, or “smart” materials, such as drug-delivery vehicles, which possesses two sets of physical or chemical properties that are accessible via the application or removal of a stimulus, or trigger.^{69, 70} Specifically, pH is one stimulus relying on acid/base chemistry. Similar to pH-responsive materials, CO₂ switchable materials are attracting more interest because of their unique properties such as the reversible solubility and acidity in an aqueous solution. The removal of CO₂ from the system is typically prompted by heating the system, or sparging with a non-reactive gas (*e.g.* Ar, N₂).

A switchable hydrophobicity solvent (SHS) is a solvent that is poorly miscible with water in one form but completely miscible with water in another form and it can be switched between these two forms by a simple change in the system.^{64, 71-73} In particular, tertiary amines and amidine SHSs have been identified which can be switched between the two forms by the addition or removal of CO₂ from the system.^{71, 74} The hydrophobicity switch is realized via the protonation and deprotonation of SHS by hydrated CO₂ or carbonic acid. Dozens of SHS are known; most of them are tertiary amines but there are also some amidines and bulky secondary amines.⁶² Because distillation is not required for separating a SHS solvent from a product, a SHS does not have to be volatile. Amines, which

display SHS behaviour, generally have $\text{Log } P$ between 1.2 and 2.5 and pK_a above 9.5. Secondary amines can also exhibit switchable behaviour but carbamate salts can form and precipitate with bicarbonate ions. It has been reported that sterically hindered groups around secondary amines could prevent the formation of carbamate salts. By utilizing the hydrophobicity switch triggered by CO_2 at one atm and room temperature, solvent removal has been realized for the production of soybean oil, algae fuel, and bitumen.^{71, 73, 75, 76}

In addition to switchable hydrophobicity solvents, a variety of novel CO_2 switchable technologies have been developed, including CO_2 -switchable surfaces and separation media. The first CO_2 -switchable polymer brushes were reported by Zhao and coworkers in 2013.⁷⁷ Brushes of poly(diethylaminoethyl methacrylate) (PDEAEMA) were grafted onto either a silicon or gold surface. At room temperature and pH 7.0, the brushes are insoluble in water and present in a collapsed state. Upon passing CO_2 through the solution, the tertiary amine groups form charged ammonium bicarbonate and render the polymer brushes soluble in water, thus resulting in the brushes being present in an extended state (Figure 1.4). Subsequently, passing N_2 through the solution can reverse the brushes to the collapsed, water insoluble state. Adsorption and desorption of proteins were observed through quartz crystal microbalance and repeated cycles of switching triggered by CO_2 was shown. Unlike the conventional pH change induced by adding acids and base, such CO_2 -switchable water solubility of the polymer brushes can be repeated many times for reversible adsorption and desorption of a protein without contamination of the solution by accumulated salts.

CO₂-switchable polymer grafted particles were also developed as drying agents. Used solvents are usually contaminated with water, altering their properties for some industrial processes. Therefore, separating water from (i.e. drying) organic liquids is a very important operation in many industrial processes like solvent recycling and the production of ethanol and biodiesel.^{62, 65} An ideal drying agent should be able to bind water strongly during the capture stage and release it easily during regeneration. Additionally, the drying agent should be easily recycled as well as inert to the solvent of interest and have a high capacity for absorbing water. Based on these criteria, Boniface *et al.* recently developed a CO₂-switchable drying agent containing tertiary amine groups and evaluated it for the drying of *i*-butanol (Fig. 1.5). Silica particles with poly(dimethylaminopropyl methacrylamide) (PDMAPMAM) chains grafted by surface initiated atom transfer radical polymerization (SI-ATRP) were used to dry solvents. The water content of wet *i*-butanol was reduced by 490 μ per gram of drying agent after application of CO₂.

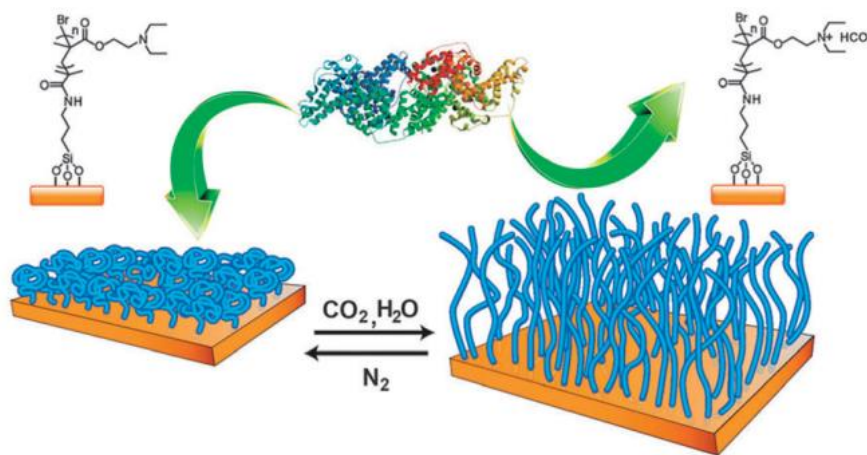


Figure 1.4 Schematic of protein adsorption and release using CO₂-switchable surface with polymer brushes. Reproduced from reference⁷⁷ with permission of The Royal Society of Chemistry.

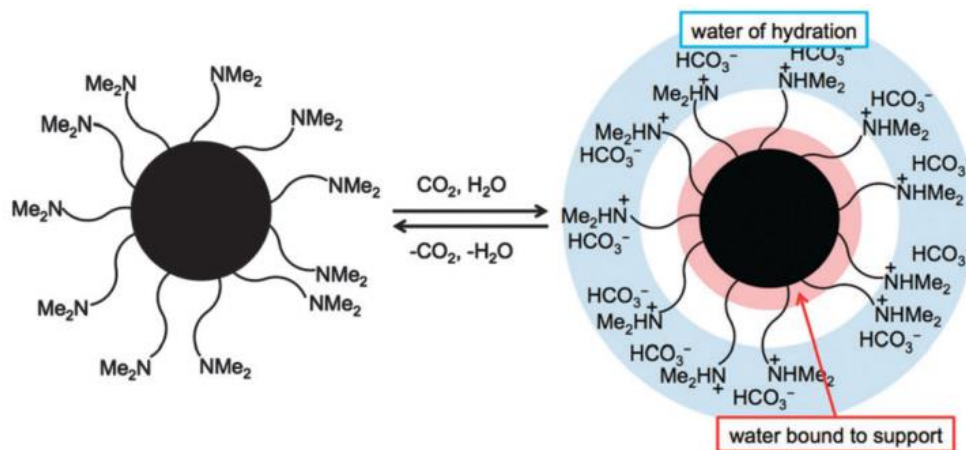


Figure 1.5 Schematic of CO_2 -switchable drying agent using silica particles grafted with PDMAPMAm chains. Reproduced from reference⁶⁵ with permission of The Royal Society of Chemistry.

CO_2 is also used for the recycle of extractant in separation processes. Yu *et al.* reported the extraction of α -tocopherol from the tocopherol homologues using polyethylenimine (PEI) as a CO_2 -switchable polymeric extractant.⁷⁸ Different PEI co-solvent solutions were employed to separate tocopherols from their hexane solutions. A simple advantage of PEI extraction is its CO_2 -switchability. PEI-extracted tocopherols are replaced and separated from PEI chains upon introduction of CO_2 . PEI - CO_2 is precipitated and separated from the extract phase, which facilitates the reverse extraction of tocopherols and the retrieval of PEI for future reuse. Precipitated PEI - CO_2 can be redissolved in the co-solvent phase for reuse by heating and N_2 bubbling (Figure 1.6).

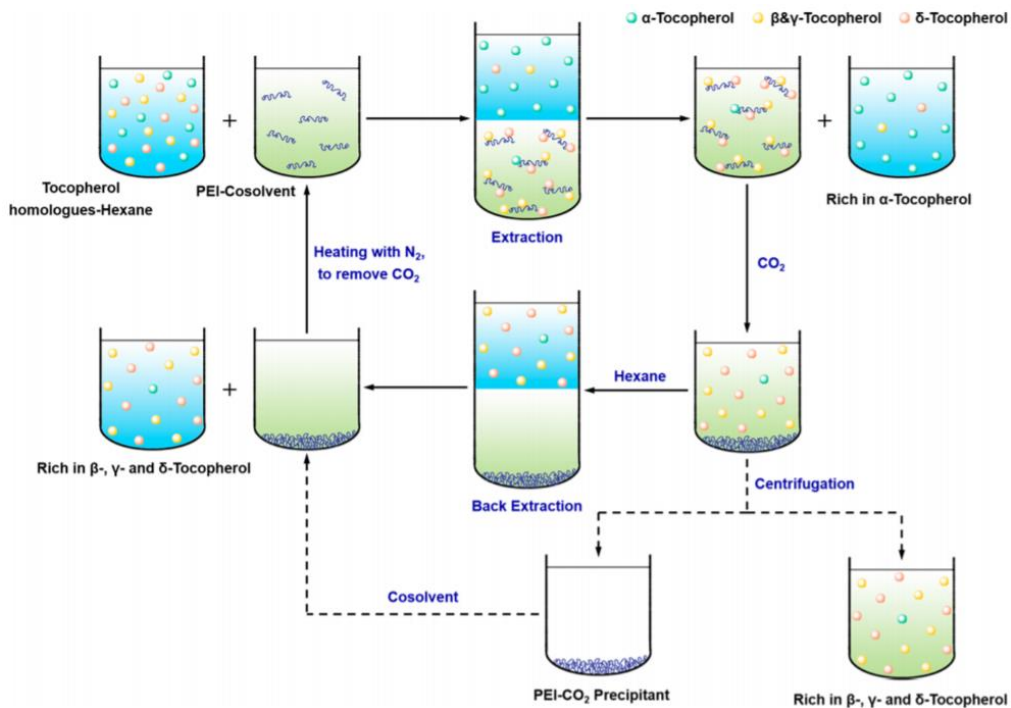


Figure 1.6 Schematic of the separation of α -Tocopherol from its homologues and recovery of the extractant. Reprinted with permission from reference.⁷⁸ Copyright © (2014) American Chemical Society.

Based on the abovementioned advances, we anticipated that the acidity of CO_2 dissolved water could be used as the basis for reversibly modifying the stationary phase and/or analytes in aqueous chromatography. CO_2 can be considered a “temporary” acid since its removal can be achieved by bubbling with an inert gas. As a result, it could be a very useful alternative to organic modifier / permanent acids. Figure 1.7 shows a schematic that, CO_2 addition and removal causes the switchable groups to convert between cationic/hydrophilic and neutral/hydrophobic states. In the case of amine groups, addition of CO_2 causes the neutral and hydrophobic groups to become cationic and hydrophilic, while removal of the CO_2 , by heating or purging with an inert gas (*e.g.* N_2 , Ar) leads to deprotonation, switching the amine groups to a neutral and hydrophobic form.

Furthermore, the pH can be carefully controlled by mixing carbonated water and water. This hypothesis is investigated in chapters 2, 3 and 4.

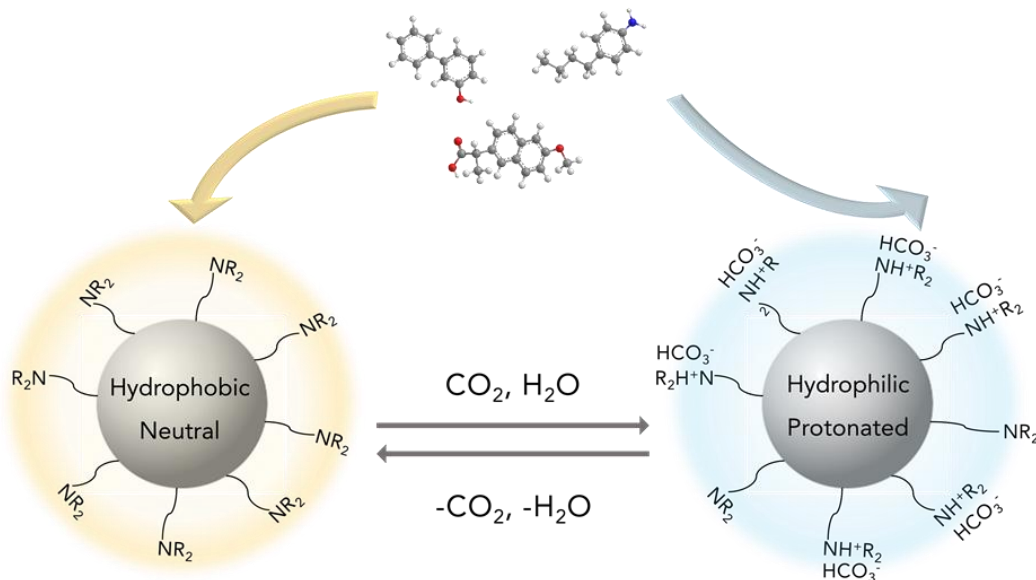


Figure 1.7 CO₂ induced “switching” of surface properties for amine functionalized stationary phase particles. Tertiary amine bonded phase before (left) and after (right) exposure to CO₂. The tertiary amine (left) presents a hydrophobic, neutral state while the tertiary amine phase (right) represents a hydrophilic and protonated state of the groups. Reproduced from reference⁶⁰ by permission of The Royal Society of Chemistry.

1.3 Principles of liquid chromatography

1.3.1 Modes of separation

Normal phase chromatography (NPC) emerged as the original form of chromatography in the 1900s.⁷⁹ The earliest chromatographic columns were packed with polar, inorganic particles, such as calcium carbonate or alumina. Less polar solvents were used as mobile phases, such as ligroin (a saturated hydrocarbon fraction from petroleum).⁷⁹ This procedure continued for the next 60 years as the most common way to carry out chromatographic separations. NPC is also known as adsorption chromatography since the

solute molecules are adsorbed onto the surface of solid particles within the column. However, some problems that are common to NPC are responsible for its decline in popularity. Those problems include poor separation reproducibility, extreme sensitivity to water content, solvent demixing, slow equilibration, *etc.* In addition to these disadvantages, the use of volatile organic solvent (*e.g.* hexanes, chloroform, *etc.*) has also become a concern. From the perspective of green chemistry, normal phase chromatography is the least environmentally friendly scenario because of its inevitable consumption of volatile organic solvent although it is still commonly used in organic synthesis labs.

In the 1970s, NPC became increasingly less common because of the introduction of high performance reversed phase chromatography (RPC) which uses a relatively more polar/aqueous solvent combination. RPC acquired the name because of the opposite polarity for stationary phase and mobile phase compared with normal phase chromatography. For reversed phase chromatography, a less polar bonded phase (*e.g.* C₈ or C₁₈) and a more polar mobile phase is used. The mobile phase is in most cases a mixture of water and either acetonitrile (ACN) or methanol (MeOH), although other organic solvents such as tetrahydrofuran and isopropanol may also be used. It is known that separations by RPC are usually more efficient, reproducible and versatile. Fast equilibration of the column is generally observed after a change in mobile phase composition. Additionally, the solvents used for RPC are less flammable or volatile compared with those in NPC because of their higher polarity in general. All of those reasons contribute to the present popularity of RPC in analytical laboratories.

Despite the popularity of RPC, certain problems exist and require the advancement of this technology. Harmful organic solvents are still needed for reversed phase chromatography. Either methanol or acetonitrile is added to modify the polarity of the mobile phase. The volatile organic solvent consumption is substantial considering the broad application of HPLC in a variety of laboratories, such as pharmaceutical and environmental analysis. The concern also becomes more apparent seeing the increasingly stringent disposal standards, more significant disposal costs, and the acetonitrile shortage in 2009. Although some progress was made in replacing acetonitrile or methanol with other greener solvents, *e.g.* ethanol, water, the lack of more environmentally friendly solvents is still a major challenge for reversed phase chromatography.

Ion exchange chromatography (IEC) was a strong candidate for the analysis of organic acids and bases before the emergence of RPC s. Although IEC is not as popular as RPC s, IEC is indispensable due to its important applications in biomolecule analysis, two-dimensional separation, inorganic ion separation, *etc.* IEC separations are carried out on columns with ionized or ionizable groups attached to the stationary phase surface. For example, anion exchange columns for IEC might contain quaternary amine groups, or charged tertiary amine groups for the separation of anionic analytes. A salt gradient is usually applied to allow the competing ion to elute the retained ionic analyte. Because buffer solutions and/or salts are used, the eluent usually contains large amount of inorganic ions. Those permanent acids, bases and salts still require costly disposal processes.

Based on this knowledge, we hypothesize that greener chromatographic methods can be developed for both reversed phase and ion exchange chromatography. Both

chromatographic modes utilize significant portions of water in the mobile phase and we propose to use CO₂ to modify the pH of the mobile phases. In this way the stationary phase hydrophobicity and/or charge may be manipulated. An important advantage of using CO₂ is its switchable properties, which allows us to introduce CO₂ or remove CO₂ without leaving any residues in the solution.

1.3.2 Functional groups of columns

The column functionality determines the retention and selectivity of different modes of chromatographic separations. A summary of functional groups for typical chromatographic modes and their eluents are presented in Table 1.3. Reversed phase chromatography usually employs stationary phases with hydrophobic alkyl groups bonded to silica particles. In some cases, unmodified particles are the stationary phase, for example, unmodified silica is used in normal phase chromatography. Ion exchange chromatography has involved stationary phases containing charged ions such as quaternary amine groups for strong anion exchange chromatography (SAX), carboxylic acid and sulfonic acid groups for weak/strong cation exchange chromatography (WCX, SCX) respectively. Interestingly, some of those groups have also been used as CO₂-switchable groups as shown earlier in Table 1.2. For example, amine-functionalized stationary phase has been used for RPC, NPC and IEC at different conditions. Therefore, some of the commercial IEC columns have been tested for their switch of hydrophobicity / charge triggered by CO₂ (Chapter 3).

Table 1.3 Functional groups for typical liquid chromatography modes and eluents.

Separation Mode	Functional group	Typical eluent
NPC	Silica (-Si-OH) Amino (-NH ₂) Cyano (-CN)	Non-polar solvents (<i>e.g.</i> hexanes, chloroform)
RPC	Butyl (C4) Octyl (C8) Octadecyl (C18) Phenyl (-C ₆ H ₅) Cyano (-CN) Amino (-NH ₂)	Aqueous solution and polar organic solvents (<i>e.g.</i> acetonitrile, methanol)
IEC	SAX Quantenary amine (-N(CH ₃) ₃ ⁺)	Buffer solutions with salt
	WAX Tertiary amine (-NH(CH ₃) ₂ ⁺) Secondary amine (-NH ₂ (CH ₃) ⁺) Primary amine (-NH ₃ ⁺)	
	SCX Sulfonic acid (-SO ₃ ⁻)	
	WCX Carboxylic acid (-COO ⁻) Phosphonic acid (-HPO ₃ ⁻) Phenolic acid (-C ₆ H ₅ O ⁻)	Buffer solutions with salt

1.3.3 Effect of pH on retention

Before we investigate the effect of CO₂ on chromatographic separations, a thorough understanding of the effect of pH is necessary. The previous studies provide valuable knowledge and models that allow us to explore the possibilities of using CO₂. Specifically, pH has a profound effect on the retention and elution of compounds and it plays different roles in different chromatographic modes (*e.g.* RPC, IEC). The effect of pH in RPC and IEC conditions is discussed separately.

1.3.3.1 Effect of pH in RPC

Because reversed phase chromatography is the most widely used chromatographic technique, the effect of mobile phase pH in RPC has been thoroughly studied. The stationary phase of RPC usually contains non-polar groups that do not dissociate into ions.

As a result, pH has a much more marked effect on the analytes if they possess ionizable functional groups.

The retention of neutral compounds is usually independent of pH of the mobile phase, and is dependent upon the hydrophobicity of the compounds. The hydrophobicity is empirically evaluated by the partition coefficient ($\text{Log } K_{ow}$, or $\text{Log } P$) of a molecule between an aqueous (water) and lipophilic (octanol) phase. Because neutral compounds do not contain ionizable groups, they are relatively more hydrophobic than ionizable compounds, *e.g.* acid (HA) or base (B). Examples of neutral compounds include alkyl hydrocarbons, aromatic hydrocarbons, ketones, alcohols, ethers, *etc.*

When a compound contains acidic or basic groups, the retention of the compound is significantly affected by the dissociation of the compound. Uncharged molecules are generally more hydrophobic (*e.g.* HA, B), they are more strongly retained in RPC. Conversely, ionized molecules are more hydrophilic and less retained in RPC. Hypothetical acidic (carboxylic acid) and basic (aliphatic amine) samples are selected as examples. Depending on the dissociation of the acid or base, the retention as a function of pH is shown in Figure 1.8. The retention factor k in RPC can be reduced 10 fold or more if the molecule is ionized. The elution order of those two compounds may also be reversed depending on the pH of the mobile phase, as shown in a hypothetical chromatogram of HA and B in Figure 1.8 b.⁷⁹ An experimental investigation of the dependence of separation on pH is shown in Figure 1.9, for a group of compounds with varying acidity and basicity.⁸⁰ The compounds whose retention time increases as pH increases are bases (nicotine and methylamphetamine); those compounds whose retention time decreases as pH increases

are acids (salicylic acid and phenobarbitone); while the retention of phenacetin shows minimal change with pH because it is neutral or fully ionized over the pH change studied.

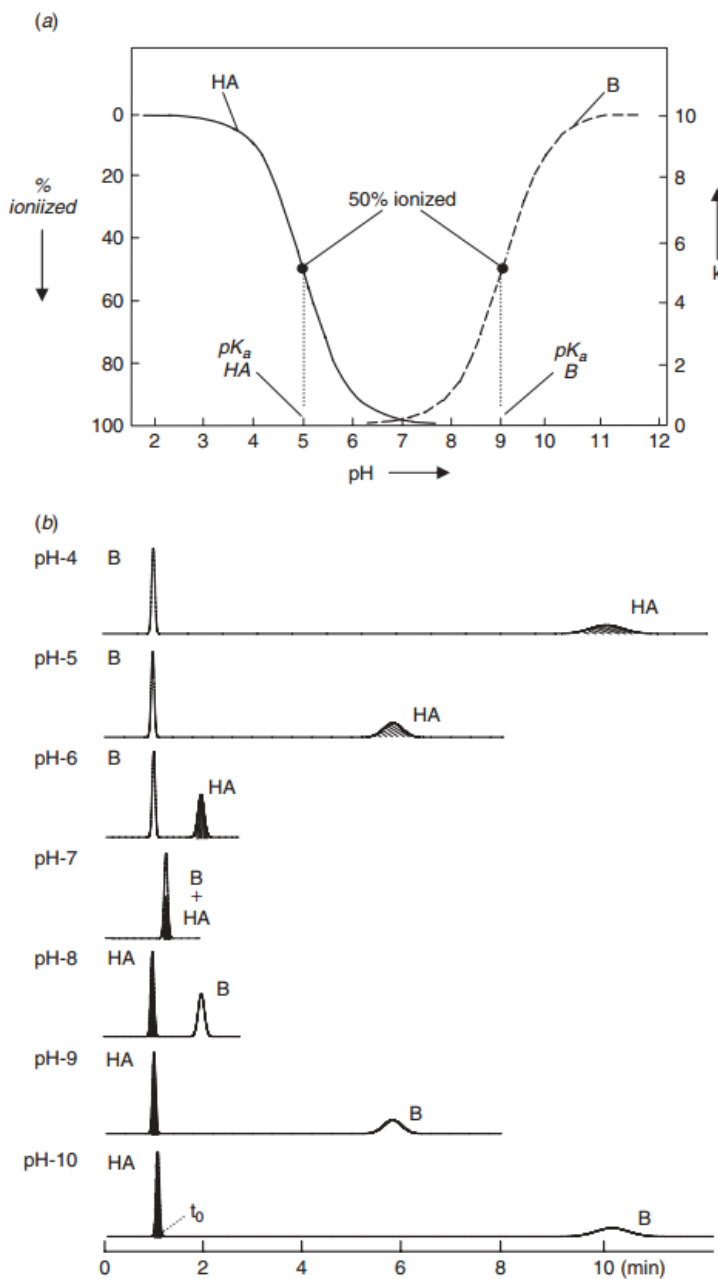


Figure 1.8 Hypothetical illustration of the RPC separation of an acidic compound HA from a basic compound B as a function of pH. (a) Ionization of HA and B as a function of mobile phase pH and effect on k. (b) separation as a function of mobile phase pH. Reprinted from reference⁷⁹ with permission. Copyright © 2010 by John Wiley & Sons, Inc.

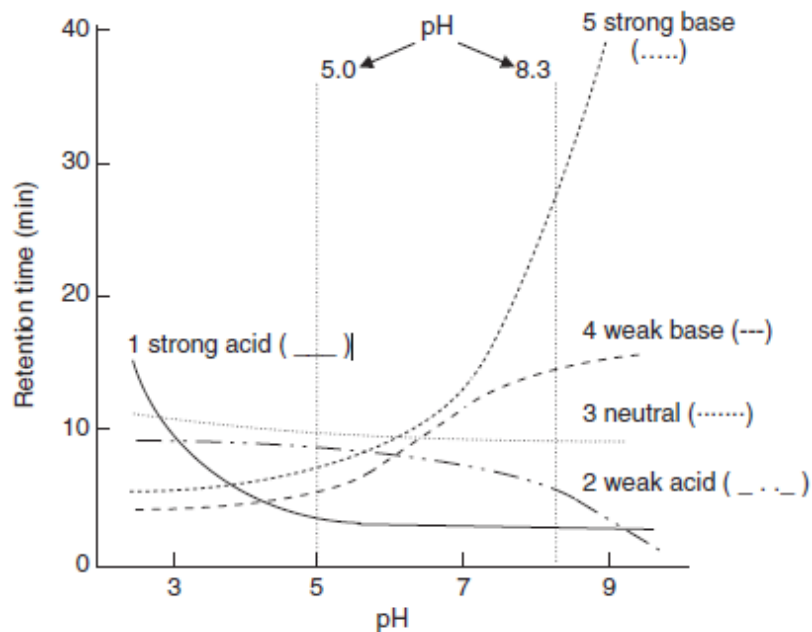


Figure 1.9 Effect of mobile-phase pH on RPC retention as a function of solute type. Sample: 1, salicylic acid; 2, phenobarbitone; 3, phenacetin; 4, nicotine; 5, methylamphetamine (shaded peak). Conditions for separations: 300 × 4.0-mm C18 column (10.0 μm particles); 40% methanol-phosphate buffer; ambient temperature; 2.0 mL/min. Reprinted from reference⁸⁰ with permission. Copyright © (1975) Elsevier.

Additionally, the retention of basic compounds may be substantially affected by the intrinsic silanol groups on the silica sphere support (less common in type-B silica), due to the electrostatic interactions. A more specific discussion regarding silanol groups and electrostatic interaction is presented in section 1.3.4.

1.3.3.2 Effect of pH in IEC

Before 1980, ion-exchange chromatography was commonly selected for the separation of acids and bases, although currently RPC has become the preferred technique for the separation of small, ionizable molecules (< 1000 Da). In the early days of HPLC,

ionic samples often presented problems for separation due to the lack of understanding of the behavior of the ionic species and limited availability of column packings.⁷⁹

As electrostatic interaction is involved in ion exchange, the effect of pH on IEC has to do with the dissociation of all the species involved considered in the chromatographic process. In appropriate pH ranges, the dissociation equilibria of the stationary phase group(s), competing ion, and solute ion may all significantly affect the retention and elution of a charged solute. To simplify the discussion, strong anion exchange chromatography is used as an example because strong anion exchangers are fully protonated over general pH ranges (2-12) and therefore their charge state is relatively constant. As a result, the effect of pH is generally subject to the change in the eluting power of the competing anion and the charge on the solute.

If a charged solute does not participate in the protolytic equilibria over the indicated pH range, the retention of the solute is solely affected by the dissociation of eluent. As shown in Figure 1.10, the capacity factor for anions (*e.g.* Cl⁻, Br⁻, I⁻) show a decrease as the eluent pH is raised because the negative charge on the phthalate eluent (pK_a 5.5) is increased. If a charged solute participates in the protolytic equilibria over the indicated pH range, the retention behaviour is more complicated because the protolytic equilibrium of eluent ion is also involved. As shown in Figure 1.10, dissociation of H₂PO₄⁻ leads to an increase in negative charge, in which case retention increases at higher pH, despite the presence of phthalate anions with stronger eluting power at higher pH values.⁸¹

Additionally, pH of the mobile phase may also affect the protolytic equilibrium of weak anion exchanger because the anion exchanger participates in the dissociation

equilibrium and therefore affect the retention of anions. For example, tertiary amine groups have a pK_{aH} value in the range of 9-11, a change in mobile phase pH around the mentioned range may cause the protonation / deprotonation of amine groups. Consequently, the retention with anions may be significantly affected.

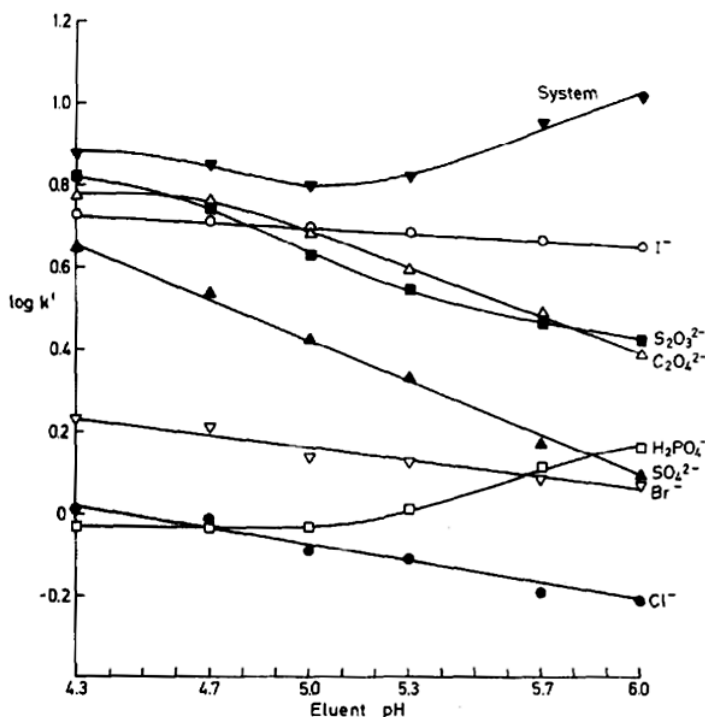


Figure 1.10 Retention data for inorganic anions in the pH range 4.3-6.0. A quaternary amine anion exchanger was used with 5.0 mM phthalate (pK_a 5.5) as eluent. Reprinted from reference⁸¹ with permission. Copyright © (1984) Elsevier.

1.3.4 Column supports

Important technical aspects of column supports are presented in this section, such as general advantages and disadvantages, preparation and functionalization routes, *etc.*

1.3.4.1 Porous polymer monolith

Back in the 1990s, some of the earliest work on porous polymer monoliths (PPM) was proposed by Hjertén, who initiated significant interest in macroporous polymer blocks

as a new class of separation media for liquid chromatography.⁸² This idea was later expanded by Svec and Fréchet, who published a number of papers and reviews exploring PPM materials, factors affecting their formation, various routes of material preparation, and applications.⁸³⁻⁸⁷

A number of factors such as an appropriate modification with functional groups, pore size adjustment and material durability have to be considered to design and prepare a satisfactory chromatographic column. The most technically straightforward method to incorporate the desired surface functionality is to co-polymerize a desired monomer with a cross-linker. Co-polymerization is well-developed for the preparation of functional polymer monoliths because of its synthesis simplicity. Many research papers have appeared using monolithic columns prepared directly from a functional monomer and a cross-linker.⁸⁸⁻⁹³ Disadvantages of copolymer monoliths result from a large amount of functional monomers are not present at the surface, instead, being buried and inaccessible within the bulk polymer.

Since the introduction of polymeric monolith columns, GMA has been used as a co-monomer in monolithic column preparations with varying modification reactions performed *in situ*.^{87, 94, 95} The epoxide groups of the polymerized glycidyl methacrylate are capable of reacting with amine groups. As a result, several researchers have used the reactive GMA group to modify a monolithic column for ion exchange^{87, 94-97} and affinity-based chromatographic separations.⁹⁸⁻¹⁰² Other reactive monomer such as 4-dimethyl-2-vinyl-2-oxazolin-5-one (VAL), and N-acryloxysuccinimide (NAS) can be incorporated

into the monolith matrix, which can be further modified to express a preferred surface chemistry.^{87, 103, 104}

Graft polymerization involves the growth of polymer moieties from the surface of a solid support, such as a polymeric monolithic column. Photo-initiated grafting offers enhanced flexibility relative to conventional co-polymerization of monomers.¹⁰⁵⁻¹¹⁰ Some photo-grafting techniques specifically use a single grafting step, i.e. initiator and monomer present simultaneously within the monolithic column. When a single grafting step is used, polymerization occurs not only from the monolith's surface as desired, but also in solution within the pores of the monolith.¹⁰⁵ As a result, solution localized polymerization can form a viscous gel, which may be difficult to remove. This method of monolith photo-grafting was improved by Stachowiak *et al.*, who employed a multi-step grafting procedure using benzophenone as an initiator.^{105, 111} The UV-irradiation procedure causes excitation of the electrons within the polymer, with consequential hydrogen abstraction from the polymer surface. The immobilization of the initiator to the monolith's surface occurs through photo-induced lysis, leaving a surface bound free radical. In the presence of monomers and subsequent UV exposure, the initiator is liberated from the surface, exposing the surface bound free radical for graft chain growth. For instance, a charged monomer 2-acrylamido-2-methyl-1-propanesulphonic acid (AMPS) and 4, 4-dimethyl-2-vinyl-2-oxazolin-5-one (VAL) was grafted to the surface of a generic poly(butyl methacrylate-co-ethylene dimethacrylate) monolithic column for ion exchange chromatography.¹⁰⁶

1.3.4.2 Silica spheres

Silica is the mostly widely used packing material for normal phase chromatography and reversed phase chromatography. Physical stability and well-defined pore structure are the major advantages of silica-based packings, although it has only limited stability beyond the pH range 2 - 8. Additionally, good chromatographic reproducibility and advanced efficiency established silica gel as a mainstream support for liquid chromatography.

Bonded stationary phases are usually made by covalently reacting an organosilane with the silanol on the surface of a silica particle. In our case, functionalization of silica gel beads was proposed to perform through a silanization reaction with organosilane reagents containing CO₂-switchable groups. For example, primary, secondary and tertiary amine bonded coupling agent such as (3-aminopropyl) triethoxysilane, trimethoxy[3-(methylamino)propyl] silane, and 3-(diethylamino) propyl trimethoxysilane can be used and they are all commercially available.

Depending on the ligands on stationary phase, as well as the solute structure and mobile phase composition, multiple retention mechanisms can be observed for a specifically designed stationary phase. A variety of interactions may be involved, such as hydrophobic interactions, steric exclusion, hydrogen bonding, electrostatic interactions, dipole-dipole interactions, and $\pi - \pi$ interactions. Depending on the purpose of the separation, some researchers have also developed mixed-mode chromatographic materials. For example, Chen *et al.* reported a polymer-modified silica stationary phase, which combines phenyl, quaternary ammonium and tertiary amine groups along with embedded polar functionalities in the dendritic shaped polymer, generating hydrophobic, electrostatic

and hydrophilic interaction (HILIC) domains simultaneously.¹¹² In this case, the modified silica was applied to the separation of basic, neutral and acidic compounds using reverse phase/anion exchange mode, as well as the separation of nucleosides under HILIC mode.

It is worth noting that, all the silanols on the support surface are not fully reacted due to the effect of steric hindrance. For example, a fully hydroxylated silica has a surface coverage of silanol groups $\approx 8.0 \mu\text{mol}/\text{m}^2$.⁷⁹ After a portion of the silanols are functionalized with silane reagents, further reaction is inhibited because of the formation of steric hindrance. The ligand concentration for a fully reacted packing will therefore seldom exceed $4.0 \mu\text{mol}/\text{m}^2$.⁷⁹ Due to the carryover of those silanol groups in reversed phase chromatography, basic analytes may interact with those leftover silanol groups and therefore affect chromatographic selectivity. If silica spheres are bonded with ionic ligands for ion exchange chromatography, the presence of silanol groups may also affect the selectivity in IEC.

1.3.5 Chromatographic parameters^{79, 113, 114}

1) Chromatographic selectivity

The selectivity of a reversed-phase separation is characterized (Synder model) via the following equation:

$$\text{Log } \alpha = \text{Log} \left(\frac{k}{k_{EB}} \right) = \eta' \cdot H + \sigma' \cdot S + \beta' \cdot A + \alpha' \cdot B + \kappa' \cdot C \quad (1.9)$$

In this case, α is the relative retention between a particular solute and the reference compound ethylbenzene, and the terms on the right-hand side describe the analyte properties in Greek letters and the corresponding column properties in capital letters. Thus,

H is the hydrophobicity of the packing, and η' is the hydrophobicity of the analyte. The first term describes the hydrophobicity contribution to the relative retention, the second term the contribution from the steric resistance to the insertion of the analyte into the stationary phase. A is the hydrogen-bond acidity of the stationary phase, which combines with the hydrogen-bond basicity β' of the analyte, while the term in B represents the hydrogen-bond basicity of the stationary phase and the hydrogen-bond acidity of the analyte. The last term reflects the ion-exchange properties of the packing which are attributed to the surface silanols and this term is pH dependent. HPLC columns can then be characterized by the parameters H , S , A , B , and C values at pH 3.0 and 7.0.

2) Retention factor

For a given solute, the retention factor k (capacity factor) is defined as the quantity of solute in the stationary phase (s), divided by the quantity in the mobile phase (m). The quantity of solute in each phase is equal to its concentration (C_s or C_m , respectively) times the volume of the phase (V_s or V_m , respectively). In practice, the retention factor is measured through this equation

$$k = \left(\frac{t_R}{t_0} \right) - 1 \quad (1.10)$$

Where: t_R is retention time of a specific solute, t_0 refers to as the column dead time.

3) Relative retention

The relative retention α is defined as the ratio of the retention factors of two compounds:

$$\alpha = \left(\frac{k_2}{k_1} \right) \quad (1.11)$$

4) Resolution

The chromatographic resolution of two peaks is defined as:

$$R = \frac{0.589 \Delta t_r}{w_{1/2av}} \quad (1.12)$$

Where: Δt_r is the difference in retention time between the two peaks, $w_{1/2av}$ is the average width of the two calculated peaks. For quantitative analysis, a resolution > 1.5 is highly desirable.

5) Tailing factor

Tailing factor (T_f) is calculated by

$$T_f = \frac{w_{0.05}}{2f} \quad (1.13)$$

Where: $w_{0.05}$ is the width of the peak at 5% peak height and f is the distance from the peak maximum to the fronting edge of the peak. A higher tailing factor value (e.g. $T_f > 3$) indicates less satisfactory peak shapes.¹¹⁵

1.4 Project outline

The primary objective of the thesis is to demonstrate environmentally friendly chromatographic techniques based on CO₂-switchable chemistry. Specifically, the main body of the thesis focuses on the demonstration of CO₂-switchable separations with a variety of column supports, such as polymer monolithic columns and silica columns.

Because porous polymer monoliths have the advantage of simple synthesis and functionalization, it was attempted first to examine its CO₂-switchable behaviour. A copolymer monolith, poly(dimethylaminoethyl methacrylate-co-ethylene glycol dimethacrylate) (poly(DMAEMA-co-EDMA)) was prepared and characterized in Chapter 2. It was found that, the copolymer monolithic column showed a slight change of retention time change triggered by acidic modifier (acetic acid). However, the chromatography with CO₂-modified solvents did not show reproducible and conclusive results, presumably due to the difficult control of CO₂ in the capillary LC columns. Potential reasons of the unsuccessful results are presented and used for alternative attempts for the objective of CO₂-switchable chromatography. Despite that, the effect of pH and temperature was explored on the poly(DMAEMA-co-EDMA) column for the separation of small organic molecules, because poly(dimethylaminoethyl methacrylate) (PDMAEMA) is a pH and thermo-responsive polymer. The presence of tertiary amine groups in the copolymer also suggest the possibility of performing ion exchange chromatography on this column. We show the effective separation of protein samples on a column in ion exchange mode.

In chapter 3, commercially available columns are used to test the concept of CO₂-switchable chromatography, because the off-the-shelf columns are well characterized and tested. A prototype set-up is assembled, to introduce gaseous carbon dioxide into HPLC, so that reliable supply of CO₂ can be delivered from CO₂ cylinder to solvent reservoir and to the HPLC system. The operational parameters of the custom CO₂ system are optimized, such as CO₂ flow rate, sparging frit type, mixing ratios, *etc.* Commercial columns containing diethylaminoethyl, polyethylenimine, and carboxymethyl groups are tested individually for their separation performance and capability using CO₂-modified solvents.

Based on the discovery and questions raised from the proof-of-concept study, another extensive study was conducted. The study in Chapter 4 focuses on addressing these goals: 1) improve separation efficiency and extend the application; 2) investigate the separation behaviour of primary amine, secondary amine, and tertiary amine functionalized column; 3) demonstrate the effect of pH / CO₂ on electrostatic interaction. Pharmaceutical compounds containing carboxylic acid groups were effectively separated using only carbonated water as the mobile phase.

The objective of the work in chapter 5 was to develop a polymer monolith surface with CO₂ triggered switchable wettability / adhesion and to use those switchable surfaces for stimuli-responsive microarrays. Template synthesis of porous polymer monolith is described, followed by photografting with stimuli-responsive polymers. The effect of different polymerization conditions presented, regarding the selection of generic polymer and functional monomer, characterization of the “top” and the “bottom” plates of the template. Water contact angles and hysteresis were measured as the evaluation of surface wettability and adhesion. Droplets with different pH values were dispensed on the surfaces and surface wettability was characterized. After characterizing the surfaces, the most promising grafted switchable surface coating was identified and those studies hold great importance for developing applications of the material.

1.5 References

1. P. T. Anastas and J. C. Warner, *Green chemistry: theory and practice*, Oxford university press, 2000.
2. C. Annex, Stockholm Convention on Persistent Organic Pollutants, <http://chm.pops.int/Portals/0/Repository/poprc4/UNEP-POPS-POPRC.4-14.English.PDF> (accessed Aug 30th, 2017).
3. J. G. Anderson, D. W. Toohey and W. H. Brune, *Science*, 1991, **251**, 39-46.
4. S. Solomon, D. J. Ivy, D. Kinnison, M. J. Mills, R. R. Neely, 3rd and A. Schmidt, *Science*, 2016, **353**, 269-274.
5. M. Koel and M. Kaljurand, *Green analytical chemistry*, Royal Society of Chemistry, 2015.
6. P. T. Anastas, *Crit Rev Anal Chem*, 1999, **29**, 167-175.
7. A. Gąluszka, Z. Migaszewski and J. Namieśnik, *Trac-Trend Anal Chem*, 2013, **50**, 78-84.
8. L. H. Keith, L. U. Gron and J. L. Young, *Chem Rev*, 2007, **107**, 2695-2708.
9. M. Tobiszewski, A. Mechlinska and J. Namiesnik, *Chem Soc Rev*, 2010, **39**, 2869-2878.
10. M. Koel, *Green Chem*, 2016, **18**, 923-931.
11. M. de la Guardia and S. Garrigues, *Handbook of green analytical chemistry*, John Wiley & Sons, 2012.
12. A. I. Olives, V. Gonzalez-Ruiz and M. A. Martin, *Acs Sustain Chem Eng*, 2017, **5**, 5618-5634.
13. C. J. Welch, N. J. Wu, M. Biba, R. Hartman, T. Brkovic, X. Y. Gong, R. Helmy, W. Schafer, J. Cuff, Z. Pirzada and L. L. Zhou, *Trac-Trend Anal Chem*, 2010, **29**, 667-680.
14. Y.-N. Hsieh, P.-C. Huang, I.-W. Sun, T.-J. Whang, C.-Y. Hsu, H.-H. Huang and C.-H. Kuei, *Anal Chim Acta*, 2006, **557**, 321-328.
15. D. W. Potter and J. Pawliszyn, *Environ Sci Technol*, 1994, **28**, 298-305.
16. V. Camel, *Analyst*, 2001, **126**, 1182-1193.

17. M. De Melo, A. Silvestre and C. Silva, *J Supercrit Fluid*, 2014, **92**, 115-176.
18. C. S. Eskilsson and E. Bjorklund, *J Chromatogr A*, 2000, **902**, 227-250.
19. K. Vilku, R. Mawson, L. Simons and D. Bates, *Innov Food Sci Emerg*, 2008, **9**, 161-169.
20. A. Arora, G. Simone, G. B. Salieb-Beugelaar, J. T. Kim and A. Manz, *Anal Chem*, 2010, **82**, 4830-4847.
21. C. Dietze, S. Schulze, S. Ohla, K. Gilmore, P. H. Seeberger and D. Belder, *Analyst*, 2016, **141**, 5412-5416.
22. M. L. Nelson, M. M. Jared, H. C. N. Alphonsus, S. Brendon, S. Neil and R. W. Aaron, *Anal Chem*, 2015, **87**, (7), 3902-3910.
23. C. Liu, K. Choi, Y. Kang, J. Kim, C. Fobel, B. Seale, J. L. Campbell, T. R. Covey and A. R. Wheeler, *Anal Chem*, 2015, **87**, 11967-11972.
24. N. S. Mei, B. Seale, A. H. C. Ng, A. R. Wheeler and R. Oleschuk, *Anal Chem*, 2014, **86**, 8466-8472.
25. J. P. Grinias and R. T. Kennedy, *Trac-Trend Anal Chem*, 2016, **81**, 110-117.
26. G. Desmet and S. Eeltink, *Anal Chem*, 2013, **85**, 543-556.
27. P. Pruijm, P. J. Schoenmakers and W. T. Kok, *Chromatographia*, 2012, **75**, 1225-1234.
28. J. P. Kutter, *J Chromatogr A*, 2012, **1221**, 72-82.
29. N. V. Lavrik, L. T. Taylor and M. J. Sepaniak, *Anal Chim Acta*, 2011, **694**, 6-20.
30. D. S. Sholl and R. P. Lively, *Nature*, 2016, **532**, 435-437.
31. R. E. Majors, *LCGC North Am*, 2012, **25**, 31-39.
32. C.-Y. Lu, in *Handbook of Green Analytical Chemistry*, John Wiley & Sons, Inc., 2012, p. 175-198.
33. H. Shaaban and T. Gorecki, *Talanta*, 2015, **132**, 739-752.
34. P. Sandra, G. Vanhoenacker, F. David, K. Sandra and A. Pereira, *LCGC Eur*, 2010, **23**, 242-259
35. K. Hartonen and M. L. Riekkola, *Trac-Trend Anal Chem*, 2008, **27**, 1-14.

36. C. J. Welch, T. Brkovic, W. Schafer and X. Gong, *Green Chem*, 2009, **11**, 1232-1238.
37. R. L. Ribeiro, C. B. Bottoli, K. E. Collins and C. H. Collins, *J Brazil Chem Soc*, 2004, **15**, 300-306.
38. C. Capello, U. Fischer and K. Hungerbühler, *Green Chem*, 2007, **9**, 927-934.
39. Y. Cui and S. V. Olesik, *J Chromatogr A*, 1995, **691**, 151-162.
40. M. C. Beilke, M. J. Beres and S. V. Olesik, *J Chromatogr A*, 2016, **1436**, 84-90.
41. T. S. Reighard and S. V. Olesik, *J Chromatogr A*, 1996, **737**, 233-242.
42. Y. Cui and S. V. Olesik, *Anal Chem*, 1991, **63**, 1812-1819.
43. S. T. Lee and S. V. Olesik, *Anal Chem*, 1994, **66**, 4498-4506.
44. A. K. Kota, G. Kwon, W. Choi, J. M. Mabry and A. Tuteja, *Nat Commun*, 2012, **3**, 1025.
45. M. A. Stuart, W. T. Huck, J. Genzer, M. Muller, C. Ober, M. Stamm, G. B. Sukhorukov, I. Szleifer, V. V. Tsukruk, M. Urban, F. Winnik, S. Zauscher, I. Luzinov and S. Minko, *Nat Mater*, 2010, **9**, 101-113.
46. M. F. X. Lee, E. S. Chan, K. C. Tam and B. T. Tey, *J Chromatogr A*, 2015, **1394**, 71-80.
47. K. Nagase, M. Kumazaki, H. Kanazawa, J. Kobayashi, A. Kikuchi, Y. Akiyama, M. Annaka and T. Okano, *ACS Appl Mater Interfaces*, 2010, **2**, 1247-1253.
48. N. Li, L. Qi, Y. Shen, Y. Li and Y. Chen, *ACS Appl Mater Interfaces*, 2013, **5**, 12441-12448.
49. E. C. Peters, F. Svec, J. M. J. Frechet, US5929214, 1999.
50. K. Nagase, J. Kobayashi, A. Kikuchi, Y. Akiyama, H. Kanazawa and T. Okano, *ACS Appl Mater Interfaces*, 2013, **5**, 1442-1452.
51. H. Kanazawa, *J Sep Sci*, 2007, **30**, 1646-1656.
52. Y. Shen, L. Qi, X. Y. Wei, R. Y. Zhang and L. Q. Mao, *Polymer*, 2011, **52**, 3725-3731.
53. M. R. Islam, Z. Lu, X. Li, A. K. Sarker, L. Hu, P. Choi, X. Li, N. Hakobyan and M. J. Serpe, *Anal Chim Acta*, 2013, **789**, 17-32.

54. R. A. Lorenzo, A. M. Carro, A. Concheiro and C. Alvarez-Lorenzo, *Anal Bioanal Chem*, 2015, **407**, 4927-4948.
55. R. Peierantozzi, Carbon Dioxide. Kirk-Othmer Encyclopedia of Chemical Technology, John Wiley & Sons, Inc., 2000.
56. K. Anton and C. Berger, *Supercritical Fluid Chromatography with Packed Columns - Techniques and Applications*, MARCEL DEKKER, Inc., New York, NY, 1997.
57. S. M. Mercer, Ph.D. thesis, Queen's University, 2012.
58. Chemicalize - Instant Cheminformatics Solutions., <http://chemicalize.com/#/calculation> (accessed April 17th, 2017).
59. L. Irving, *J Biol Chem*, 1925, **63**, 767-778.
60. X. Yuan, E. G. Kim, C. A. Sanders, B. E. Richter, M. F. Cunningham, P. G. Jessop and R. D. Oleschuk, *Green Chem*, 2017, **19**, 1757-1765.
61. J. B. Levy, F. M. Hornack and M. A. Levy, *J. Chem. Educ.*, 1987, **64**, 260-261.
62. A. Darabi, P. G. Jessop and M. F. Cunningham, *Chem Soc Rev*, 2016, **45**, 4391-4436.
63. J. Durelle, J. R. Vanderveen and P. G. Jessop, *Physical chemistry chemical physics : PCCP*, 2014, **16**, 5270-5275.
64. J. R. Vanderveen, J. Durelle and P. G. Jessop, *Green Chem*, 2014, **16**, 1187-1197.
65. K. J. Boniface, R. R. Dykeman, A. Cormier, H. B. Wang, S. M. Mercer, G. J. Liu, M. F. Cunningham and P. G. Jessop, *Green Chem*, 2016, **18**, 208-213.
66. X. Su, P. G. Jessop and M. F. Cunningham, *Green Materials*, 2014, **2**, 69-81.
67. J. Durelle, J. R. Vanderveen, Y. Quan, C. B. Chalifoux, J. E. Kostin and P. G. Jessop, *Physical chemistry chemical physics : PCCP*, 2015, **17**, 5308-5313.
68. P. G. Jessop, *Aldrichim Acta*, 2015, **48**, 18-21.
69. A. M. Ross, H. Nandivada and J. Lahann, *Handbook of Stimuli-responsive Materials*, Wiley-VCH, Weinheim, M.W. Urban ed., 2011.
70. V. C.T., *Modern Drug Discovery*, 2001, 49-52.
71. P. G. Jessop, L. Phan, A. Carrier, S. Robinson, C. J. Durr and J. R. Harjani, *Green Chem*, 2010, **12**, 809-814.

72. P. G. Jessop, L. Kozycz, Z. G. Rahami, D. Schoenmakers, A. R. Boyd, D. Wechsler and A. M. Holland, *Green Chem*, 2011, **13**, 619-623.
73. A. R. Boyd, P. Champagne, P. J. McGinn, K. M. MacDougall, J. E. Melanson and P. G. Jessop, *Bioresour Technol*, 2012, **118**, 628-632.
74. P. G. Jessop, S. M. Mercer and D. J. Heldebrant, *Energ Environ Sci*, 2012, **5**, 7240-7253.
75. A. Holland, D. Wechsler, A. Patel, B. M. Molloy, A. R. Boyd and P. G. Jessop, *Can J Chem*, 2012, **90**, 805-810.
76. C. Samorì, D. López Barreiro, R. Vet, L. Pezzolesi, D. W. F. Brilman, P. Galletti and E. Tagliavini, *Green Chem*, 2013, **15**, 353-356.
77. S. Kumar, X. Tong, Y. L. Dory, M. Lepage and Y. Zhao, *Chem Commun*, 2013, **49**, 90-92.
78. G. Q. Yu, Y. Y. Lu, X. X. Liu, W. J. Wang, Q. W. Yang, H. B. Xing, Q. L. Ren, B. G. Li and S. P. Zhu, *Ind Eng Chem Res*, 2014, **53**, 16025-16032.
79. L. R. Snyder, J. J. Kirkland and J. W. Dolan, *Introduction to Modern Liquid Chromatography*, A John Wiley & Sons Inc., Hoboken, NJ, 3rd ed., 2009.
80. P. J. Twitchett and A. C. Moffat, *J Chromatogr*, 1975, **111**, 149-157.
81. P. R. Haddad and C. E. Cowie, *J Chromatogr*, 1984, **303**, 321-330.
82. S. Hjerten, J. L. Liao and R. Zhang, *J Chromatogr A*, 1989, **473**, 273-275.
83. Q. C. Wang, F. Svec and J. M. J. Frechet, *Anal Chem*, 1993, **65**, 2243-2248.
84. F. Svec and J. M. Frechet, *Science*, 1996, **273**, 205-211.
85. F. Svec and J. M. J. Frechet, *Macromolecules*, 1995, **28**, 7580-7582.
86. F. Svec and J. M. J. Frechet, *Chem Mater*, 1995, **7**, 707-715.
87. F. Svec and J. M. J. Frechet, *Anal Chem*, 1992, **64**, 820-822.
88. Z. Liu, Y. Peng, T. Wang, G. Yuan, Q. Zhang, J. Guo and Z. Jiang, *J Sep Sci*, 2013, **36**, 262-269.
89. Z. Jiang, N. W. Smith, P. D. Ferguson and M. R. Taylor, *J Sep Sci*, 2009, **32**, 2544-2555.

90. Z. Jiang, N. W. Smith, P. D. Ferguson and M. R. Taylor, *Anal Chem*, 2007, **79**, 1243-1250.
91. Z. Jiang, J. Reilly, B. Everatt and N. W. Smith, *J Chromatogr A*, 2009, **1216**, 2439-2448.
92. P. Jandera, M. Stankova, V. Skerikova and J. Urban, *J Chromatogr A*, 2013, **1274**, 97-106.
93. M. Stankova, P. Jandera, V. Skerikova and J. Urban, *J Chromatogr A*, 2013, **1289**, 47-57.
94. J. P. Hutchinson, E. F. Hilder, R. A. Shellie, J. A. Smith and P. R. Haddad, *Analyst*, 2006, **131**, 215-221.
95. D. Sykora, F. Svec and J. M. Frechet, *J Chromatogr A*, 1999, **852**, 297-304.
96. I. N. Savina, I. Y. Galaev and B. Mattiasson, *J Mol Recognit*, 2006, **19**, 313-321.
97. D. Schaller, E. F. Hilder and P. R. Haddad, *J Sep Sci*, 2006, **29**, 1705-1719.
98. Q. Luo, H. Zou, X. Xiao, Z. Guo, L. Kong and X. Mao, *J Chromatogr A*, 2001, **926**, 255-264.
99. Z. Pan, H. Zou, W. Mo, X. Huang and R. Wu, *Anal Chim Acta*, 2002, **466**, 141-150.
100. R. Mallik and D. S. Hage, *J Sep Sci*, 2006, **29**, 1686-1704.
101. L. P. Erika, P. Marie Laura, M. D. Courtney and S. H. David, *Anal Bioanal Chem*, 2012, **405**, 2133-2145.
102. E. L. Pfaunmiller, M. L. Paulemond, C. M. Dupper and D. S. Hage, *Anal Bioanal Chem*, 2013, **405**, 2133-2145.
103. T. Mohammad, R. D. Arrua, G. Andras, A. L. Nathan, W. Qian, R. H. Paul and F. H. Emily, *Anal Bioanal Chem*, 2012, **405**, 2233-2244.
104. H. Wang, J. Ou, H. Lin, Z. Liu, G. Huang, J. Dong and H. Zou, *J Chromatogr A*, 2014, **1367**, 131-140.
105. T. B. Stachowiak, F. Svec and J. M. J. Fréchet, *Chem Mater*, 2006, **18**, 5950-5957.
106. T. Rohr, E. F. Hilder, J. J. Donovan, F. Svec and J. M. J. Frechet, *Macromolecules*, 2003, **36**, 1677-1684.

107. S. Currvivan, D. Connolly and B. Paull, *J Sep Sci*, 2015, **38**, 3795-3802.
108. R. J. Vonk, S. Wouters, A. Barcaru, G. Vivó-Truyols, S. Eeltink, L. J. de Koning and P. J. Schoenmakers, *Anal Bioanal Chem*, 2015, **407**, 3817-3829.
109. C. Lianfang, O. Junjie, L. Zhongshan, L. Hui, W. Hongwei, D. Jing and Z. Hanfa, *J Chromatogr A*, 2015, **1394**, 103-110.
110. Z. P. Xu and R. D. Oleschuk, *Electrophoresis*, 2014, **35**, 441-449.
111. T. B. Stachowiak, D. A. Mair, T. G. Holden, L. J. Lee, F. Svec and J. M. J. Fréchet, *J Sep Sci*, 2007, **30**, 1088-1093.
112. Y. Li, J. Yang, J. Jin, X. Sun, L. Wang and J. Chen, *J Chromatogr A*, 2014, **1337**, 133-139.
113. D. C. Harris, *Quantitative Chemical Analysis*, W.H. Freeman and Company, NY, 8th ed. edn., 2009.
114. U. D. Neue, *HPLC Columns: Theory, Technology, and Practice*, Wiley-VCH, 1997.
115. J. W. Dolan, *LCGC North Am*, 2003, **21**, 612-616.

Chapter 2 Chromatographic characteristics of a DMAEMA-co-EDMA polymeric monolithic column

2.1 Introduction

In classic chromatographic separations, elutropic strength is typically manipulated through the change of mobile phase composition. For example, reversed phase chromatography uses a change in organic phase composition to alter the retention time of analytes. In normal phase chromatography the polarity of the mobile phase is controlled by adjusting the composition of solvent mixtures. However, the hydrophobicity and charge state change of stationary phase materials have been barely explored. The concept of “stimuli-responsive stationary phases” has been raised in the past decade, where the stationary phase itself can have its properties altered during the chromatographic run while the mobile phase composition remains relatively constant.¹⁻⁶ Because the property of the stationary phase may be selectively manipulated, the conventional binary mixture of the mobile phase may be replaced by other solvent systems, a temperature gradient, pH gradient, *etc.*⁷⁻⁹ Therefore, stimuli-responsive stationary phases hold great potential of reducing the consumption of harmful organic solvents while also providing an alternative chromatographic mechanism.

The significant interest in stimuli-responsive stationary phases has been facilitated by the substantial advances in stimuli-responsive materials. Advances in polymer chemistry and surface chemistry allow for the preparation of various smart, or stimuli-responsive materials (pH, temperature, light responsive, *etc.*).¹⁰⁻¹⁴ Stimuli-responsive groups are typically incorporated on various chromatographic supports (*e.g.* silica,

monolith) as stimuli-responsive stationary phase groups. Functionalization of silica particles with stimuli-responsive polymers has been previously studied, using different grafting approaches. Nagase *et al.* reported the thermo-responsive poly(N-isopropylacrylamide-co-n-butyl methacrylate) (poly(IPAAm-co-BMA)) brush surfaces on silica spheres through surface-initiated atom transfer radical polymerization (ATRP).¹⁵ Manipulation of the hydrophobic interaction at various temperatures was demonstrated using a group of benzoic acid and phenol compounds. Recently, Sepehrifar *et al.* reported the utilization of poly(2-dimethyl-aminoethyl methacrylate)-block-poly(acrylic acid) (PDMAEMA-b-PAA) grafted silica spheres as stimuli-responsive separation media at various temperature, ionic strength and pH conditions.^{16, 17} Silica spheres are considered more advantageous for the separation of small molecules because of their higher surface area. However, although silica spheres are the most commonly used packing materials, they have disadvantages that limit their capability. Packing of silica spheres in micro LC and nano LC columns is technically challenging. Silica particles are also susceptible to hydrolysis at low pH (< 2.0) and high pH (> 8.0). Alternatively, polymer monolithic supports have the potential to be *in situ* synthesized and they are durable over a wider pH range (1.0 – 13.0).

Stimuli-responsive polymer monoliths were demonstrated as alternative separation media via the incorporation of functional monomers/polymers. Shen *et al.* reported the preparation of poly(2-(dimethylamino)ethyl methacrylate) (PDMAEMA) brushes on the monolithic surface via two-step ATRP.¹⁸ Li *et al.* demonstrated all aqueous chromatography using thermo-responsive oligo(ethylene glycol)-based polymer brushes on polymer monoliths.¹⁹ However, in those previous studies, the separation performance

of the stimuli-responsive columns was not satisfactory and there was no direct evidence showing the advantage of using ATRP for the PPM preparation.²⁰ Additionally, because DMAEMA also contains tertiary amine groups that are considered potential CO₂-switchable groups, we proposed that a copolymer DMAEMA-co-EDMA monolith might be prepared for the investigation of CO₂-switchable chromatography. Because poly(DMAEMA) is a weakly basic polymer exhibiting stimuli-responsive behaviour triggered by a change in pH or temperature, a further investigation of different pH and temperature conditions was performed. Furthermore, because of the introduction of ionizable groups on DMAEMA, the column was also used for ion exchange chromatography of bio-molecules.

In brief, this chapter addresses the following topics: 1) the preparation and characterization of copolymer monolith; 2) CO₂-switchability of the copolymer column; 3) effect of temperature and pH on the chromatography; 4) ion exchange chromatography using the copolymer column.

2.2 Experimental

2.2.1 Materials

Chemicals such as glacial acetic acid, formic acid, ammonium hydroxide, 2-propanol, 1,4-butanediol, and HPLC grade acetonitrile were acquired from Fisher Scientific (Nepean, ON, Canada). To prepare the polymer monolith, 3-(trimethoxysilyl) propyl methacrylate (γ -MAPS), dimethylaminoethyl methacrylate (DMAEMA), ethylene glycol dimethacrylate (EDMA), and 2, 2'-azobis (2-methylpropionitrile) (AIBN) were acquired from Sigma-Aldrich (Milwaukee, WI, USA). Ultrapure water was prepared from

a Milli-Q system (Bedford, MA, USA). All analytes involved were acquired from Sigma-Aldrich (Milwaukee, WI, USA).

2.2.2 Preparation of polymer monolith columns

The column formation process has been described in our previous work with some modified conditions.^{21, 22} Briefly, fused silica capillary (100 μm I.D., 360 μm O.D. Polymicro Technologies; Phoenix, AZ) was employed as a vessel for the monoliths. Prior to polymerization, the inner wall of the capillary was pretreated with a solution of 3-(trimethoxysilyl)propyl methacrylate, water, and glacial acetic acid (20:50:30; volume percentage unless otherwise stated) to functionalize them with vinyl groups (facilitating monolith polymer attachment). A syringe (3.0 mL Monoject, Covidien Canada) was attached to the capillary via a Female Luer to 10-32 Female adapter (P-629, IDEX Health and Science), a Fingertight 10-32 Coned PEEK fitting (F-120), and a NanoTight Sleeve (F-242, 1/16 O.D., 0.0155' I.D.). Afterwards, the capillary was filled with the pretreatment mixture via syringe pump (Pico Plus, Harvard Apparatus, Holliston, MA, USA) at a flow rate of 0.50 $\mu\text{L min}^{-1}$ for 12 hours. The pretreated capillary was then thoroughly rinsed with water and acetonitrile and dried with a stream of nitrogen. Following, a PPM polymerization mixture comprising initiator (AIBN, 2.5 mg mL^{-1}), monomer (DMAEMA), crosslinker (EDMA), porogenic solvents was introduced into the capillary with a syringe pump at a flow rate of 5.0 $\mu\text{L min}^{-1}$. Detailed composition of the polymerization mixture is shown in Table 2.1 and Table 2.2. Gas chromatography septa (Supelco, Thermogreen, 9.5 mm, Bellefonte, PA, USA) were used to seal the capillary at each end. Then, the sealed capillary was left in the oven at 60 $^{\circ}\text{C}$ for 12 hours, then 80 $^{\circ}\text{C}$ for 2 hours.

Table 2.1 Compositions of the polymerization mixture for poly(DMAEMA-co-EDMA) monolithic column with varying ratios of monomer / crosslinker.

Sample	Reagent composition (μL)				
	DMAEMA	EDMA	Water	2-Propanol	1,4-Butanediol
A1	50	200	75	450	225
A2	75	175	75	450	225
A3	100	150	75	450	225

Table 2.2 Compositions of the polymerization mixture for poly(DMAEMA-co-EDMA) monolithic column with varying amounts of 2-propanol and 1,4-butanediol.

Sample	Reagent composition (μL)				
	DMAEMA	EDMA	Water	2-Propanol	1,4-Butanediol
B1	200	50	75	450	225
B2	200	50	75	465	210
B3	200	50	75	480	195
B4	200	50	75	495	180

Following polymerization, the septa were removed. Both ends of the capillary were trimmed off 1.0 cm, and the capillary column was flushed with 95.0% ACN in water using an HPLC pump (Water NanoAcquity UPLC) to remove the remaining polymerization solvent mixture. The columns are ready for use thereafter. A parallel polymerization

reaction is performed in a 3.0 mL syringe, allowing for enough material for further material characterization. In order to prepare a polymer monolith with appropriate permeability, the morphology of the polymer monolith was examined with scanning electron microscopy. The backpressure of the columns was also measured so that an optimal monolithic column can be selected. Additionally, attenuated total reflection infrared spectroscopy (ATR-IR) was used to characterize the prepared polymer material.

2.2.3 Chromatographic conditions

The individual analyte in Table 2.3 was dissolved in acetonitrile at a concentration of 5.0 mg mL⁻¹ as the stock solution. The stock solutions were diluted accordingly in 80:20 water/acetonitrile in sample vials for chromatographic analysis. For example, naphthalene is diluted 100 times, which corresponds to a concentration of 50 µg mL⁻¹. For the compound mixture used in section 2.3.2, the concentrations of benzene, naphthalene and anthracene were 0.10 mg mL⁻¹, 50 µg mL⁻¹ and 20 µg mL⁻¹, respectively. For the compound mixture used in section 2.3.3 and 2.3.4, the concentrations of 4-butylaniline, phenanthrene and ketoprofen were 0.50 mg mL⁻¹, 50 µg mL⁻¹, and 20 µg mL⁻¹, respectively. Protein samples in Table 2.4 were prepared by dissolving them in 10 mM Tris buffer solution (pH 7.6). For the protein mixture used in section 2.3.5, the concentrations of myoglobin, transferrin and bovine serum albumin were all 5.0 mg mL⁻¹.

A Waters NanoAcquity UHPLC was used for the capillary liquid chromatography. The NanoAcquity is equipped with a binary solvent manager with the capability of solvent delivery as low as 100 nL min⁻¹, a sample manager module with 2 µL sample loop used in the experiments, and a tunable UV detector with a 10 nL flow cell. Firstly, the custom PPM

column (10.0 cm) was connected with the outlet port on the switching valve of the sample manager. Afterwards, the capillary column was connected with a capillary tubing towards UV detector inlet through a Teflon sleeve tubing (0.01" I.D., 186002690), so that minimal dead volume is introduced. UV detection was used at wavelength 254 nm for the organic compounds in Table 2.3 and 214 nm for the protein sample in Table 2.4. The injection volume was 2.0 μL . A column diameter of 100 μm was used for the experiments in section 2.3.2-2.3.4, at a mobile phase flow rate 1.0 $\mu\text{L}/\text{min}$. It was found that peak tailing was very significant for this column if protein samples were introduced, therefore, a column diameter of 200 μm was used for the experiments in section 2.3.5 for protein analysis, at a mobile phase flow rate 4.0 $\mu\text{L}/\text{min}$. Column temperature was controlled in a column compartment affiliated with the sample manager.

Table 2.3 List of organic compounds used for the reversed phase chromatography with polymer monolithic column.

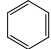
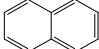
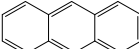
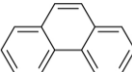
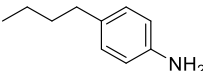
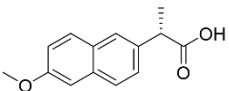
Analyte	Structure	<i>Log P</i>	<i>pK_a</i> (<i>pK_{atH}</i>)
Benzene		2.0	-
Naphthalene		3.0	-
Anthracene		4.0	-
Phenanthrene		4.0	-
4-Butylaniline		3.0	4.9
Ketoprofen		3.6	3.9

Table 2.4 List of proteins used for the ion exchange chromatography with the polymer monolithic column. Theoretical *pI* was calculated using ExPasy.²³

Protein sample	UniProtKB ID	Theoretical <i>pI</i>	MW (kDa)
Myoglobin horse heart	P68082	7.2	17
Transferrin human	P02787	6.8	77
Bovine serum albumin	P02769	5.8	66

2.2.4 Mobile phase preparation

A gradient method using water (A) and acetonitrile (B) was first developed to effectively separate the three neutral compounds. Acidic modifier (acetic acid, 0.05%) was first added in both water and acetonitrile to generate acidic mobile phases. The retention time of modifier-free and acid-modified conditions was compared to confirm the effect of pH on retention time. Afterwards, gaseous CO₂ was introduced into the water bottle to generate carbonated water (1 bar). The same gradient was used again to investigate the effect of CO₂ on retention time. In particular, a CO₂ delivery system was used, which contains a CO₂ cylinder, a two-stage regulator, a flow gauge and a sparging tube submerged in the water reservoir.

Acid and base were also used as mobile phase modifiers in section 2.3.3 to investigate the effect of pH on the separation of neutral, acidic and basic compounds. Both water (A) and acetonitrile (B) were modified with either glacial acetic acid (0.05%, v/v) or ammonium hydroxide (0.05%, v/v).

Tris buffer was used in ion exchange separations in section 2.3.5. In particular, 1.211 g (10 mM) tris(hydroxymethyl)aminomethane was dissolved in 1 L deionized water. The pH of the tris buffer was adjusted to pH 7.6 using 1 M HCl. Afterwards, the 10 mM tris buffer was used as the buffer A. Buffer B was prepared by adding 1 M NaCl (58.44 g for 1 L) in buffer A.

2.3 Results and Discussion

2.3.1 Column preparation and characterization

The free radical polymerization process allows one to control several variables that enable the preparation of monoliths with different properties. These variables include choice of monomers, cross-linkers, porogens, polymerization time and temperature, *etc.*²⁴ However, it remains a major challenge to independently control the morphology/properties of the monolith such as, the size of throughpores, permeability of the polymer monolith, density of functional groups, *etc.* A miniscule change in composition of the polymerization mixture may lead to a significant change in column permeability.²⁵ For example preparing a monolith using a 59.3:40.7 (v/v) methanol/dodecanol mixture as the porogenic solvent in a 10 cm × 75 μm I.D. capillary produced a column that was barely permeable, with a backpressure of 22 MPa at a flow rate of only 300 nL/min. In contrast, a porogen with a 66.5:33.5 ratio produced a column exhibiting at the same flow rate a backpressure of only 0.24 MPa indicating the presence of very large pores through pores.

In order to find a column with appropriate permeability and robustness, the composition of our DMAEMA-co-EDMA polymerization mixture has to be optimized. First, a tertiary mixture containing water, acetonitrile and ethanol was used as the porogenic

solvent according to previous studies.^{21,26} However, we were not able to prepare a polymer monolithic column with satisfactory robustness, stability and permeability. Several types of unsatisfactory monolithic columns are shown in Figure 2.1. For example, polymer monoliths without pores were produced at an initial attempt, which is a result of very high monomer concentration. The monomer used in our experiment, DMAEMA, was found to produce a soft and jelly-like material, due to its higher hydrophilicity. It was also found that a polymer monolithic column can crack or peel off the wall, as shown in Figure 2.1. It was considered a result of small throughpores (high density) and softness of the monolithic material. Therefore, the ratio of monomer/crosslinker was optimized in subsequent experiments. Another mixture of porogenic solvents was considered an alternative approach to preparing the intended copolymer monolith.^{27,28}

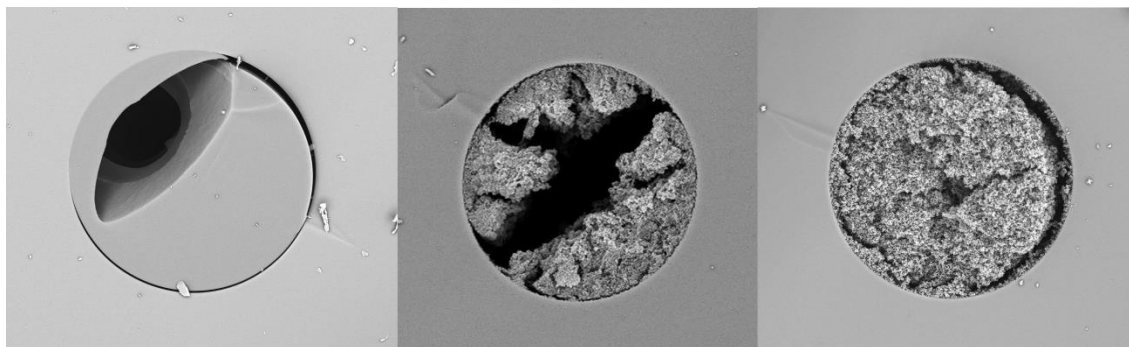


Figure 2.1 Scanning electron microscope images of unsatisfactory polymer monolithic columns. The inner diameter of the columns is 75 μm .

Firstly, the ratio of monomer/crosslinker was investigated. Various percentages (5.0%, 7.5%, 10.0%, v/v) of DMAEMA were used to prepare the monolithic columns as shown in Table 2.1 (sample A1 - A3). It was found that, both column A3 and column A3 (7.5% and 10.0% DMAEMA, respectively) were not able to allow significant flow, with the backpressure exceeding 5000 psi at a 0.2 $\mu\text{L}/\text{min}$ flow rate. The column A1 containing

5.0% DMAEMA produces a satisfactory backpressure at 660 ± 40 psi at 1.0 $\mu\text{L}/\text{min}$ of acetonitrile. As it shows in Figure 2.2, column A1 (5.0% DMAEMA) has much larger throughpores instead of smaller throughpores and denser morphology for column A2 and column A3. Therefore, the monomer/crosslinker ratio of column A1 was used for further investigation.

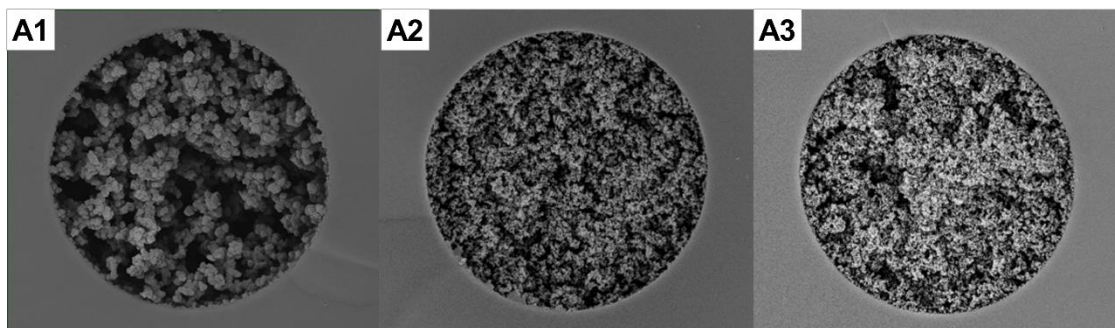


Figure 2.2 Scanning electron microscope images of poly(DMAEMA-co-EDMA) monolithic column with different volume ratios of monomer/crosslinker: (A1) 20:80 (A2) 30:70 (A3) 40:60; corresponding to the composition of polymerization mixture A1 - A3 in Table 2.1.

A major factor defining the permeability of a porous polymer column is the composition of the porogenic solvent. Because the polymer monolith produced in the above experiment has large throughpores and relatively low backpressure (indicating low surface area), the composition of porogenic solvents was further optimized. The updated tertiary solvent mixture contains water, 2-propanol and 1,4-butanediol. Specifically, the ratio of 2-propanol and 1,4-butanediol was investigated because it was reported that the ratio of those two solvents has a significant impact on the morphology.²⁸ Column B1-B4 were prepared as shown in Table 2.2, with percentage of 2-propanol varying from 60.0% to 66.0%. SEM imaging showed that a monolithic column with larger throughpores and larger globules was produced if a higher percentage of 2-propanol was used (Figure 2.3 and Figure 2.4).

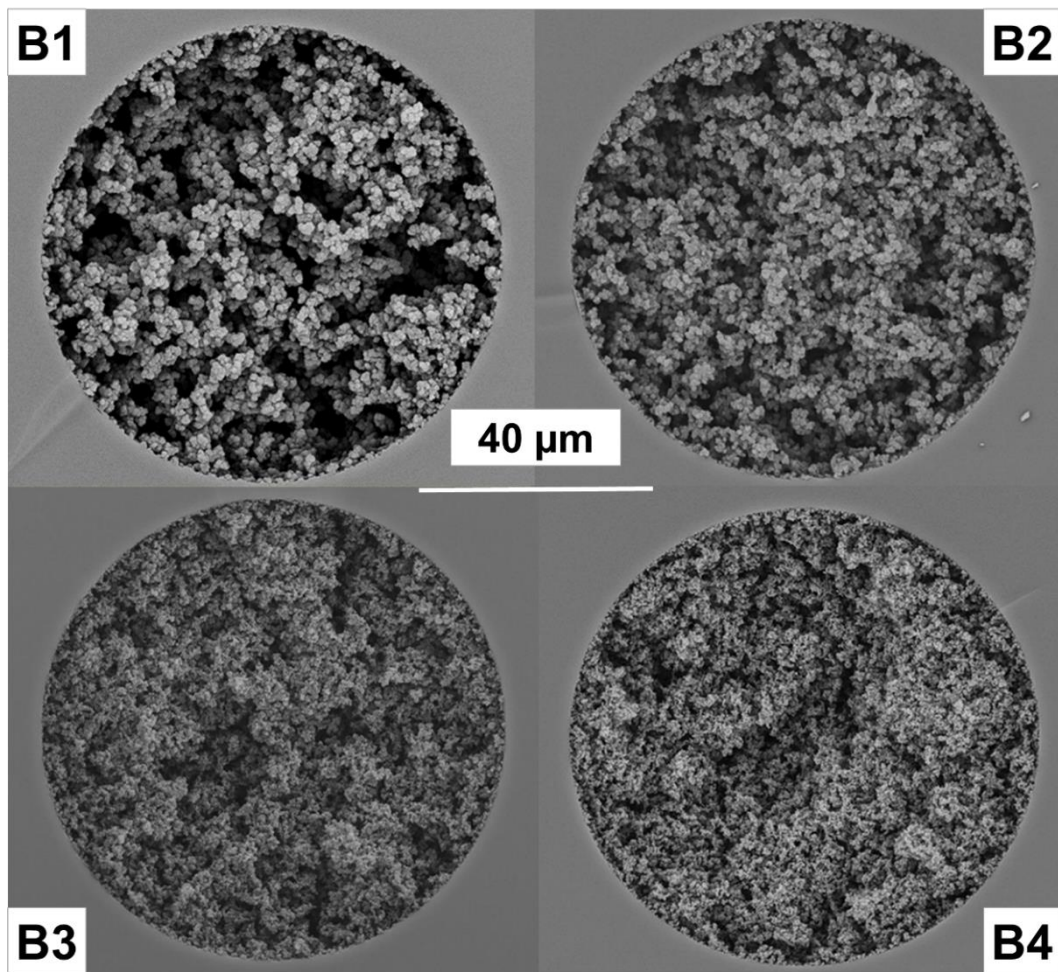


Figure 2.3 Scanning electron microscope images of poly(DMAEMA-co-EDMA) monolithic column with different volume ratios of 2-propanol and 1,4-butanediol: B1) 60:30; B2) 62:28; B3) 64:26; B4) 66:24; corresponding to the column B1-B4 in Table 2.2.

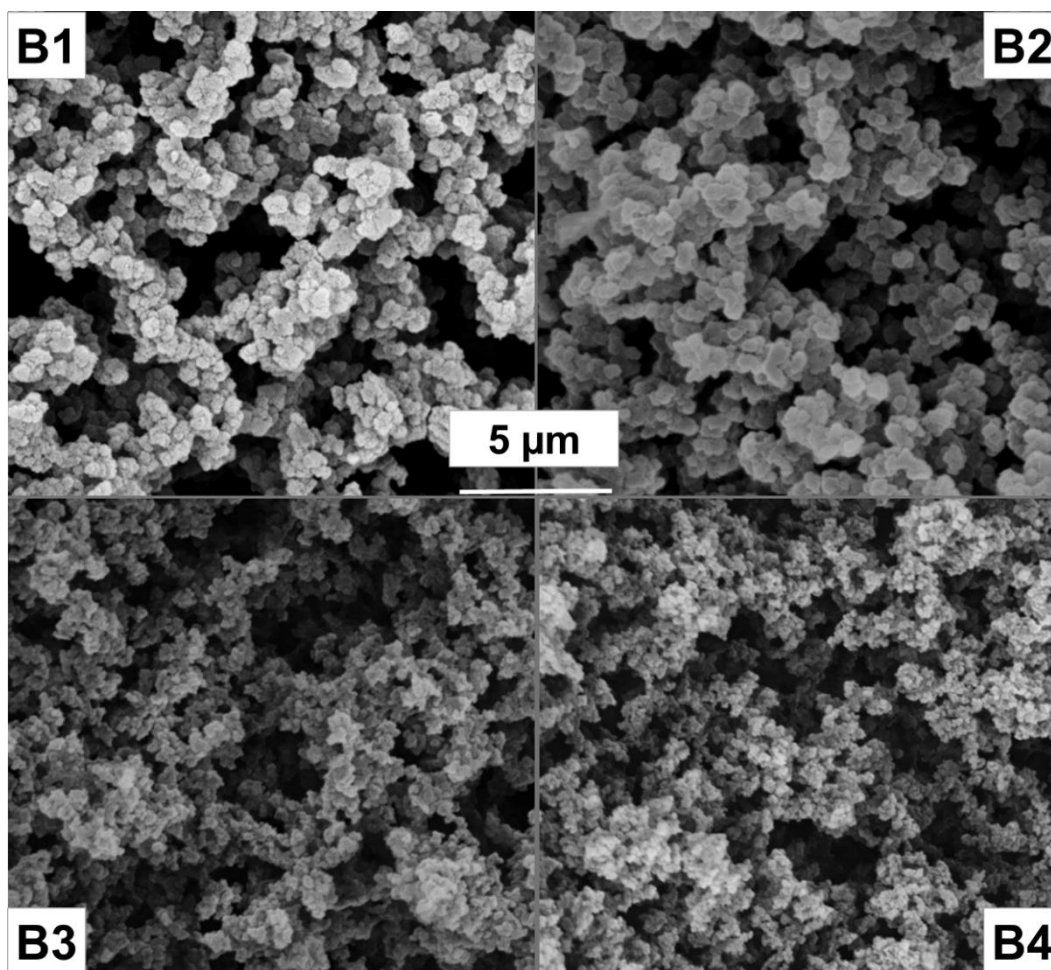


Figure 2.4 Scanning electron microscope images (magnified) of poly(DMAEMA-co-EDMA) monolithic column with different ratios of 2-propanol and 1,4-butanediol: B1) 60:30; B2) 62:28; B3) 64:26; B4) 66:24; corresponding to the column B1-B4 in Table 2.2.

According to a previous study, this effect may be explained by the differential solvation polarity of solvent mixtures.²⁹ A volume weighted solvent polarity (VWSP) was used to evaluate the properties of mixed solvents by calculating a weighted average of the dielectric constant of the individual solvents. Higher polarity solvents (higher VWSP value) have poorer solvation ability to polymers composed of hydrophobic monomers. The backpressure versus the volume weighted solvent polarity is plotted to demonstrate the effect of solvent polarity on the density of the monolith (Figure 2.5). Because poorer

solvation (higher VWSP) causes a later onset of phase separation, polar solvents result in monoliths with larger globules and throughpores. With a slight change of VWSP from 29.63 to 28.94, a significant increase of column backpressure was observed.

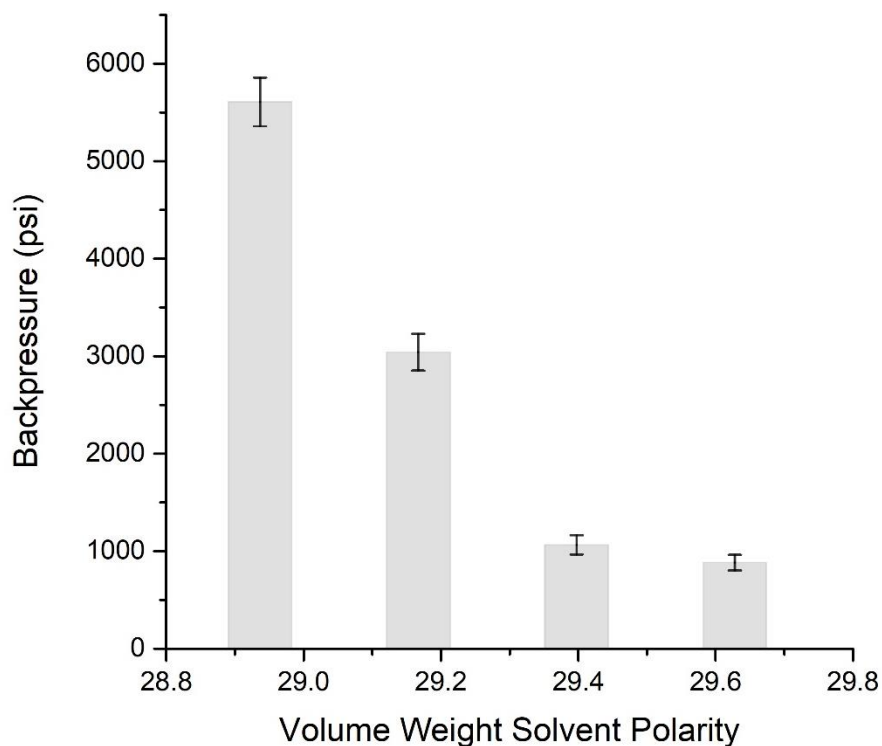


Figure 2.5 Backpressure of the poly(DMAEMA-co-EDMA) monolithic columns made from different solvents represented by the volume weighted solvent polarity. Column dimension: 10.0 cm \times 100 μ m I.D. Solvent: 95.0% acetonitrile at 1.0 μ L min⁻¹.

ATR-IR was used to confirm the presence of amine groups in the copolymer monolith (Figure 2.6). The IR spectrum of the monomer, DMAEMA was first collected and it was noticed that, a weak absorbance at 2770 nm and 2821 nm was observed. Those peaks are attributed to the symmetric stretching vibrations of $-N-CH_3$. The IR spectrum of the copolymer was then collected and it showed the absorbance at 2770 nm and 2821 nm

as well although the peaks were not very strong. The weak intensity may result from a large portion of DMAEMA being buried within the polymer bulk and not able to be detected.

Based upon those characterizations, column B3 was found to have the most satisfactory properties, including an intermediate backpressure (< 5000 psi, $1.0 \mu\text{L min}^{-1}$) and appropriate size of through-pores. Therefore, the polymerization mixture in column B3 was utilized for the chromatographic characterization experiments.

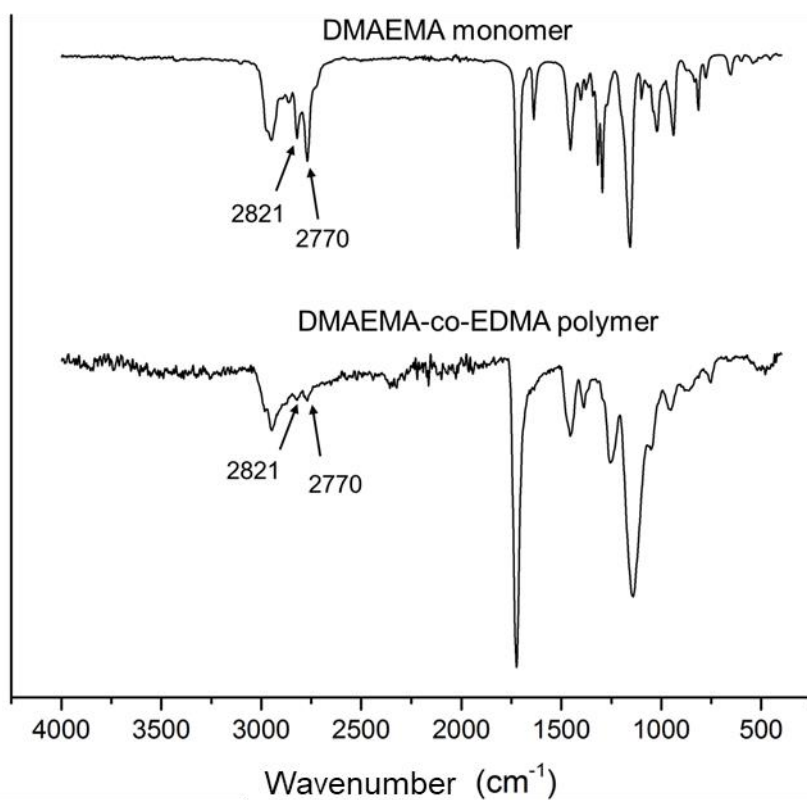


Figure 2.6 ATR-IR spectroscopy of DMAEMA and the poly(DMAEMA-co-EDMA) monolithic material.

2.3.2 CO_2 -switchability of the column

DMAEMA was selected as the potential CO_2 -switchable monomer because of the presence of tertiary amine groups and reports about its pH/thermo-responsive

properties.^{3, 30-32} Another group reported the preparation of pH/salt responsive polymer brushes on monolithic surfaces by a two-step atom transfer radical polymerization method. However, there is no direct comparison of the performance of copolymer and grafted monoliths, to validate the advantages of ATRP methods. Additionally, copolymerization is a very straightforward way of preparing monolithic columns and it does not require the strict experimental conditions (*e.g.* oxygen free, heavy metal catalysts). Therefore, the poly(DMAEMA-co-EDMA) monolithic column was tested for its performance with CO₂-switchable separations.

A gradient method was first developed to separate the selected neutral compounds, benzene, naphthalene and anthracene. As shown in Figure 2.7 A, three compounds were successfully separated in 15 minutes with a gradient of water and acetonitrile. To investigate the effect of acidic modifier, acetic acid was first added in the mobile phases (both A and B) because it is more straightforward to study the effect of an acidic modifier. As shown in Figure 2.7 B, the three compounds were separated in a similar chromatogram, with slightly shorter retention times. The retention time was about one minute shorter using the acid modified solvents, compared with the retention time without a modifier. This indicates that the column has been slightly switched to a more hydrophilic state although the scale of retention time change is not very significant.

The effect of CO₂ on the retention time was also attempted by carefully introducing CO₂ into the aqueous phase reservoir. Care was taken to optimize the delivery of CO₂ in order to generate a stable supply of CO₂-modified water. However, the chromatograms were not reproducible, showing an obvious deviation between chromatograms. As it shows

in Figure 2.8, the two typical chromatograms with CO₂-modified solvents are very different in peak shape and retention time. It was considered that, effective and reliable delivery of CO₂ in the nano LC system is difficult. In the nano LC system, all the experiments have to be performed at a micro liter or nano liter flow (0.50 – 5.0 μL min⁻¹). It takes a very long time (> 2 hours) for the solvents to travel through the tubing from the solvent reservoirs and bubbles may form in the tubing between the pump and column. Therefore, the solvent tubing is not capable for minimizing the formation of bubbles and subsequent consistent flow rate of solvents. Solvent tubing was primed more frequently to avoid the generation of bubbles. However, the irreproducibility was still not fixed. Another disadvantage of using nano LC for CO₂-based experiments was that the pH of the eluent was very difficult to measure because of the very small volume of eluent generated.

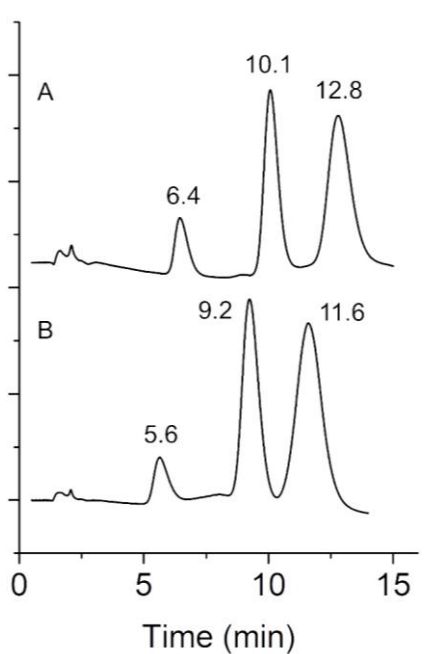


Figure 2.7 Chromatograms of benzene, naphthalene and anthracene (in the order of elution) separated (A) without modifier and (B) with 0.10% acetic acid in the mobile phases. Conditions: poly(DMAEMA-co-EDMA) monolithic column, 100 μm I.D., 15.0 cm; mobile phase is a gradient of water and acetonitrile, 0-1 min, 80% water; 1-10 min, 80% - 50% water; 10-15 min, 50% water; flow rate 1.0 μL min⁻¹, injection volume 2.0 μL, UV detection 254 nm.

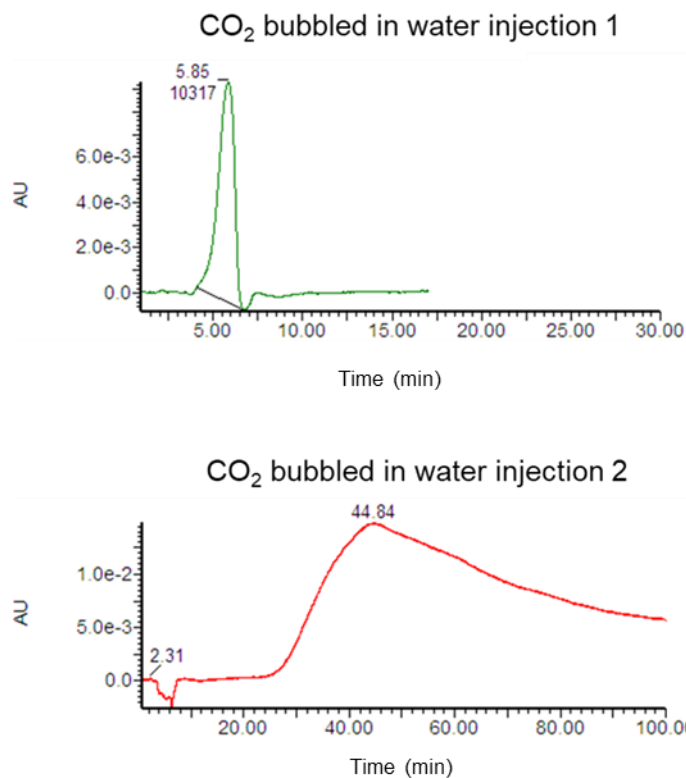


Figure 2.8 Representative chromatograms showing the irreproducibility of using CO₂-modified solvent with repeated injections on nano LC. Conditions: poly(DMAEMA-co-EDMA) monolithic column, 100 μm I.D., 15.0 cm; mobile phase: 0-1 min, 80% carbonated water; 1-10 min, 80% - 50% carbonated water; 10-15 min, 50% carbonated water; flow rate 1.0 $\mu\text{L min}^{-1}$; injection volume 2.0 μL ; sample: naphthalene; UV detection 254 nm.

In brief, the attempt of using CO₂-modified solvent to separate compounds was not very successful although acidic modifier slightly switched the hydrophobicity of the column. It was suggested that it could be more feasible to demonstrate the concept of CO₂-switchable chromatography in a conventional HPLC system. The flow rate of conventional HPLC is considerably faster and it uptakes the mobile phase more quickly reducing the chances for bubble formation. Thus, a CO₂-delivery set-up was applied to experiments on an Agilent 1100 conventional HPLC system, with a typical solvent flow rate of 1.0 mL min⁻¹.

2.3.3 Effect of pH on retention time

Despite the unfavorable results from CO₂-switchable experiments, there are also some interesting aspects about the poly(DMAEMA-co-EDMA) that are worth exploring. First, there have been no reports about the possibility of reversed phase separation with a copolymer monolith column based on DMAEMA. Furthermore, the intrinsic pH and thermo-responsive properties of PDMAEMA indicates the potential application of this column for stimuli-responsive separation at different pH and temperature conditions.

As discussed in the first chapter, if a neutral compound is retained on a traditional reversed phase column, the pH should have minimal effect on the retention because it does not affect the states of either stationary phase groups or the neutral compound. If a stationary phase contains ionizable groups within the range of pH change (equation 2.1), the selectivity of the stationary phase may be significantly affected. The pK_a of the polymeric DMAEMA is 7.4, which may show a significant protonation / deprotonation by a switch of pH from acidic to basic. Therefore, the retention time of charged analytes may be controlled through the electrostatic interaction between the analytes and the stationary phase. Additionally, the ionization of the analyte may also participate in the retention time change over the range of pH change triggered by a solvent modifier. Therefore, three compounds, an acidic, a neutral, and a basic compound were selected to test their retention time at various conditions.

Protonation of amine stationary phase



Initially a gradient method with water and acetonitrile was developed to completely separate the three compounds, at pH 7.0 (no modifier). As it shows in Figure 2.9, 4-butylaniline and phenanthrene were retained on the column for shorter times than ketoprofen.

The chromatogram of the three compounds with acidic modifier (pH 3.4) was significantly different. Firstly, the retention time of phenanthrene was slightly shorter at pH 3.4 ($t_R = 19.1$ min) compared with the retention time at pH 7.0 ($t_R = 19.9$ min). This result corroborated the results in Figure 2.7, where the retention time of all neutral compounds decreased slightly. It indicated that hydrophobicity of the stationary phase was decreased due to the protonation of amine groups. The retention time of both 4-butylaniline and ketoprofen was decreased with the acidic modifier added. Presumably, the ionization of those two compounds may have an effect on the retention time, because both of them have a pK_a (pK_{aH}) ~ 5 . As shown in the equilibria equations 2.2 and 2.3, the basic analyte (4-butylaniline) is protonated at a significant fraction if the pH is lower than its pK_a . The acidic analyte (ketoprofen) is converted to a neutral form at a significant fraction when the pH is lower than its pK_a . That being said, both the protonation of stationary phase amine groups and dissociation of analytes contributed to the decrease in retention time. A schematic of the charge states of the analytes and the stationary phase groups is shown in Figure 2.10.

Basic analyte dissociation equilibrium



Acidic analyte dissociation equilibrium



The chromatography of the three compounds with basic modifier further confirmed the contribution of both stationary phase and the analytes. At pH 10.3, the retention time of 4-butylaniline was slightly longer ($t_R = 18.1$ min) than the retention time without modifier ($t_R = 17.9$ min). It is reasonable, considering that the stationary phase becomes slightly more hydrophobic because of deprotonation, and the compound 4-butylaniline mostly remains in deprotonated form because of the high pH. The retention time of ketoprofen was significantly reduced ($t_R = 11.0$ min) compared with the retention time without modifier ($t_R = 31.8$ min). The electrostatic interaction between the protonated amine and the negatively charged ketoprofen is diminished because the amine groups are deprotonated at elevated pH. As shown in Figure 2.9, the retention time of ketoprofen was significantly reduced because of its self-dissociation and its higher polarity thereafter.

Those results verified the hypothesis of using pH to manipulate the selectivity of compounds on a DMAEMA-co-EDMA column. The protonation and deprotonation of amine functional groups indicates the potential application of this copolymer material for CO₂-switchable chromatography, because CO₂ performs as a weak acid in aqueous solutions. In reversed phase chromatography, electrostatic interaction may be exploited in the manipulation of retention time in addition to hydrophobic interaction.

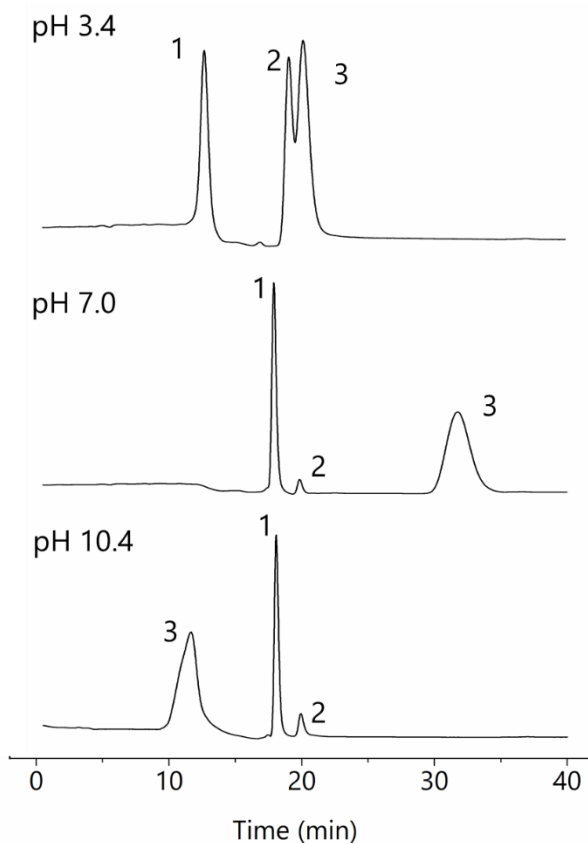


Figure 2.9 Chromatograms of 1) 4-butylaniline, 2) phenanthrene, and 3) ketoprofen separated using poly(DMAEMA-co-EDMA) column using acidic (pH 3.4), neutral (pH 7.0) and basic (pH 10.4) solutions. Conditions: poly(DMAEMA-co-EDMA) monolithic column, 100 μm I.D., 15.0 cm; mobile phase, 0-1 min, 80% water; 1-10 min, 80% - 50% water; 10-15 min, 50% water; flow rate $1.0 \mu\text{L min}^{-1}$, injection volume $2.0 \mu\text{L}$, UV detection 254 nm. The concentration of phenanthrene in the top panel chromatogram is higher because stock solution of phenanthrene was spiked in the mixture to increase the intensity of peak 2.

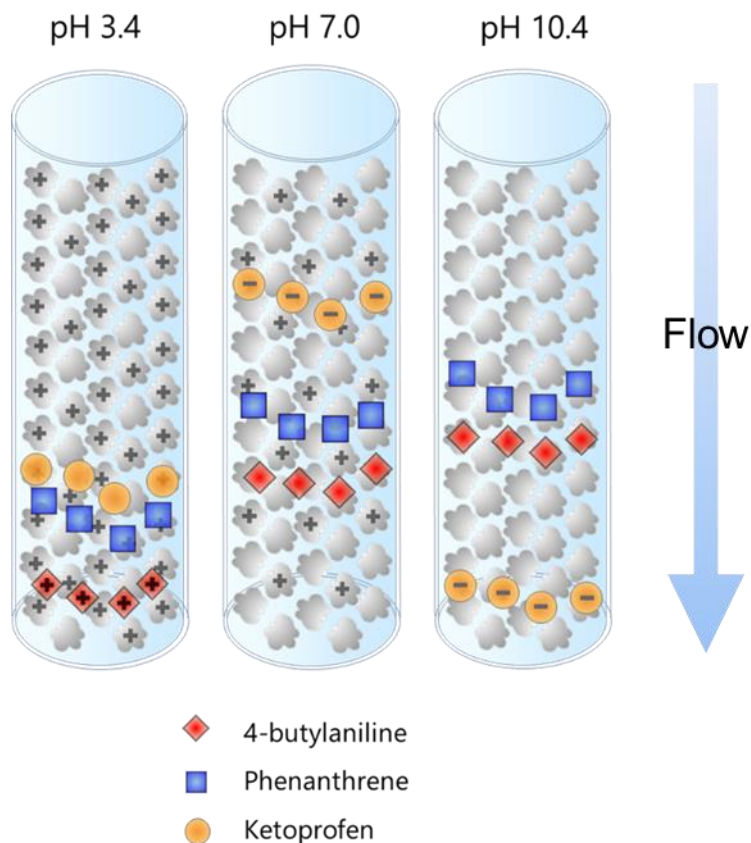


Figure 2.10 Retention scheme of the basic (4-butylaniline), neutral (phenanthrene), and acidic (ketoprofen) analytes on the poly(DMAEMA-co-EDMA) monolithic column, showing the protonation of stationary phase and dissociation of the analytes.

2.3.4 Effect of temperature on the chromatography

The temperature responsiveness of polymers has been well explored, including some chromatographic applications using thermo-responsive polymers, such as poly(N-isopropylacrylamide) (PNIPAAm). A reversible phase transition of the polymer in aqueous solutions is reported at a temperature near to 32 °C, which is also called the lower critical solution temperature (LCST). That being said, the hydrophobicity and charge state are potentially switchable at different temperatures, enabling an additional level of control for the separation of charged compounds. Generally, thermo-responsive polymers are grafted

on the surface of silica spheres or polymers. However, the incorporation of thermo-responsive polymers in a copolymer monolith is less explored. Therefore, it is considered valuable to investigate the thermo-responsive chromatographic behaviour of the copolymer monolithic column.

Three representative compounds (acidic, neutral and basic) were selected and separated with a gradient method using water and acetonitrile. Although ketoprofen is less polar ($\text{Log } P$ 3.6) than phenanthrene ($\text{Log } P$ 4.0), the retention time of ketoprofen is relatively longer. That being said, electrostatic attraction of the anionic ketoprofen with the protonated amine groups contributed to the extended retention time, as also demonstrated earlier (section 2.3.3).

The chromatogram at an elevated temperature (65 °C) is shown in Figure 2.11. The retention time of phenanthrene and 4-butylaniline showed a slight retention decrease of less than 1 minute, indicating that the hydrophobicity of the stationary phase is switched slightly. Interestingly, the retention time of ketoprofen decreased from 31.8 min at 25 °C to 22.0 min at 65 °C and a much narrower peak of ketoprofen was observed. This behaviour is consistent with the results reported by Sepehrifar *et al.*¹⁷ In their study, the retention time of 2-fluorobenzoic acid, ketoprofen and amitriptyline decreased at a higher temperature (65 °C) on a silica sphere column grafted with a (PDMAEMA-*b*-PAA).¹⁷ In that example, the positively charged amitriptyline interacts with the ionized carboxyl groups of PAA more strongly at a lower temperature. However, a decrease in retention occurs due to the thermally induced collapse of the polymeric framework together with the shielding of the charged groups from an extended morphology to a more compressed morphology.

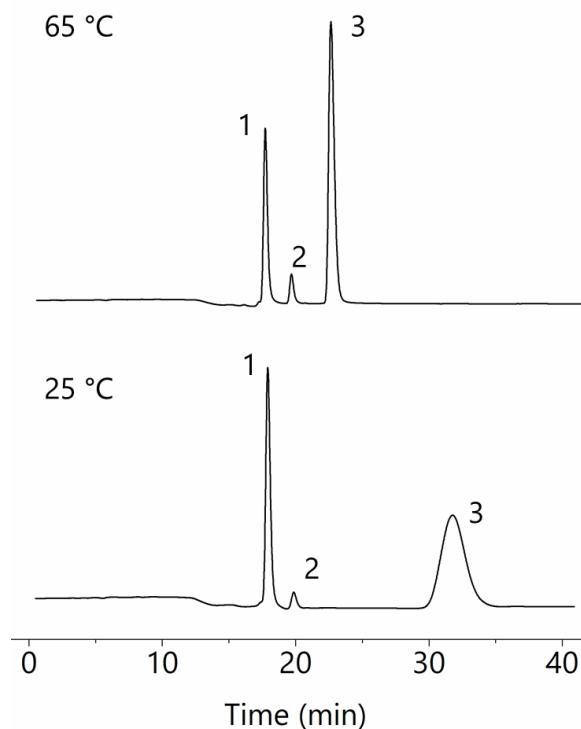


Figure 2.11 Chromatograms of 1) 4-butylaniline, 2) phenanthrene, and 3) ketoprofen separated using poly(DMAEMA-co-EDMA) column at 25 °C and 65 °C. Conditions: poly(DMAEMA-co-EDMA) monolithic column, 100 μm I.D., 15.0 cm; mobile phase, 0-1 min, 80% water; 1-10 min, 80% - 50% water; 10-15 min, 50% water; flow rate 1.0 $\mu\text{L min}^{-1}$, injection volume 2.0 μL , UV detection 254 nm.

In brief, the decreased retention time is considered an effect of less accessible positive charge from collapsed polymeric DMAEMA, resulting from elevated temperature, as depicted in Figure 2.12. The results from our experiment confirmed the effectiveness of using copolymer monolithic column as a thermo-responsive media. Additionally, a satisfactory efficiency was observed in the chromatographic separation with the poly(DMAEMA-co-EDMA) monolithic column, which provides an alternative to the commonly adopted grafting approach to prepare thermo-responsive moieties. It is worth noting, the incorporation of EDMA in the copolymer monolith makes the column generally

more hydrophobic, which requires the use of organic solvent for chromatography. Future attempts may involve the introduction a more hydrophilic crosslinker, which may allow the development of all-aqueous separation methods.

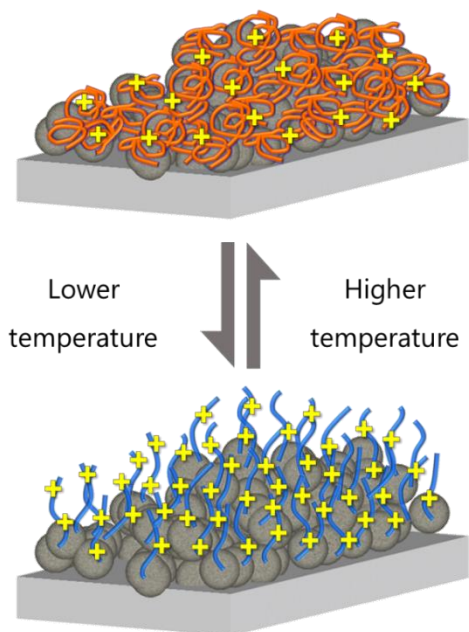


Figure 2.12 Schematic of the thermo-responsive change of the poly(DMAEMA-co-EDMA) monolithic column between a collapsed form at low temperature and an extended form at higher temperature.

2.3.5 Ion exchange separation using the copolymer monolith

It is known that quaternary amine groups are used as strong anion exchangers, tertiary amine groups are often used as weak anion exchangers. It indicates that, the tertiary amine groups on DMAEMA could also be used as ion exchangers for the separation of protein samples. Sepehrifar *et al.* reported the use of PDMAEMA-*b*-PAA grafted silica column for the ion exchange separation of horse heart myoglobin, hen egg white lysozyme, and bovine heart cytochrome c.¹⁷ Therefore, an ion exchange separation was performed for myoglobin, transferrin and bovine serum albumin using a salt gradient. At 25 °C, a

successful separation of the three proteins was performed with a gradient of sodium chloride in the Tris-HCl buffer at pH 7.6, as shown in Figure 2.13.

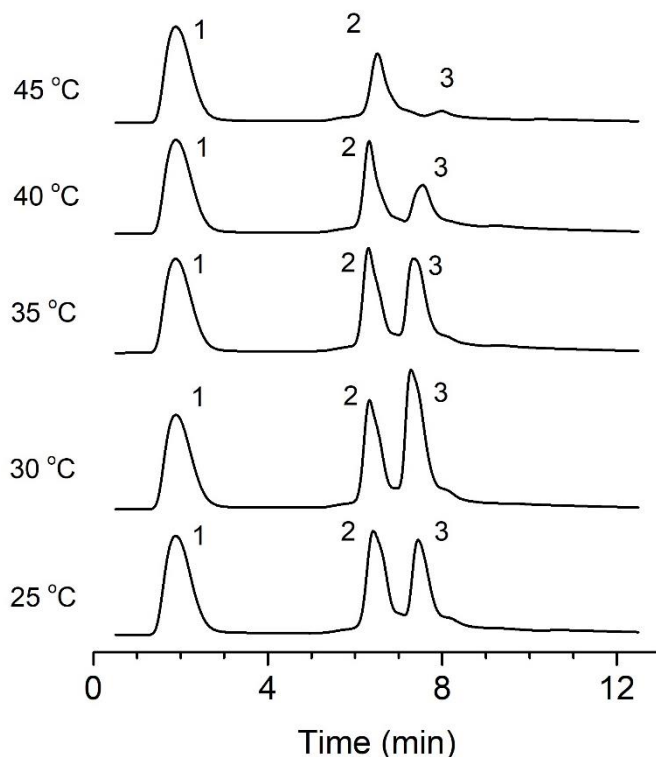


Figure 2.13 Chromatograms of 1) myoglobin, 2) transferrin, 3) bovine serum albumin separated at various temperatures. Conditions: poly(DMAEMA-co-EDMA) monolithic column, 200 μm I.D., 15.0 cm; mobile phase A: Tris-HCl buffer at pH 7.6, mobile phase B, same as A except with 1 M NaCl; Gradient: 0-2 min, 100% water; 2-17 min, 100% A \sim 100% B; flow rate 4.0 $\mu\text{L min}^{-1}$, injection volume 2.0 μL , UV detection 214 nm.

In an earlier section (2.3.4), it was demonstrated that the accessible charge on the surface of poly(DMAEMA-co-EDMA) was manipulated with temperature for the separation of organic molecules in reversed phase mode. Herein, the ion exchange chromatography of the protein samples was performed at elevated temperatures, *e.g.* 30 °C, 35 °C, 40 °C, 45 °C. It was observed that the retention time of all three proteins was relatively constant at various temperatures (Figure 2.13).

The results reported by Sepehrifar *et al.* also lead to a similar conclusion, indicating a minimal change of retention time for proteins caused by elevated temperature. It is believed that, an additional level of complexity is involved because both the protein analyte and the immobilized polymeric DMAEMA are flexible in their conformations, as it is in the case of the interaction of proteins with poly(DMAEMA-co-EDMA) stationary phases. This makes the interpretation of retention time much more difficult. Some change of peak areas of the proteins have also been observed. Especially, the peak area of bovine serum albumin shows a slight increase at 30 °C and 35 °C, and an obvious decrease at 40 °C and 45 °C (Figure 2.13). It implies the conformational change of proteins at higher temperature, as also reported in earlier studies.^{17, 33}

In general, this attempt has demonstrated the ion exchange separation of proteins with the poly(DMAEMA-co-EDMA) monolithic column. The peak area variation at higher temperatures indicates a possible conformational change of the protein sample, which affects the intensity of UV detection. A more complicated mechanism about the interaction of a protein sample with the stationary phase is likely involved because of the temperature sensitivity of protein molecules. This again points toward the drawback of thermo-responsive separations of biological samples due to their thermal instability.

2.4 Conclusive remarks

In this chapter, a poly(DMAEMA-co-EDMA) was prepared for the investigation of CO₂-switchable chromatography, pH/thermo-responsive separations and ion exchange separations. Composition of the porogenic solvent was optimized to allow the preparation of monolithic columns with appropriate permeability and robustness. After the

characterization of morphology (by SEM imaging) and backpressure, an optimal composition containing 10.0% water, 64.0% 2-propanol, and 26.0% 1,4-butanediol was adopted for preparing the monolithic columns used in each of the experiments. The investigation of CO₂-switchable chromatography on a copolymer column was not successful, presumably due to the technical challenge of introducing CO₂ into the nano LC system. In the studies in following chapters, a conventional HPLC system is used, together with conventional column dimensions (*e.g.* 4.6 mm I.D.). A further study using polymer monolith in a conventional column is proposed, but the swelling / shrinking of monolithic columns will become another technical fabrication challenge. Thereafter, commercial columns and functionalized-silica columns were used in a conventional HPLC instrument in the demonstration of CO₂-switchable chromatography.

The demonstration of pH and thermo-responsive properties of the copolymer monolith provides a valuable alternative to the commonly used grafting approach. The results indicate a more effective switch for the charge states (*e.g.* protonation) of the stationary phase than for the stationary phase hydrophobicity. The dissociation of analytes at different pH values may also be considered in the manipulation of chromatographic selectivity. Additionally, an ion exchange separation of protein samples was performed successfully on the copolymer monolithic column and the poly(DMAEMA-co-EDMA) is considered a versatile media for the separation in reversed phase mode and ion exchange mode.

2.5 References

1. H. Kanazawa, M. Nishikawa, A. Mizutani, C. Sakamoto, Y. Morita-Murase, Y. Nagata, A. Kikuchi and T. Okano, *J Chromatogr A*, 2008, **1191**, 157-161.
2. P. Maharjan, M. T. W. Hearn, W. R. Jackson, K. De Silva and B. W. Woonton, *J Chromatogr A*, 2009, **1216**, 8722-8729.
3. X. Han, X. Zhang, H. Zhu, Q. Yin, H. Liu and Y. Hu, *Langmuir*, 2013, **29**, 1024-1034.
4. R. A. Lorenzo, A. M. Carro, A. Concheiro and C. Alvarez-Lorenzo, *Anal Bioanal Chem*, 2015, **407**, 4927-4948.
5. A. J. Satti, P. Espeel, S. Martens, T. Van Hoeylandt, F. E. Du Prez and F. Lynen, *J Chromatogr A*, 2015, **1426**, 126-132.
6. P. Maharjan, E. M. Campi, K. De Silva, B. W. Woonton, W. R. Jackson and M. T. Hearn, *J Chromatogr A*, 2016, **1438**, 113-122.
7. K. Nagase, J. Kobayashi, A. Kikuchi, Y. Akiyama, M. Annaka, H. Kanazawa and T. Okano, *Langmuir*, 2008, **24**, 10981-10987.
8. K. Nagase, J. Kobayashi, A. Kikuchi, Y. Akiyama, H. Kanazawa and T. Okano, *ACS Appl Mater Interfaces*, 2013, **5**, 1442-1452.
9. K. Nagase and T. Okano, *J Mater Chem B*, 2016, **4**, 6381-6397.
10. C. d. I. H. Alarcon, S. Pennadam and C. Alexander, *Chem Soc Rev*, 2005, **34**, 276-285.
11. M. A. Stuart, W. T. Huck, J. Genzer, M. Muller, C. Ober, M. Stamm, G. B. Sukhorukov, I. Szleifer, V. V. Tsukruk, M. Urban, F. Winnik, S. Zauscher, I. Luzinov and S. Minko, *Nat Mater*, 2010, **9**, 101-113.
12. A. M. Ross, H. Nandivada and J. Lahann, *Handbook of Stimuli-responsive Materials*, Wiley-VCH, Weinheim, M.W. Urban ed., 2011.
13. Q. Yan and Y. Zhao, *Chem Commun*, 2014, **50**, 11631-11641.
14. A. K. Kota, G. Kwon, W. Choi, J. M. Mabry and A. Tuteja, *Nat Commun*, 2012, **3**, 1025.
15. K. Nagase, M. Kumazaki, H. Kanazawa, J. Kobayashi, A. Kikuchi, Y. Akiyama, M. Annaka and T. Okano, *ACS Appl Mater Interfaces*, 2010, **2**, 1247-1253.

16. R. Sepehrifar, R. I. Boysen, B. Danylec, Y. Yang, K. Saito and M. T. Hearn, *Anal Chim Acta*, 2016, **917**, 117-125.
17. R. Sepehrifar, R. I. Boysen, B. Danylec, Y. Yang, K. Saito and M. T. Hearn, *Anal Chim Acta*, 2017, **963**, 153-163.
18. Y. Shen, L. Qi, X. Y. Wei, R. Y. Zhang and L. Q. Mao, *Polymer*, 2011, **52**, 3725-3731.
19. N. Li, L. Qi, Y. Shen, Y. Li and Y. Chen, *ACS Appl Mater Interfaces*, 2013, **5**, 12441-12448.
20. S. Frantisek and L. Yongqin, *Anal Chem*, 2015, **87**, 250-273.
21. A. B. Daley, Z. P. Xu and R. D. Oleschuk, *Anal Chem*, 2011, **83**, 1688-1695.
22. Z. P. Xu and R. D. Oleschuk, *J Chromatogr A*, 2014, **1329**, 61-70.
23. ExPasy Bioinformatics resource portal, http://web.expasy.org/compute_pi/ (accessed September 6th, 2017).
24. F. Svec, *J Chromatogr A*, 2012, **1228**, 250-262.
25. K. Liu, H. D. Tolley and M. L. Lee, *J Chromatogr A*, 2012, **1227**, 96-104.
26. Z. P. Xu, G. T. T. Gibson and R. D. Oleschuk, *Analyst*, 2013, **138**, 611-619.
27. W. Niu, L. Wang, L. Bai and G. Yang, *J Chromatogr A*, 2013, **1297**, 131-137.
28. D. Moravcová, P. Jandera, J. Urban and J. Planeta, *J Sep Sci*, 2003, **26**, 1005-1016.
29. K. J. Bachus, K. J. Langille, Y. Q. Fu, G. T. T. Gibson and R. D. Oleschuk, *Polymer*, 2015, **58**, 113-120.
30. P. Cotanda, D. B. Wright, M. Tyler and R. K. O'Reilly, *J Polym Sci A1*, 2013, **51**, 3333-3338.
31. L. Zhou, W. Yuan, J. Yuan and X. Hong, *Mater Lett*, 2008, **62**, 1372-1375.
32. S. Kumar, X. Tong, Y. L. Dory, M. Lepage and Y. Zhao, *Chem Commun*, 2013, **49**, 90-92.
33. C. Kulsing, A. Z. Komaromy, R. I. Boysen and M. T. Hearn, *Analyst*, 2016, **141**, 5810-5814.

Chapter 3 CO₂-switchable separation with commercial columns

3.1 Introduction

Chemical separations account for about half of US industrial energy use and 10-15% of the nation's total energy consumption.¹ Immense amounts of energy and harmful organic solvents are consumed in chemical separation processes. Developing alternative green separation and purification approaches is a high priority. As an important separation technique, chromatographic separation is widely used in purification separation and analysis of chemicals. In chromatography, elution strength is usually adjusted by utilizing organic solvents, salt gradients, pH gradients, *etc.* The adverse impact of solvent use to the environment and human health has driven the development of alternative solvents.^{2,3} Salt and permanent acids/bases are very difficult to remove and they require higher cost for recovery and disposal. Furthermore, utilization of organic solvents can permanently denature analytes such as proteins or nucleic acids through structure modification.⁴

Although stimuli-responsive materials are widely utilized in sensors, smart surfaces, and oil-water separation, *etc.*,⁵⁻⁷ they have not been extensively exploited for chromatographic separations. Thermo-responsive stationary phases on silica or polymer surfaces were demonstrated to separate organic molecules using various temperature conditions.^{8,9} However, the thermo-responsive approach is limited by the thermal conductivity of the chromatographic column and biomolecules can be susceptible to high temperature. Alternatively, pH and salt responsive surfaces are exploited for separation, although permanent salts are still difficult to remove afterwards.¹⁰

Recently, the groups of Jessop and Cunningham, working together, have reported solid-liquid systems using CO₂ as an useful trigger for the reversible modification of the surfaces of switchable latex particles¹¹ and drying agents¹². Based on a similar mechanism, Zhao *et al.* modulated the protein adsorption properties on a modified silicon surface in the presence and absence of CO₂.^{13, 14} Muñoz-Espí *et al.* observed the coagulation of the polystyrene nanoparticles modified with a carboxymethyl-based monomer when bubbled with CO₂. Re-dispersion of the coagulated particles was achieved with ultrasonication or heat to recover the coulombic repulsion between the particles.¹⁵

CO₂ is easy to eliminate, non-flammable and non-toxic. In supercritical fluid chromatography and extraction, CO₂ is extensively used as a solvent due to its ability to solubilize non-polar compounds in a supercritical state.¹⁶⁻¹⁸ Elution strength is manipulated by varying the density of the supercritical CO₂ through pressure and temperature control. “Enhanced fluidity liquids” have also been demonstrated as an alternative to SFC mobile phases which are operated at subcritical conditions.^{16, 17, 19}

We anticipated that the acidity of CO₂ dissolved in water could be used as the basis for reversibly modifying the stationary phase and/or analytes in aqueous chromatography. CO₂ lowers the pH of water because it forms carbonic acid and hydrated CO₂, both of which are acidic. For example, CO₂ bubbled water at 1 bar shows a pH of 3.9, and 0.03% v/v CO₂ in air makes a solution of pH 5.6.²⁰ CO₂ can be considered a “temporary” acid since its removal can be achieved by bubbling with an inert gas. As a result, it is a very useful alternative to permanent acids and minimizes salt formation through neutralization with a

base. Furthermore, the pH can be carefully controlled by mixing carbonated and uncarbonated water.

The objective of the study in this chapter was to verify the concept of CO₂ responsive chromatography, where raising or lowering the amount of CO₂ dissolved in the aqueous eluent would control retention times. We sought to demonstrate the chromatographic separations with aqueous solvents modified with CO₂ and showed that the change of selectivity and elution strength depending on the amount of CO₂ involved. A CO₂ delivery system was assembled to sparge CO₂ in the solvent reservoir at 1 bar. All the CO₂ sparging was performed at ambient temperature and pressure. Only a small amount of CO₂ (mole fraction 0.00061) is dissolved in water at ambient conditions (approx. 25 °C, 1 bar), the CO₂-modified aqueous solvents do not present the properties of supercritical fluids or even CO₂-expanded liquids.²¹ Instead, CO₂ serves as a “temporary” weak acid in the aqueous phase. In this work, three commercially available columns were tested representing diethylaminoethyl (DEAE) groups, polyethylenimine (PEI) groups and carboxymethyl (CM) groups respectively. Neutral, weakly acidic (phenol) and basic (amine) compounds were used to assess the impact of CO₂ on the retention of different analyte classes. Zeta potential measurements were used to examine the degree of protonation/deprotonation of surface groups in contact with CO₂-modified water or aqueous mixtures.

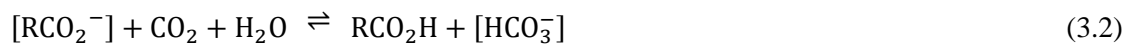
3.2 Theory

The reversible “switch” results from the protonation of surface-bound basic groups when CO₂ is introduced into the system in the presence of water (Equation 3.1). In

particular, amine, amidine, phenolate, and carboxylate groups have been identified as CO₂-switchable groups.²² Figure 3.1 shows how retention factor *k* is expected to be affected by the hydrophobicity change of the stationary phase particles when CO₂ addition and removal causes the switchable groups to switch between ionic/hydrophilic and neutral/hydrophobic. In the case of amine groups, addition of CO₂ causes the neutral and hydrophobic groups to become cationic and hydrophilic, while removal of the CO₂, by heating or purging with an inert gas (*e.g.* N₂, Ar) leads to deprotonation, switching the amine groups to a neutral and hydrophobic form.



Although not as widely explored, an opposite way of CO₂ switching, in Equation 3.2, has also been reported. Instead of amines as the switchable groups, carboxylate and phenolate groups can undergo CO₂ switching. The addition of CO₂ switches the anionic basic group to a hydrophobic, uncharged form.^{23, 24} Therefore, two amine based columns and one carboxymethyl column were tested in this study for their CO₂ switching performance.



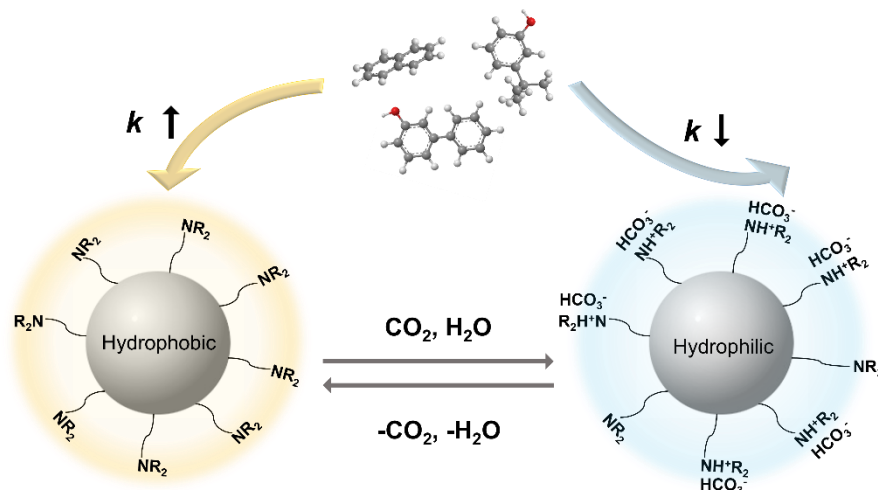


Figure 3.1 CO_2 induced “switching” the surface properties of amine functionalized stationary phase particles. Tertiary amine bonded phase before (left) and after (right) exposure to CO_2 . The neutral tertiary amine presents a hydrophobic state favourable for retention (\uparrow retention factor, k) while the protonated tertiary amine phase favours elution ($\downarrow k$).

3.3 Experimental

3.3.1 Instrumentation

Chromatographic separations of all compounds were performed at room temperature with an Agilent 1100 HPLC system. A flow rate of 1.0 mL/min with an injection volume of 5 μL was applied. The UV/vis. detector was set to monitor 254 nm. Reciprocating piston pumps were used to mix solvents therefore CO_2 is manipulated more easily than in bulk liquids. All system control and data acquisition were performed with the CDS ChemStation software. The retention factors (k) were obtained under isocratic conditions. All k values were derived from repeated measurements ($n \geq 5$) to obtain the relative standard deviation.

Compressed liquefied CO₂ (Bone Dry Grade) and a two-stage regulator were acquired from Praxair Canada Inc. (Mississauga, ON, Canada). An Omega FL-1461-S rotameter (Stamford, CT, USA) and a stainless-steel solvent filter (10 µm porosity) from VWR International (Radnor, PA, USA) were utilized in the CO₂ delivery system. The vacuum degasser of HPLC was bypassed to allow the CO₂ laden solvents to be introduced into the pumping system.

3.3.2 The CO₂ Delivery System

The addition of a gas to a mobile phase is contrary to conventional HPLC wisdom. The formation of bubbles can cause considerable trouble for the pumping, separation, and detection components of the liquid chromatography system. Dissolved gas is typically removed by either sparging with helium or more recently by vacuum degassing.²⁵ In this study we intentionally introduce CO₂ into the mobile phase to facilitate a “hydrophobicity switch” of the stationary phase. It was expected that using mobile phases heavily laden with CO₂ would cause significant pumping and mobile phase delivery difficulties. Therefore, a CO₂ delivery system was assembled (Figure 3.2) to probe the system capability for different CO₂ mobile phase concentrations and sparging flow rates. Local atmosphere pressure was monitored and it averaged 100.7 kPa with less than 2% daily variance.²⁶ Room temperature was maintained at 23 °C (± 1 °C). Based on the variance of Henry’s constant and acid dissociation constant depending on temperature and pressure,²⁷ ²⁸ the pH variance of CO₂ dissolved water at 1 bar was found to be less than 1.4%. Therefore, these variations should not significantly influence the pH of CO₂ dissolved water.

To initially form a CO₂-saturated mobile phase a high flow rate of CO₂ is desired, but once the solution is saturated with CO₂, that saturation could be maintained with lower sparging flow rates of 20 mL/min without excessive bubble formation and resulting pressure fluctuations. Therefore, a CO₂ sparging flow rate of 20 mL/min was used to maintain mobile phase saturation. However, with optimization of the equipment, it is quite likely that much lower CO₂ flow rates would be sufficient to maintain consistent carbonation in the solvent reservoir. In order to prepare mobile phases with different concentrations of dissolved CO₂, a CO₂-free solvent (i.e. reservoir A, 80% water 20% acetonitrile) and a CO₂-saturated solvent (reservoir B, otherwise identical with A in composition) were mixed in different ratios to investigate the backpressure stability of different CO₂ concentrations. Figure 3.3 shows the pressure fluctuations encountered when pumping an 80/20 water/acetonitrile mobile phase with different percentages of CO₂-saturated solvent (B). The backpressure is stable (i.e. < 1% variation) over days when 25% CO₂-saturated solvent is applied. Pumping 50% CO₂-saturated solvent shows a stable pressure plot although the pressure might drop after operation for hours. In that case, the pump has to be primed again. However, when using 100% CO₂-saturated solvent the pressure can vary significantly due to bubble formation in the fluidic system which can prevent a complete HPLC experiment or cause considerable retention time variation. Therefore, < 50% CO₂-saturated solvent was used to perform all the chromatographic experiments. The pH of different percentage CO₂-saturated solvent is discussed in the results section (*vide infra*).

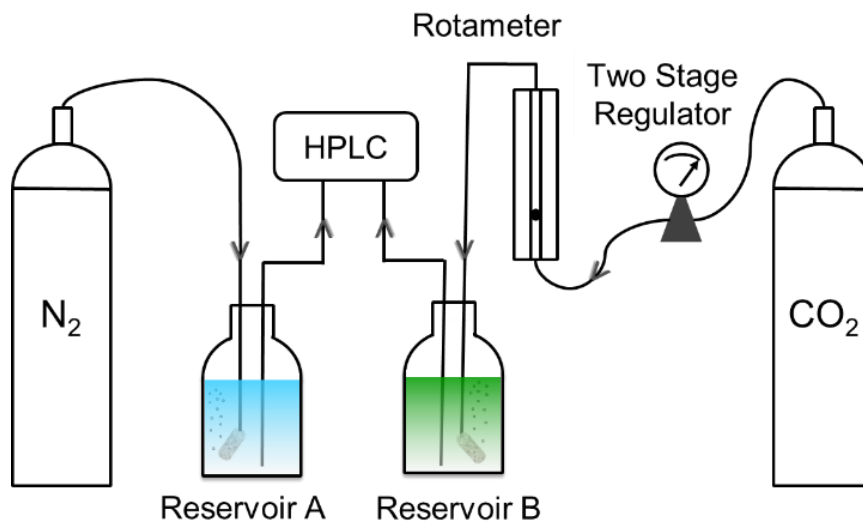


Figure 3.2 Gas delivery system coupled with HPLC, including a two-stage regulator, a rotameter, and a gas dispersion tube. (Gaseous CO_2 flow rate, 20 mL/min; HPLC degasser bypassed; < 50% CO_2 -saturated solvent B utilized). N_2 bubbling was used to remove the dissolved ambient CO_2 in Reservoir A and maintain pH 7.0.

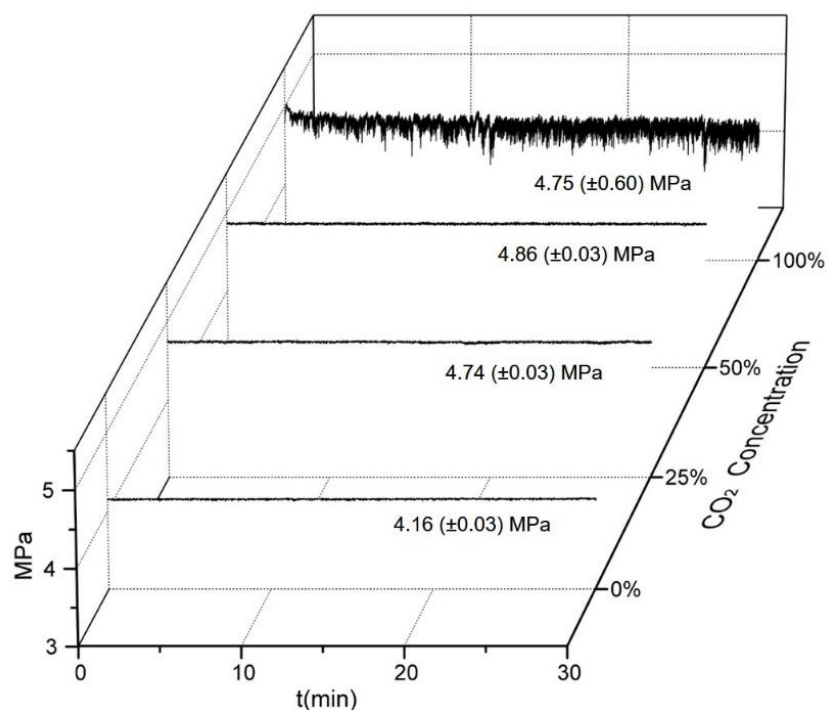


Figure 3.3 System backpressure plots for 0%, 25%, 50%, and 100% CO_2 -saturated solvents. Conditions: Agilent Bio-monolith DEAE column; mobile phase: 80/20 (v/v%) H_2O /acetonitrile; flow rate: 1.0 mL/min.

3.3.3 Chromatographic Columns

Three different types of commercial columns (Table 3.1) were utilized to perform the chromatographic experiments. The Agilent Bio-monomer Diethylaminoethyl (DEAE) column was obtained from Agilent Technologies (Santa Clara, CA, USA). The polyethylenimine (PEI) functionalized column (CA-103) and carboxymethyl (CM) functionalized column (CCM-103) were obtained from Eprogen (Downers Grove, IL, USA). Ultrapure water was obtained from a Milli-Q Purification System (Bedford, MA, USA). HPLC grade acetonitrile and glacial acetic acid (HOAc) were purchased from Fisher Scientific (Ottawa, ON, CANADA). All analytes were acquired from Sigma-Aldrich (Milwaukee, WI, USA).

3.3.4 Sample Preparation

Six analytes were tested (naphthalene, anthracene, 3-*tert*-butylphenol, 3-phenylphenol, 4-butylaniline, and diphenylamine). A table of the structures, *Log P* and *pK_a* values is included in Table 3.2. The stock solutions (5.0 mg/mL) of all analytes were prepared in acetonitrile and then diluted 10-fold using a mixed solvent (water/acetonitrile 80/20 v/v). The final concentration of each individual compound was 0.50 mg/mL. Mixtures of compounds were prepared by diluting the individual stock solutions. *Mixture A* had a final concentration of 0.10 mg/mL naphthalene, 0.50 mg/mL 3-*tert*-butylphenol and 0.25 mg/mL 3-phenylphenol. *Mixture B* contains 0.25 mg/mL anthracene, 0.25 mg/mL 4-butylaniline and 0.10 mg/mL diphenylamine.

Table 3.1 Column dimensions (obtained from manufacturer data sheets).

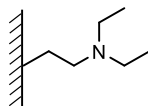
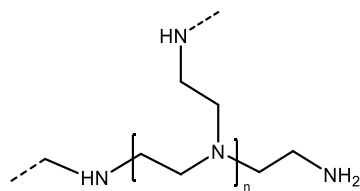
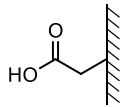
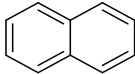
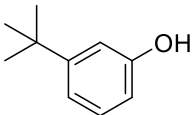
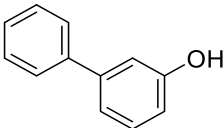
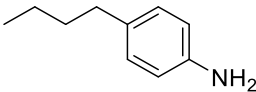
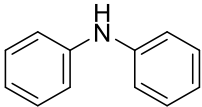
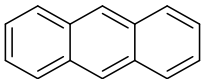
Columns	Support	Dimensions (L × I.D. mm × mm)
<p>Diethylaminoethyl (DEAE)</p> 	<p>Functionalized poly(glycidyl methacrylate-co-ethylene dimethacrylate)</p>	<p>5.2 × 4.95</p>
<p>Polyethylenimine (PEI)</p> 	<p>Crosslinked polyethylenimine phase on 6.5 μm, 300 Å silica</p>	<p>100 × 4.6</p>
<p>Carboxymethyl (CM)</p> 	<p>Polyamide coating containing carboxymethyl groups on 6.5 μm, 300 Å silica</p>	<p>100 × 4.6</p>

Table 3.2 Analytes structure, $\log P$ and pK_a values.²⁹

Number	Analyte	Structure	$\log P$	pK_a (pK_{aH})
1	Naphthalene		3.0	-
2	3-tert-Butylphenol		3.2	10.1
3	3-Phenylphenol		3.3	9.8
4	4-Butylaniline		3.0	4.9
5	Diphenylamine		3.4	0.8
6	Anthracene		4.0	-

3.3.5 $\Delta\Delta G^\circ$ Determination

The retention of compounds is associated with the chemical equilibrium of the analytes between the stationary phase and the mobile phase. In the Gibbs free energy equation, $\Delta G^\circ = -RT \ln K$, K refers to the equilibrium constant of the retention process. Based on the relationship between K and retention factor k ($K = k/\beta$), $\Delta\Delta G^\circ$ is expressed in Equation 3.3 assuming a constant phase ratio β . α represents the ratio of the retention factors for the modified condition (k_2) and modifier-free condition (k_1), $\alpha = k_2/k_1$. The Gibbs free energy difference ($\Delta\Delta G^\circ$) was used to evaluate the energy difference in retention

between conditions.³⁰ Obtaining a positive value for the Gibbs free energy difference ($\Delta\Delta G^\circ$) suggests that elution is favoured, whereas a negative value indicates that retention is favoured. Retention factor data (k) was obtained for modifier-free and modified mobile phases (10% CO₂-saturated solvent and 0.05% (v/v) acetic acid) to determine $\Delta\Delta G^\circ$.

$$\Delta\Delta G^\circ = -RT \ln\alpha \quad (3.3)$$

3.3.6 Zeta Potential Measurement

Zeta potential measurements (ζ) were carried out according to an approach developed by Buszewski *et al.*³¹⁻³³ Prior to preparing the suspension, the bulk polymer of DEAE stationary phase was ground into a fine powder. Briefly, the stationary phase material was rinsed with ultrapure water, methanol and vacuum dried. A 0.20 mg/mL suspension sample was prepared in ultrapure water and agitated in an ultrasonic bath for 2 min. The measurement was carried out immediately after removing the suspension from the ultrasonicator. To observe the zeta potential change with CO₂, 5.0 mL gaseous CO₂ in a syringe was purged via a needle into 900 μ L of the suspension sample in 10 seconds. Then the suspension was shaken for another 10 seconds manually. The CO₂ purged suspension was immediately transferred into the folded capillary cell for zeta potential measurement. The acetic acid modified suspension was prepared by adding 0.05% acetic acid (v/v) to the suspension. All measurements were determined (n=6) using a Zetasizer Nano ZS (Malvern Instruments Ltd, Worcestershire, UK) by measuring electrophoretic mobility (μ_{ep}) of the particles.³⁴ Both the viscosity (η) and dielectric constant (ϵ) of water were used in the calculation of ζ based on Henry's Law in Equation 3.4. The Smoluchowski approximation was utilized with $f(Ka) = 1.5$.

$$\mu_{ep} = \frac{2\varepsilon\zeta f(Ka)}{3\eta} \quad (3.4)$$

3.4 Results and discussion

3.4.1 CO₂ Partial Pressure and pH

At a given temperature, the pH of an aqueous solution containing dissolved CO₂ is determined by the partial pressure (pCO_2) of carbon dioxide above the solution. According to the Henry's constant of CO₂ and the dissociation constant of carbonic acid, the pH of CO₂ dissolved water at different partial pressure level can be calculated and is shown in Figure 3.4.^{20, 35} The presence of CO₂ in water ($pCO_2 = 1$ bar) results in a solution with pH 3.9. Reducing the CO₂ partial pressure to 0.1 bar produces a solution with pH 4.4. To examine the pH of CO₂-containing water pumped through the HPLC pumps, we mixed CO₂-saturated water (1 bar) with N₂-bubbled water in different ratios producing water with different CO₂ concentrations corresponding to different partial pressure levels. For example, 1% CO₂-saturated water at 1 bar corresponds to a CO₂ partial pressure of 0.01 bar. The mixed fluids were collected after the pump (column not connected), and the pH was measured after 10.0 mL of mobile phase had been collected. A plot of measured pH and pCO_2 is shown in Figure 3.4. Experimental data shows that 100% CO₂-saturated water (1 bar) presents pH 4.0 (± 0.1 , $n \geq 3$), and 10% CO₂-saturated water (0.1 bar) presents pH 4.6 (± 0.1). The measurements also outline the range of pH values accessible with a CO₂ delivery system (pH 3.9 ~ 6.5 with ≤ 1 bar pCO_2). In theory, the upper end of the pH range could be expanded significantly through the use of basified H₂O as the co-phase. The lower end of the pH range could be potentially extended using compressed CO₂ in the system. The calculated pH of carbonated water at different pCO_2 correlates well with the measured

pH of the HPLC mixed mobile phases verifying that the saturated CO₂/ ultrapure water mixing is reliable for delivering reproducible mobile phase compositions. However, there is a constant systematic error associated with the pH determination; as the mobile phase is being collected for pH determination it begins to re-equilibrate with air.

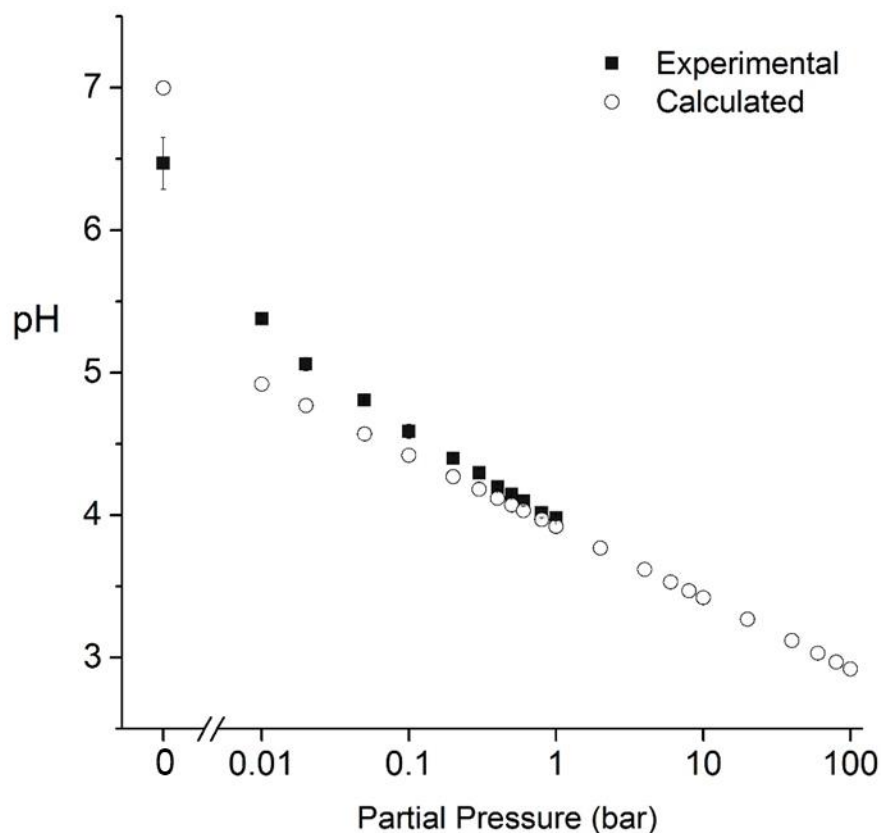


Figure 3.4 The measured pH of CO₂ dissolved in water produced post-pump by mixing different ratios of CO₂-saturated water (1 bar) and N₂ bubbled water; calculated pH of CO₂ dissolved water at different CO₂ partial pressure. The plot identifies the pH range accessible with a water / CO₂-modified solvent system.

3.4.2 Diethylaminoethyl Column (DEAE)

To investigate the ability to switch the hydrophobicity of a stationary phase we utilized a reversed phase separation performed with the DEAE column. In early reports,

diethylaminoethyl groups have been shown to be very promising as CO₂-switchable groups.³⁶ Although poor chromatographic efficiency stemming from the column's dimensions was both anticipated and observed, this column serves as a good model material to explore the concept of a CO₂-based switch of column hydrophobicity. The CO₂-saturated solvent (B) and CO₂-free solvent (A) were mixed in different ratios to examine how the CO₂ content of the eluent affects the chromatographic behaviour of each analyte. A plot of retention factors (n=6) with errors is shown in Figure 3.5. The RSD% of retention factors for all the analytes are less than 3.0%.

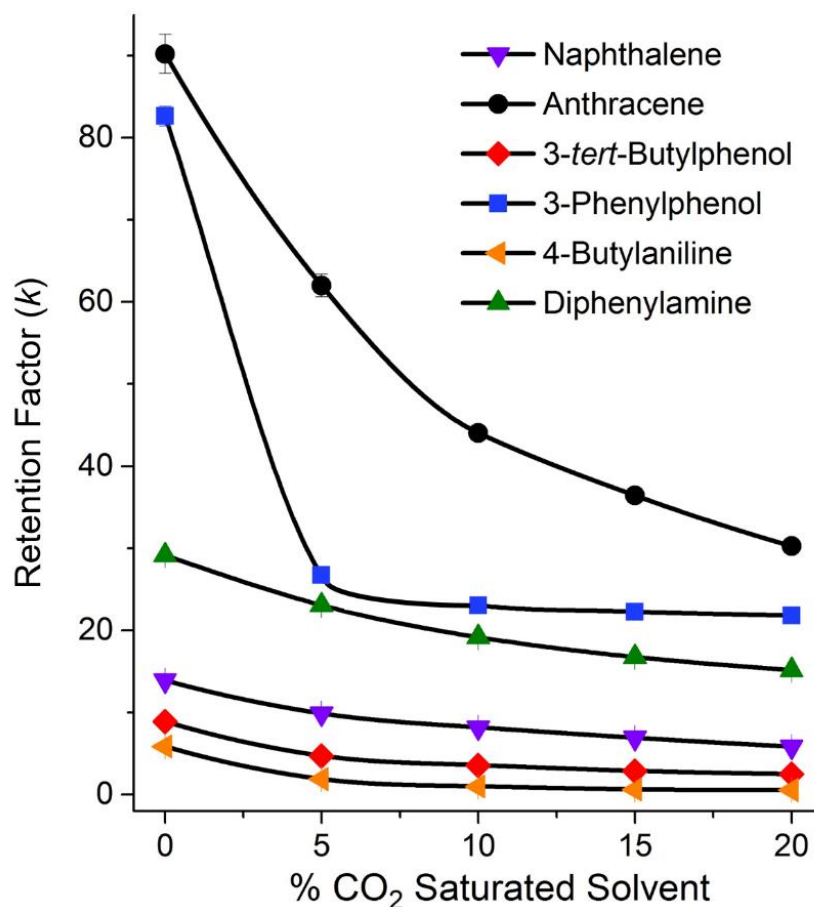


Figure 3.5 Plots of retention factors with varying percentages of CO₂-saturated solvent measuring naphthalene, anthracene, 3-*tert*-butylphenol, 3-phenylphenol, 4-butylaniline, and diphenylamine.

Conditions: Agilent Bio-monolith DEAE column; Solvent A: 80% water/20% acetonitrile; Solvent B: identical to A except saturated with CO₂ at 1 bar; flow rate: 1.0 mL/min; UV 254 nm.

The retention decreased for anthracene and naphthalene with increased amounts of CO₂-modified solvent. As Figure 3.5 shows, naphthalene and anthracene showed retention factors of 13.9 and 90.2 respectively on the DEAE column using the CO₂-free solvent (0%). When 5% CO₂-saturated solvent was used, the retention factors of both compounds were decreased to 9.9 and 62.0 respectively. Higher percentages of CO₂-saturated solvent reduced the retention factors further. This is a simple scenario where both analytes lack ionizable groups, so it is assumed that any retention changes are due solely to changes to the stationary phase. The absolute change in retention time is larger for anthracene than naphthalene however the relative retention time differences are very similar (32% and 29% respectively). The retention factors of all the other compounds also decrease with the addition of CO₂ as shown in Figure 3.5. Interestingly, 3-phenylphenol exhibits a different selectivity with increasing CO₂ concentration where it shows a more significant change initially at the introduction of CO₂ and a reduced change at higher CO₂. This experiment was carried out several times to ensure validity. Additionally, zeta potential measurements in Table 3.3 provide additional evidence for the stationary phase surface switch. Zeta potential measurements were carried out with CO₂-modified solvent, compared to both a modifier-free and 0.05% acetic acid-modified sample (pH 3.4). Suspended in water, DEAE particles exhibit a positive zeta potential of 17.1 ± 3.6 mV, but when CO₂ is introduced, the zeta potential almost doubles to 30.4 ± 1.9 mV. The increased zeta potential is also observed in 0.05% acetic acid, giving an even greater value of 37.4 ± 0.6 mV. The zeta potential data corroborates the chromatography data where the introduction of CO₂ causes

the stationary phase to switch to a protonated, more hydrophilic form reducing the retention factor of compounds.

Table 3.4 lists the $\Delta\Delta G^\circ$ values for the test compounds on the DEAE column. The positive values of Gibbs free energy difference ($\Delta\Delta G^\circ$) show that desorption is favoured when CO₂ is present in the system, which reduces the retention time. The majority of the compounds exhibit $\Delta\Delta G^\circ$ between 1.9 and 3.3 kJ·mol⁻¹ with CO₂-modified solvents. The $\Delta\Delta G^\circ$ value was very similar for naphthalene (2.3) and anthracene (2.7). The phenols exhibit a slightly higher value ≈ 3.3 , suggesting secondary interactions (i.e. electrostatic forces) affecting the selectivity with or without CO₂. 4-Butylaniline, however, exhibits the most significant $\Delta\Delta G^\circ$ at 6.0 kJ·mol⁻¹. Of the test compounds, 4-butylaniline has a pK_{aH} value of 4.9, which falls within the range of pH values observed in water/CO₂ mixtures (Figure 3.4). As a result, not only does the stationary phase exhibit reduced hydrophobicity due to protonation but 4-butylaniline also becomes protonated (positively charged) and therefore sorption is even less favoured due to electrostatic repulsion. In particular, it is interesting that the retention factor of the compounds had a significant decrease when only 10% CO₂-saturated solvent was applied. It implies that even with 10% CO₂, the hydrophobicity of the column can be switched quite efficiently with stable backpressure of the system maintained. In brief, retention on DEAE column is switched significantly by CO₂-modified solvents and a selectivity change was observed for 4-butylaniline. Although the efficiency of the column is low, it demonstrated the feasibility of using tertiary amine groups as a switchable stationary phase. Elution strength and selectivity can be adjusted using CO₂-modified solvents. It should be noted that, because the chromatographic peaks

of those compounds are very broad (e.g. peak width > 10 min), this column is not appropriate for efficient separation.

Table 3.3 Zeta potential (mV) of stationary phase suspensions.

Columns	Modifier-free	CO ₂	0.05% HOAc
DEAE	17.1 ± 3.6	30.4 ± 1.9	37.6 ± 0.6
PEI	-13.8 ± 2.2	-4.5 ± 2.4	3.3 ± 2.5
CM	-34.4 ± 1.8	-35.0 ± 1.8	-25.7 ± 0.9

Table 3.4 Gibbs free energy difference ($\Delta\Delta G^\circ$, kJ mol⁻¹) of chromatographic adsorption between the modified solvents and the modifier-free solvents. (*data was not acquired due to non-retention of 4-butylaniline)

Analytes	Columns					
	DEAE		PEI		CM	
	Modifiers					
	CO ₂	HOAc	CO ₂	HOAc	CO ₂	HOAc
Naphthalene	2.3	5.3	2.7	3.0	0.1	0.0
Anthracene	2.7	6.3	2.3	3.8	0.2	0.0
3-tert-Butylphenol	3.3	8.1	3.9	4.5	0.0	0.1
3-Phenylphenol	3.3	6.8	3.3	4.1	0.1	0.1
4-Butylaniline	6.0	-*	-*	-*	3.9	5.5
Diphenylamine	1.9	6.6	2.8	3.5	0.1	0.0

3.4.3 Polyethylenimine Column (PEI)

Another commercial amine-functionalized column was examined in the presence of CO₂. The PEI column comprises a silica particle support, with crosslinked polyethylenimine groups. The longer column length (100 × 4.6 mm) and more conventional dimensions (6.5 μm, 300 Å) should improve separation efficiency. Furthermore, the PEI column does not require an organic modifier to produce reasonable analyte retention times (i.e. < 40 minutes) and therefore, in terms of organic solvent consumption, is more environmentally friendly. The enhanced resolution and efficiency enabled the simultaneous analysis of two test mixtures. The test compounds were prepared in two mixtures that were chromatographically discernable. Naphthalene, 3-*tert*-butylphenol and 3-phenylphenol were present in *Mixture A*, and were separated on the PEI column (Figure 3.6 a). The compounds 4-butylaniline, diphenylamine and anthracene were present in *Mixture B* (Figure 3.6 b). The chromatographic separation is reproducible with RSD% (n ≥ 5) of retention time less than 2.4%.

As with the DEAE column there is a pattern of decreasing retention time for each of the analytes with the addition of CO₂. Furthermore, the greater the CO₂ concentration the more the retention of analytes was reduced. The retention factor of each of the test compounds decreases significantly with the introduction of 10% CO₂-saturated water. Higher percentages of CO₂-saturated water cause a further reduction in retention time, however, the change is not as significant.

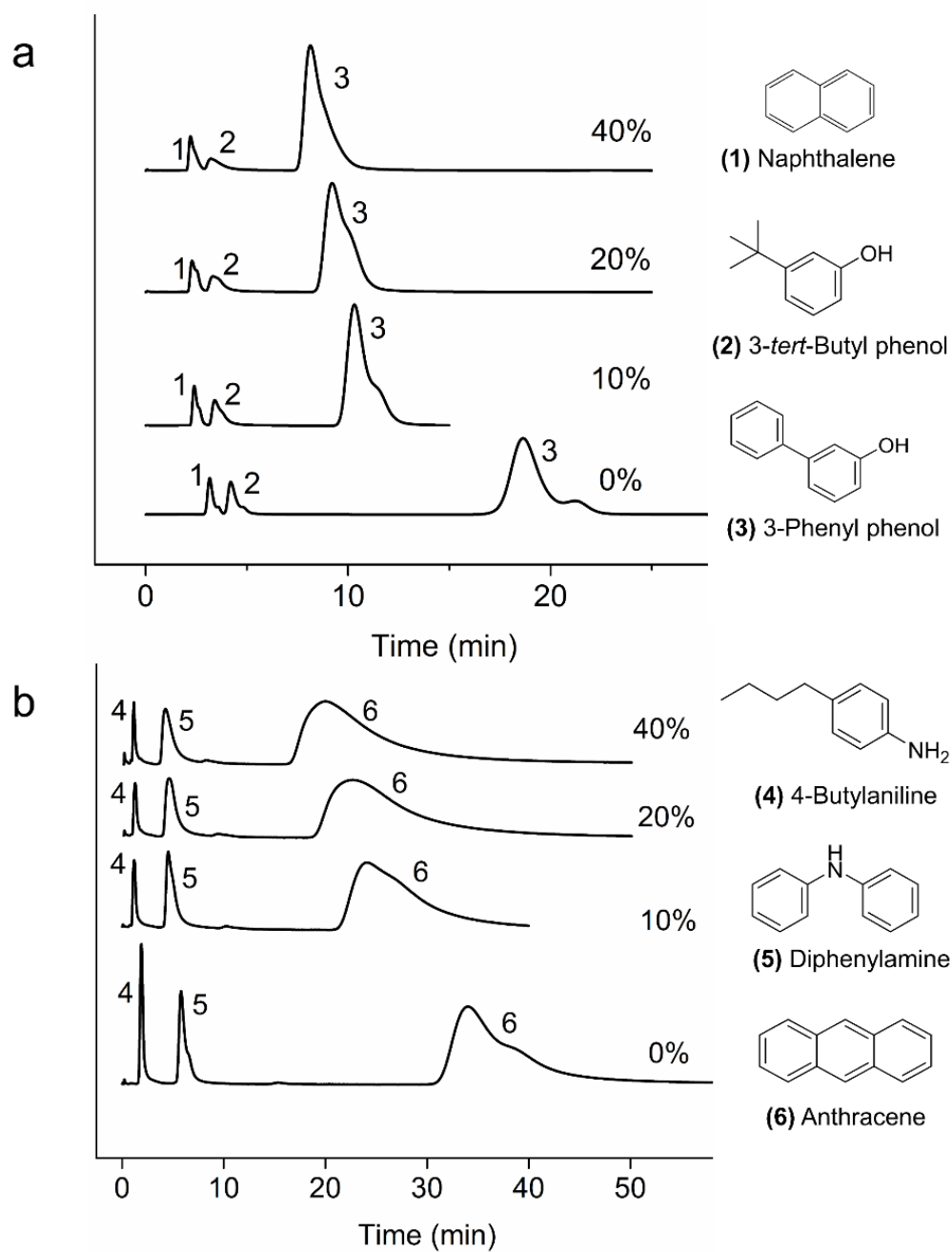


Figure 3.6 Chromatograms produced using different CO₂-modified solvents (%B) for a) a mixture of naphthalene, 3-*tert*-butylphenol, 3-phenyl phenol and b) a mixture of 4-butylaniline, diphenylamine and anthracene. Conditions: Eprogen PEI column; solvent A: water, solvent B: CO₂-saturated water; isocratic; flow rate: 1.0 mL/min; UV 254 nm.

Although the PEI column showed limited efficiency, it is valuable to compare the performance and solvent consumption between CO₂/water solvent and conventional acetonitrile/water system. Therefore, we analyzed the previous chromatograms produced using 85%/15% water/acetonitrile phase and 40% CO₂ saturated water and compared their efficiency, resolution, analysis time and organic solvent consumption (Figure 3.7). The separation using 85%/15% water/acetonitrile phase presents a slightly higher theoretical plate number, N=105 (for 3-phenylphenol), while the separation using 100% water (40% CO₂ saturated) presents a plate number of 86 (for 3-phenylphenol). It was found that naphthalene and 3-*tert*-butylphenol were not resolved completely using either conditions, but the 85%/15% water/acetonitrile mobile phase produces higher efficiency. Conversely a resolution of 0.476 is shown for compound 1 and 2 using 85%/15% water/acetonitrile mobile phase compared to 0.842 observed when using 40% CO₂ saturated water. The analysis time is comparable for both conditions. Theoretically speaking in this example, a saving of 15% organic solvent can be achieved if CO₂ modified solvent is utilized. This results in up to \approx 17 liters of solvent saving/ instrument (analytical scale) in a year (1.0 mL/min, 5 days per week 8 hours/day operation), however, this saving would be considerably higher for preparative scale separations.

Polyethylenimine is a crosslinked polymer containing primary, secondary and tertiary amine groups (Table 3.1) unlike DEAE which presents a single tertiary amine functionality. Although it is difficult to characterize the ionization state of the primary, secondary and tertiary amine groups on the stationary phase surface, we are able to see the change of zeta potential on the stationary phase with the addition of CO₂. PEI particles exhibit a zeta potential value of -13.8 ± 2.2 mV in the absence of CO₂. The negative zeta

potential stems presumably from the presence of silanols on the surface of silica, some of which are deprotonated at pH 7.0 (similar to the observed negative zeta potential on silica microfluidic substrate walls).³⁷⁻³⁹ When CO₂ is bubbled into a suspension of the PEI functionalized particles, the zeta potential becomes close to neutral at -4.5 ± 2.4 mV. The decreased pH partially protonates the amine groups causing the switch to a more positive potential. This information corroborates the reduced retention shown as a positive $\Delta\Delta G^\circ$ (Table 3.4). However, the zeta potential measurements should be only taken as a guide. The in-solution measurements do not directly mimic the conditions within a packed column where surface charge on adjacent particles will influence surface pK_a 's. Improved efficiency was observed due to both smaller particle size and longer column compared to the DEAE monolithic disk. With a 100% water mobile phase and the polyethylenimine column, the test compounds exhibited comparable retention to an 80% water / 20% acetonitrile mobile phase on diethylaminoethyl column. Similar retention with a lower elutropic strength suggests that the PEI column possesses a lower hydrophobicity than the DEAE column which enables more environmentally friendly “aqueous only” chromatography.

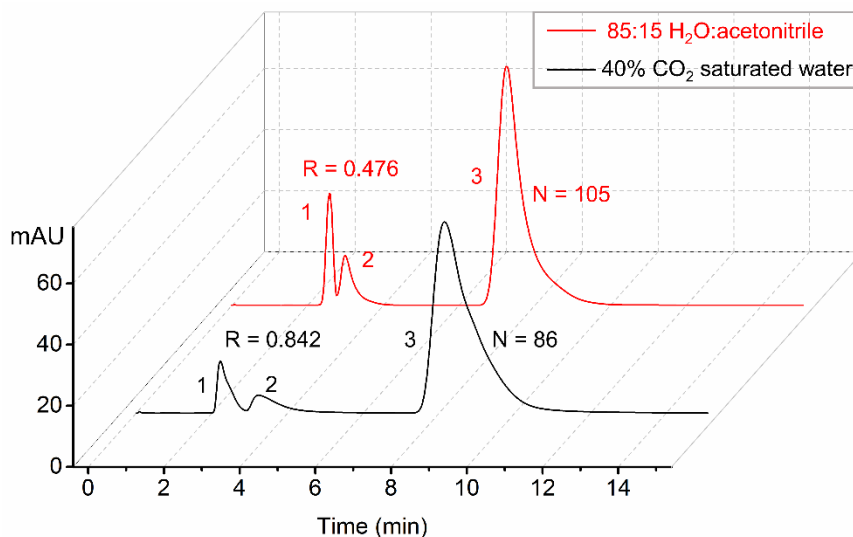


Figure 3.7 Comparison of an acetonitrile/H₂O and a CO₂-saturated water mobile phase based separation using the PEI column.

3.4.4 Carboxymethyl Column (CM)

The CM column possesses a silica particle support with carboxymethyl functional groups. An eluent mixture of 95/5 (v/v%) water/acetonitrile was utilized to perform a separation of compounds (*Mixtures A* and *B*) at an isocratic condition. The chromatographic separation is reproducible with RSD% ($n \geq 5$) of retention time less than 4.1%. In theory this column could produce an increased retention factor responding to CO₂, according to Equation 3.2 where an increase in hydrophobicity of the stationary phase is expected by the addition of CO₂. However, zeta potential measurements (Table 3.3) showed that the surface charge of CM particles did not significantly switch upon the addition of CO₂ to the mobile phase. Chromatograms of *Mixtures A* and *B* suggested the retention times were virtually identical with either CO₂-modified or CO₂-free solvent (Figure 3.8 a and b) with the exception of 4-butylaniline. The retention and zeta potential

data both suggest that the pH change by addition of CO₂ did not cause significant protonation / deprotonation of carboxylic acid groups on the surface of the CM stationary phase. Using ambient conditions, the accessible solution pH range is limited to 3.9-6.5. To produce a significant switch on the CM phase a larger accessible pH range should be required. Therefore, analytes without a pK_a or pK_{aH} in the accessible range (3.9-6.5) do not show appreciable changes in retention behaviour. The 4-butylaniline was the only compound that showed a significant change in retention time when CO₂-modified solvents are applied. Increasing the CO₂-saturated solvent concentration from 10%, to 20% and 40% CO₂ decreased the retention time accordingly. This is explained by considering the ionization of 4-butylaniline. The percentage protonation of 4-butylaniline is plotted versus pH in Figure 3.9. The solution pK_{aH} of 4-butylaniline is 4.9, while the pH of CO₂-modified solvent is 4.59 (i.e. 10% solvent B). Under these conditions a significant portion of the 4-butylaniline is protonated, from the addition of CO₂. Therefore, for analytes having pK_a (or pK_{aH}) values within the pH range accessible with carbonated water, the amount of carbonation significantly influences retention, which provides the control of compound selectivity. Overall, the CM column is not switchable with pH changes caused by the introduction of CO₂, but a selectivity change due to analyte ionization is observed. This selectivity control might be very useful for the separation of compounds with accessible pK_a 's.

In summary, for the purpose of validating the concept, the above tests were performed using commercially available columns that were never designed for such use. Future work will involve the design and testing of new columns specifically for use with CO₂-modified aqueous eluent. Such columns should make it possible to further

demonstrate the concept of CO₂-switchable stationary phases while obtaining better resolution and peak shapes than were possible using the currently-available columns.

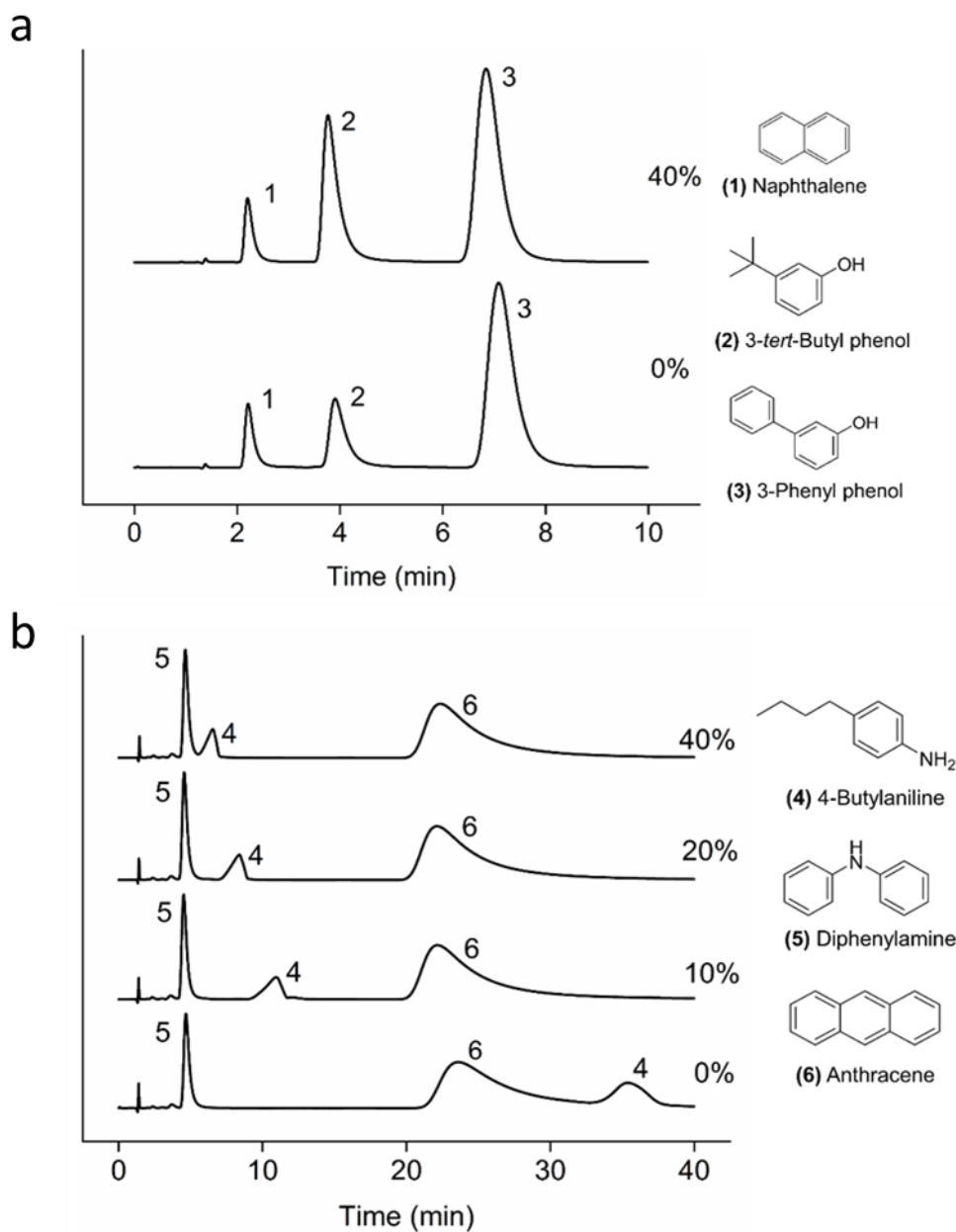


Figure 3.8 Chromatograms produced using different CO₂-modified solvents (%B) for mixture of a) naphthalene, 3-*tert*-butylphenol, 3-phenylphenol; b) 4-butylaniline, diphenylamine, anthracene. Conditions: Eprogen CM column; solvent A: 95% H₂O/5% acetonitrile; solvent B: CO₂-saturated solvent A; isocratic; flow rate: 1.0 mL/min; UV 254 nm.

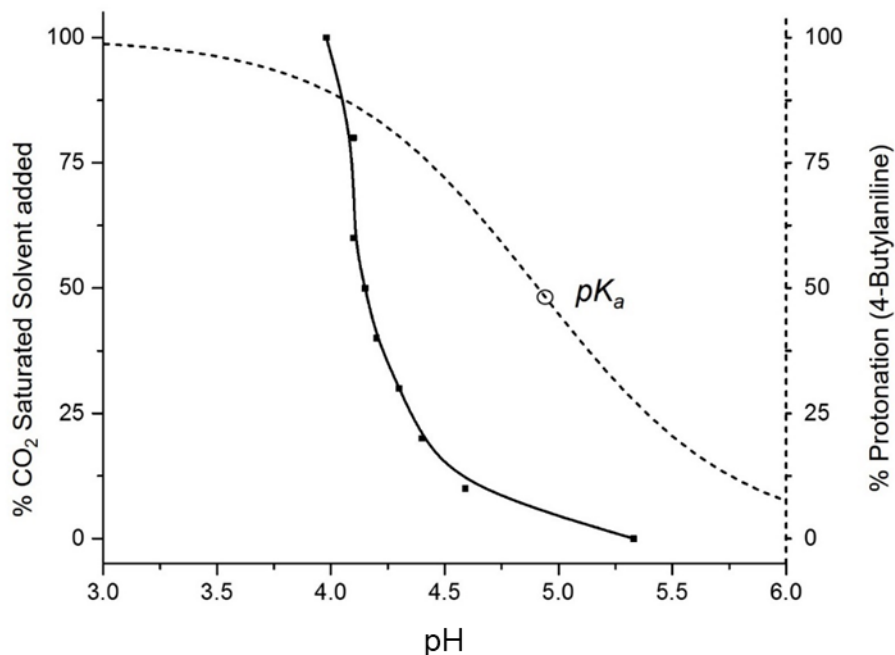


Figure 3.9 Plot of pH vs percentage of CO₂ saturated water in HPLC as the mobile phase (solid line), percentage protonation of 4-butylaniline versus pH (dashed line).

3.5 Conclusions

In this work, CO₂ is shown to be a promising mobile phase modifier in high performance liquid chromatographic systems. CO₂-modified phases offer advantages such as lower environmental impact and lower cost (purchase and disposal). The mobile phase pH can be carefully controlled by mixing carbonated and noncarbonated water providing an accessible pH range of 3.9 - 6.5. The investigation verified the CO₂-triggered hydrophobicity switch of the amine-based columns (DEAE and PEI). The PEI column can be used for separation with a 100% aqueous mobile phase (i.e. no organic modifier). The CM column was not switched by a CO₂ triggered pH change therefore indicating more significant CO₂ concentrations may be required for the switching. The observed selectivity change of 4-butylaniline on the CM column is potentially valuable for the separation of compounds with accessible pK_a 's. The addition of CO₂ to mobile phases has not been

extensively explored and may be a powerful tool to tune chromatographic selectivity. This conceptual study, employing isocratic liquid chromatographic conditions, demonstrates the ability to change the retention behavior of analytes with the addition of CO₂ to the mobile phase. The effects of dynamically changing the CO₂ concentration of the mobile phase will be the subject of a future study featuring custom stationary phases to enhance chromatographic resolution and efficiency. Furthermore, chromatographic performance and accessible pH range could be further improved using pressures and chromatographic particle sizes associated with ultrahigh pressure chromatography.

Although the columns were demonstrated in analytical liquid chromatography one can envision the possibility of employing a similar paradigm for solid phase extraction and preparative processes, where compounds may be separated with carbonated water only. The use of CO₂ as a “temporary acid” should aid in reducing the environmental footprint of chemical separations and analysis.

3.6 References

1. D. S. Sholl and R. P. Lively, *Nature*, 2016, **532**, 435-437.
2. C. J. Welch, N. J. Wu, M. Biba, R. Hartman, T. Brkovic, X. Y. Gong, R. Helmy, W. Schafer, J. Cuff, Z. Pirzada and L. L. Zhou, *Trac-Trend Anal Chem*, 2010, **29**, 667-680.
3. J. Plotka, M. Tobiszewski, A. M. Sulej, M. Kupska, T. Gorecki and J. Namiesnik, *J Chromatogr A*, 2013, **1307**, 1-20.
4. U. R. Desai and A. M. Klibanov, *J Am Chem Soc*, 1995, **117**, 3940-3945.
5. G. M. Whitesides and P. E. Laibinis, *Langmuir*, 1990, **6**, 87-96.
6. M. A. Stuart, W. T. Huck, J. Genzer, M. Muller, C. Ober, M. Stamm, G. B. Sukhorukov, I. Szleifer, V. V. Tsukruk, M. Urban, F. Winnik, S. Zauscher, I. Luzinov and S. Minko, *Nat Mater*, 2010, **9**, 101-113.
7. A. K. Kota, G. Kwon, W. Choi, J. M. Mabry and A. Tuteja, *Nat Commun*, 2012, **3**, 1025.
8. K. Nagase, M. Kumazaki, H. Kanazawa, J. Kobayashi, A. Kikuchi, Y. Akiyama, M. Annaka and T. Okano, *ACS Appl Mater Interfaces*, 2010, **2**, 1247-1253.
9. N. Li, L. Qi, Y. Shen, Y. Li and Y. Chen, *ACS Appl Mater Interfaces*, 2013, **5**, 12441-12448.
10. Y. Shen, L. Qi, X. Y. Wei, R. Y. Zhang and L. Q. Mao, *Polymer*, 2011, **52**, 3725-3731.
11. Y. Liu, P. G. Jessop, M. Cunningham, C. A. Eckert and C. L. Liotta, *Science*, 2006, **313**, 958-960.
12. K. J. Boniface, R. R. Dykeman, A. Cormier, H. B. Wang, S. M. Mercer, G. J. Liu, M. F. Cunningham and P. G. Jessop, *Green Chem*, 2016, **18**, 208-213.
13. S. Kumar, X. Tong, Y. L. Dory, M. Lepage and Y. Zhao, *Chem Commun*, 2013, **49**, 90-92.
14. Q. Yan and Y. Zhao, *Chem Commun*, 2014, **50**, 11631-11641.
15. V. Fischer, K. Landfester and R. Munoz-Espi, *Acs Macro Lett*, 2012, **1**, 1371-1374.
16. S. T. Lee, S. V. Olesik and S. M. Fields, *J Microcolumn Sep*, 1995, **7**, 477-483.

17. M. C. Beilke, M. J. Beres and S. V. Olesik, *J Chromatogr A*, 2016, **1436**, 84-90.
18. C. West, E. Lemasson, S. Bertin, P. Hennig and E. Lesellier, *J Chromatogr A*, 2016, **1440**, 212-228.
19. Y. Cui and S. V. Olesik, *J Chromatogr A*, 1995, **691**, 151-162.
20. L. Irving, *J Biol Chem*, 1925, **63**, 767-778.
21. S. T. Lee, T. S. Reighard and S. V. Olesik, *Fluid Phase Equilibr*, 1996, **122**, 223-241.
22. J. R. Vanderveen, J. Durelle and P. G. Jessop, *Green Chem*, 2014, **16**, 1187-1197.
23. L. M. Scott, T. Robert, J. R. Harjani and P. G. Jessop, *RSC Advances*, 2012, **2**, 4925-4931.
24. E. R. Moore and N. A. Lefevre, US4623678, 1986.
25. J. W. Dolan, *LCGC North Am*, 2014, **32**, 482-487.
26. Environment Canada - Historical Climate Data, <http://climate.weather.gc.ca/> (accessed October 2016).
27. N. N. Greenwood and A. Earnshaw, *Chemistry of the Elements (2nd Edition)*, Elsevier, 1997.
28. F. J. Millero and R. N. Roy, *Croat Chem Acta*, 1997, **70**, 1-38.
29. Chemicalize - Instant Cheminformatics Solutions., <http://chemicalize.com/#/calculation> (accessed April 17th, 2017).
30. U. D. Neue, *HPLC Columns: Theory, Technology, and Practice*, Wiley-VCH, 1997.
31. B. Buszewski, S. Bocian and E. Dziubakiewicz, *J Sep Sci*, 2010, **33**, 1529-1537.
32. B. Buszewski, M. Jackowska, S. Bocian and E. Dziubakiewicz, *J Sep Sci*, 2013, **36**, 156-163.
33. S. Bocian, E. Dziubakiewicz and B. Buszewski, *J Sep Sci*, 2015, **38**, 2625-2629.
34. *Zetasizer Nano Series User Manual*, Malvern Instruments Ltd., UK, MAN0317 edn., 2003.
35. J. B. Levy, F. M. Hornack and M. A. Levy, *J. Chem. Educ.*, 1987, **64**, 260-261.

36. P. G. Jessop, L. Kozycz, Z. G. Rahami, D. Schoenmakers, A. R. Boyd, D. Wechsler and A. M. Holland, *Green Chem*, 2011, **13**, 619-623.
37. B. J. Kirby and E. F. Hasselbrink, *Electrophoresis*, 2004, **25**, 187-202.
38. J. K. Beattie, *Lab Chip*, 2006, **6**, 1409-1411.
39. M. R. Monton, M. Tomita, T. Soga and Y. Ishihama, *Anal Chem*, 2007, **79**, 7838-7844.

Chapter 4 Carbonated water for the separation of carboxylic acid compounds

4.1 Introduction

The environmental impact of harmful organic solvents is a growing concern due to their risks to human health, as well as the costly disposal. Reduction of organic solvent consumption is a major goal of green analytical chemistry, especially for greener chromatographic separations. Liquid chromatographic separations are widely utilized for chemical purification and analysis in both chemical research and production. Liquid chromatography can be broadly classified as either normal or reversed phase by the nature of the stationary phase and mobile phases employed to carry out the separation. Normal phase chromatography uses a polar stationary phase with non-polar solvents as mobile phases (*e.g.* hexanes, chloroform, THF, *etc.*). However, because those solvents are usually non-polar, they are far from environmentally friendly. Alternatively, reversed phase chromatography utilizes a non-polar stationary phase (*e.g.* octadecyl) with polar aqueous mobile phases containing significant concentrations of organic modifiers. Organic modifier such as methanol or acetonitrile is mixed with aqueous phase (water) to change the elutropic strength of the mobile phase. In this way, the retention and separation of hydrophobic analytes can be carried out in a reasonable amount of time. Compared with normal phase chromatography, reversed phase requires less organic solvents, but it still generates substantial amounts of mixed organic/aqueous waste. Additionally, ion exchange chromatography usually requires aqueous mobile phases, but permanent salts, acids, bases are usually introduced. The aqueous waste still requires expensive disposal processes. As

a result, there is a growing interest in the development of greener chromatographic techniques in order to reduce the consumption of harmful organic solvents and waste generated.

In the field of green analytical chemistry, the three R principles refer to efforts towards the 'R'eduction of solvents consumed and waste generated, 'R'eplacement of existing solvents with greener alternatives, and 'R'ecycling via distillation or other approaches.¹ Researchers have utilized smaller particle size and reduced column diameter (*e.g.* micro and nano flow chromatography) to reduce solvent consumption.²⁻⁸ Furthermore, the development of more versatile stationary phase materials (*e.g.* pH, thermal or photo-responsive) is of significant interest because of their potential to meet all three "R" principles.^{5, 9-12} For example, thermo- / pH-responsive polymers such as poly(*N*-isopropylacrylamide) and poly(dimethylaminoethyl methacrylate), have been utilized as stimuli-responsive stationary phases for the separation of steroids and benzoic acids using 100% aqueous mobile phase.^{9, 13-15} Also, pH tunable water stationary phases were developed in supercritical fluid chromatography and gas chromatography through the addition of CO₂ or an acidic modifier.^{16, 17} In this way, the aqueous HPLC effluent may be directly poured down the drain unless a toxic analyte is present. Despite significant advantages, challenges remain for the wider application of those green chromatographic techniques. In particular, the thermo-responsive approach is limited by the thermal conductivity across the column, and the potential susceptibility of biomolecules to higher temperature (*e.g.* denaturing). Additionally, the pH responsive approaches usually require permanent acids, bases or buffered mobile phases. Thus aqueous chemical waste would

still necessitate costly processes to remove or neutralize the permanent acids/bases and salts prior to disposal.

Compared with other organic or acid/base modifier, CO₂ has some major benefits. CO₂ is easy to remove, non-flammable and non-toxic. CO₂ has been extensively used as a solvent in pressurized and heated conditions in supercritical fluid chromatography and enhanced fluidity chromatography.¹⁸⁻²⁰ However, the acidity of CO₂ has not been exploited as a modifier. CO₂ saturated water at 1 bar exhibits a pH of 3.9 because of the weak acidity of carbonic acid. Therefore, pH can be carefully controlled by mixing carbonated and non-carbonated water at different ratios.²¹ Liu and Boniface *et al.* reported the stimuli-responsive properties of latex particles and drying agents using CO₂ as a benign stimulus.²² Zhao *et al.* reported switchable protein adsorption on a modified silicon surface in the presence and absence of CO₂.²⁴ The temporary acidity of CO₂ can trigger a chromatographic retention switch by “switching” either the stationary phase or analyte. Recently we reported the all-aqueous separation of small molecules on a polyethylenimine based column using carbonated water at 1 bar.²¹ Following that, CO₂ could evaporate from the aqueous solutions and it does not generate extra waste. It is worth noting that this carbon dioxide generated is not a net addition to the environment, since industrial carbon dioxide is typically derived as a by-product from natural gas processing or alcohol fermentation.¹

To the best of our knowledge, there has not been a study using CO₂ as an aqueous modifier for ion exchange separation. In this work, a pH dependent ion exchange mechanism is described considering the protonation of both amine groups and carboxylic acid compounds. Zeta potential measurements are used to corroborate an ion exchange

mechanism for analyte retention. The retention and selectivity of carboxylic compounds are manipulated by changing the amount of CO₂ introduced into the mobile phase.

The objective of this work is to demonstrate the separation of carboxylic acid compounds with amine functionalized columns, with gaseous CO₂ as a weak acid modifier. It was reported that different types of amine functional groups show different efficacy as CO₂ switchable hydrophilicity solvents and CO₂ switchable drying agents.^{22, 25, 26} Therefore, primary, secondary and tertiary amine functionalized silica spheres were prepared, and high pressure packed in columns for chromatographic testing. Detailed physical, chemical and chromatographic characterization of the functionalized materials was performed. The separation of anti-inflammatory drugs was demonstrated using only mixtures of water and carbonated water. Compared to conventional reversed phase conditions, the CO₂-based separation requires no organic solvent, therefore the risks of flammability, smog formation, and health impacts from inhalation of organic solvents are eliminated.

4.2 Experimental

4.2.1 Materials and instruments

Silane coupling agents including (3-aminopropyl) triethoxysilane, trimethoxy[3-(methylamino)propyl] silane, and 3-(diethylamino) propyl trimethoxysilane were obtained from TCI America (Portland, OR, USA). Regarding the packing material, 3.5 μm silica particles were acquired as a gift from Agilent Technologies. Glycolic acid, HOCH₂CO₂H, (70 wt. % in H₂O) and sodium hydroxide were obtained from Sigma-Aldrich (Milwaukee, WI, USA). All analytes including ibuprofen, naproxen, and ketoprofen were also acquired

from Sigma-Aldrich. Ultrapure water was generated using a Milli-Q Purification System (Bedford, MA, USA). Compressed liquefied CO₂ (Bone Dry grade), compressed Nitrogen gas (Purity > 99.998%) and a two-stage regulator were acquired from Praxair Canada Inc. (Mississauga, ON, Canada). An Omega FL-1461-S rotameter and a gas dispersion tube (7.0 mm × 135 mm, porosity 4.0 – 8.0 μm) (Sigma-Aldrich, WI, USA) were utilized in the gas delivery system. A Zetasizer Nano ZS (Malvern Instruments Ltd., Worcestershire, UK) was used to measure the zeta potential values for the functionalized and non-functionalized silica spheres.

4.2.2 Functionalization of silica spheres

Silica spheres were modified using a silane coupling reaction following a previously reported procedure.^{27, 28} Ten grams of silica spheres were first activated in 50.0 mL 3 M HCl for two hours, rinsed with DI water until neutral, then dried at 160 °C for 12 h. The activated silica spheres were then suspended in 50.0 mL dry toluene, with 50.0 mmol silane coupling agent (primary, secondary or tertiary amine) added, and refluxed in an oil bath at 110 °C for 12 hours. After the reaction, silica spheres were isolated by centrifugation, washed with toluene, methanol and water, then dried at 60 °C overnight. The functionalized silica spheres were characterized and then packed in columns for chromatographic tests.

4.2.3 Characterization of prepared silica spheres

After the silane coupling reaction, the primary, secondary and tertiary amine functionalized silica spheres were analyzed for elemental composition (C, H, N) using a Flash 2000 Elemental Analyzer. Physical morphology was examined using a FEI MLA

650 FEG Scanning Electron Microscopy. Structural identification was performed using CP-MAS NMR on a Bruker Avance 600 model.

Zeta potential measurements were performed according to an approach developed by Buszewski *et al.*²⁹⁻³¹ Because the pH of carbonated water may fluctuate if handled in the air, therefore, glycolic acid was used as a substitute for carbonic acid.³² Various pH solutions were prepared by mixing 0.010 M glycolic acid solution with 0.001 M sodium hydroxide solution in different ratios using gradient capable HPLC pumps. Thereafter, functionalized or non-functionalized silica particles were suspended (0.20 mg mL^{-1}) in the various solutions (pH 2.8 - 9.0). The zeta potential of amine-functionalized silica in carbonated solutions was also measured to examine their surface charge in the presence of CO_2 . Specifically, carbonated solutions were prepared by passing CO_2 through a dispersion tube at 100 mL min^{-1} . Before the zeta potential measurement, ultra-sonication (30 s) was performed to agitate the particles. Zeta potential values were determined ($n = 6$) using the Smoluchowski equation within the Zetasizer software by measuring the electrophoretic mobility of the particles. After characterization, the functionalized silica spheres were packed by Agilent Technologies R&D group in stainless steel columns ($2.1 \text{ mm} \times 50 \text{ mm}$) with $2 \text{ }\mu\text{m}$ stainless steel frits on each end.

4.2.4 CO_2 delivery system

The custom CO_2 delivery system was used to facilitate a stable mobile phase delivery (Figure 3.2) based on a the set-up in Chapter 3.²¹ Specifically, a two-stage regulator and a rotameter were sequentially connected to the CO_2 cylinder. A gas dispersion tube was inserted into *Reservoir B* to generate the carbonated solution (1 bar). A supply of

N₂ was used to degas the modifier-free water in *Reservoir A*, so that the pH of the water was not affected by atmospheric gas absorption. The optimal conditions for carbonation and delivery of carbonated solutions were investigated. It was found that carbonation with a CO₂ flow rate at 20 mL min⁻¹ and having the HPLC vacuum degasser bypassed resulted in stable delivery of carbonated solutions. Water in *Reservoir A* and *Reservoir B* was mixed in different ratios to produce solutions with a pH between 7.0 and 3.9. A pressure drop after stable operation for hours was observed for high mixing ratios (*e.g.* 80% B). However, ≤50% CO₂-saturated water was used in all chromatographic experiments.

4.2.5 Mobile phase solutions

The pH of carbonated water is determined by the partial pressure (pCO_2) of carbon dioxide above the solution at a given temperature.³³ According to both the Henry's law constant for CO₂ and the dissociation constants (pK_{a1} , pK_{a2}) of carbonic acid, the pH of carbonated water at different partial pressure (pCO_2) levels can be calculated.^{34, 35} The presence of CO₂ in water ($pCO_2 = 1$ bar, 25 °C) results in a solution with theoretical pH 3.9. Correspondingly, reducing the CO₂ partial pressure to 0.1 bar should produce a solution with pH 4.4. Figure 3.2 in Chapter 3 shows the HPLC mobile phase reservoirs containing CO₂ saturated water (B) at 1 bar and N₂ bubbled water (A). Therefore, the various ratios of solution A and B correspond to different partial pressures of CO₂. For example, 1% CO₂ saturated water corresponds to a CO₂ partial pressure of 0.01 bar. We have employed the system shown in Figure 3.2 to mix carbonated and noncarbonated water in different ratios to generate mixed carbonated water solutions at various pH values. Using this system 100% CO₂ saturated water (1 bar) generated a pH 4.0 (± 0.1), and 10% CO₂ saturated water (0.1 bar) produced a pH 4.6 (± 0.1) as measured after HPLC mixing. A plot

of measured pH vs pCO_2 is presented in the Figure 3.4 in Chapter 3. The measured pH of mixed carbonated water correlates well with theoretical pH values.

Solutions of glycolic acid (0.010 M) and sodium hydroxide (0.001 M) were used in some experiments as aqueous solutions with various pH's because the pH of carbonated water may fluctuate if exposed in air. Additionally, glycolic acid and sodium hydroxide can produce a wider range of pH values than can CO_2 in water. Glycolic acid was chosen because its anion, glycolate, has similar size and hydrogen-bonding ability to bicarbonate anion.³² The purpose was to investigate the chromatographic behaviour at a broader pH range (2.8 – 9.0). Specifically, 0.010 M glycolic acid (pH 2.8) was mixed with 0.001 M sodium hydroxide (pH 11.0) in different ratios to generate solutions with pH between 2.8 and 9.0. The pH values of the mixed solutions were monitored by measuring the pH of the effluent as it exited the HPLC pump.

4.2.6 Chromatographic conditions

Individual analyte solutions were prepared at a concentration of 0.50 mg mL⁻¹ in 80/20 v/v water/acetonitrile. The test mixture contained the following concentrations of the analytes: ibuprofen, 0.20 mg mL⁻¹; naproxen, 0.025 mg mL⁻¹; and ketoprofen, 0.010 mg mL⁻¹. Structures and reference pK_a values of the compounds are shown in Figure 4.1.³⁶ The HPLC flow rate was maintained at 0.40 mL min⁻¹ and a 2.0 μ L injection volume was used. UV absorbance was monitored at 254 nm. All chromatographic data were measured at least in triplicate ($n \geq 3$) for standard deviation calculations. Selectivity (α) is calculated based on retention factors (*e.g.* k_2/k_1). Tailing factor (T_f) is calculated by $T_f = W_{0.05}/2f$, where $W_{0.05}$ is the width of the peak at 5% peak height and f is the distance from the peak maximum to

the fronting edge of the peak. A higher tailing factor value (*e.g.* $T_f > 3$) indicates less satisfactory peak shapes.³⁷

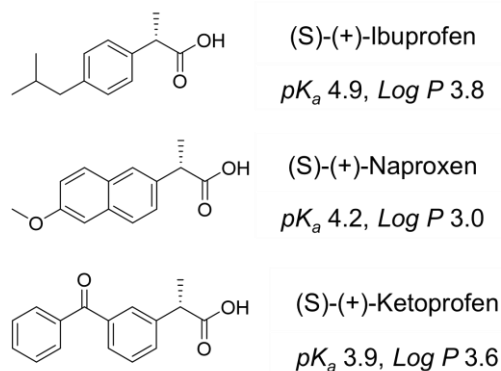


Figure 4.1 Analyte structures and predicted pK_a values and $\text{Log } P$ values.

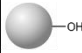
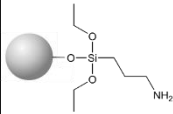
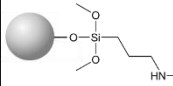
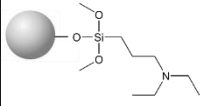
4.3 Results and discussion

4.3.1 Silica sphere characterization

This study was a test of the feasibility of using amine functionalized silica columns with carbonated water as a mobile phase. Primary, secondary and tertiary amine silanization reagents were used to bond the amines to the silica spheres. A low stir rate (200 rpm) was used during the silane coupling reactions to minimize the particle breakage caused by magnetic stirring. Scanning electron microscopy confirmed the intact morphology of the particles after reaction (Figure 4.2). Solid-state ^{13}C and ^{29}Si CP-MAS-NMR (Figure 4.3) was performed on the functionalized particles to probe the presence of functional groups. Primary, secondary and tertiary amine groups were confirmed by comparing the measured and predicted chemical shifts in the ^{13}C NMR. It is worth noting that ^{29}Si NMR indicates the presence of Si-C bonds (-64.8, -72.6 ppm), as well as the presence of silanol groups (Si-OH, 108.2 ppm).³⁸ The amine-functionalized silica spheres were analyzed for their organic elemental composition (Table 4.1). Amine (1° , 2° , 3°)

functionalized silica spheres contain N% between 0.51 – 0.64% (w/w). This N% corresponds with an amine functional group density $\approx 0.36\text{-}0.45 \text{ mmol g}^{-1}$. Comparably, commercial anion exchange resins usually contain 0.10 – 1.0 mmol g^{-1} monovalent charged groups.³⁹ Therefore, the density of amine groups was considered satisfactory for further experiments.

Table 4.1 Elemental composition of bare silica and primary, secondary and tertiary amine functionalized silica spheres.

Functionalization	Surface	Elemental composition		
		N%	C%	H%
Bare Silica		0	0.25	0.87
Primary amine (1°)		0.51	2.11	0.54
Secondary amine (2°)		0.64	2.09	0.59
Tertiary amine (3°)		0.58	3.10	0.72

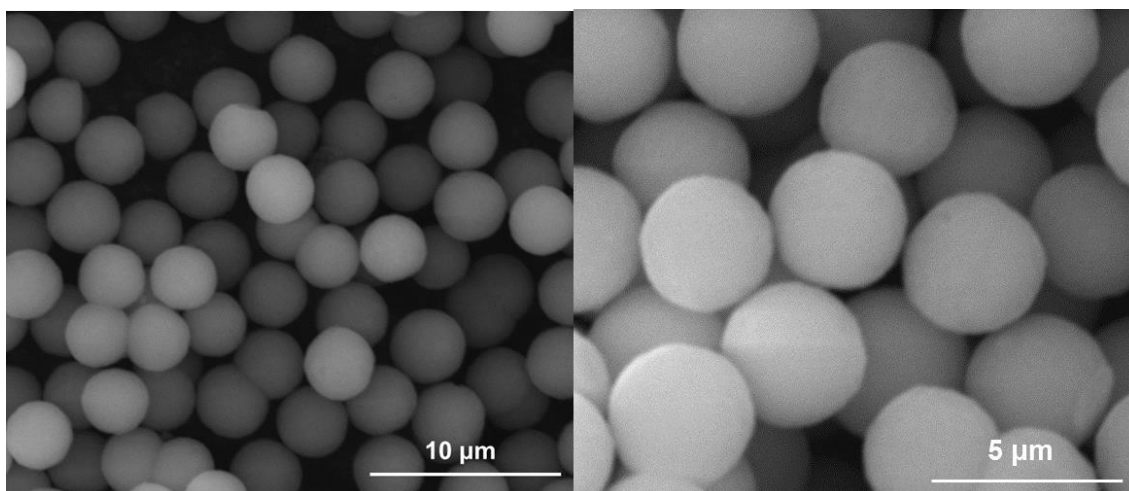


Figure 4.2 Representative scanning electron microscope images of silica spheres after the functionalization reaction at two different magnifications. The images are obtained from a FEI MLA 650 FEG Scanning Electron Microscopy.

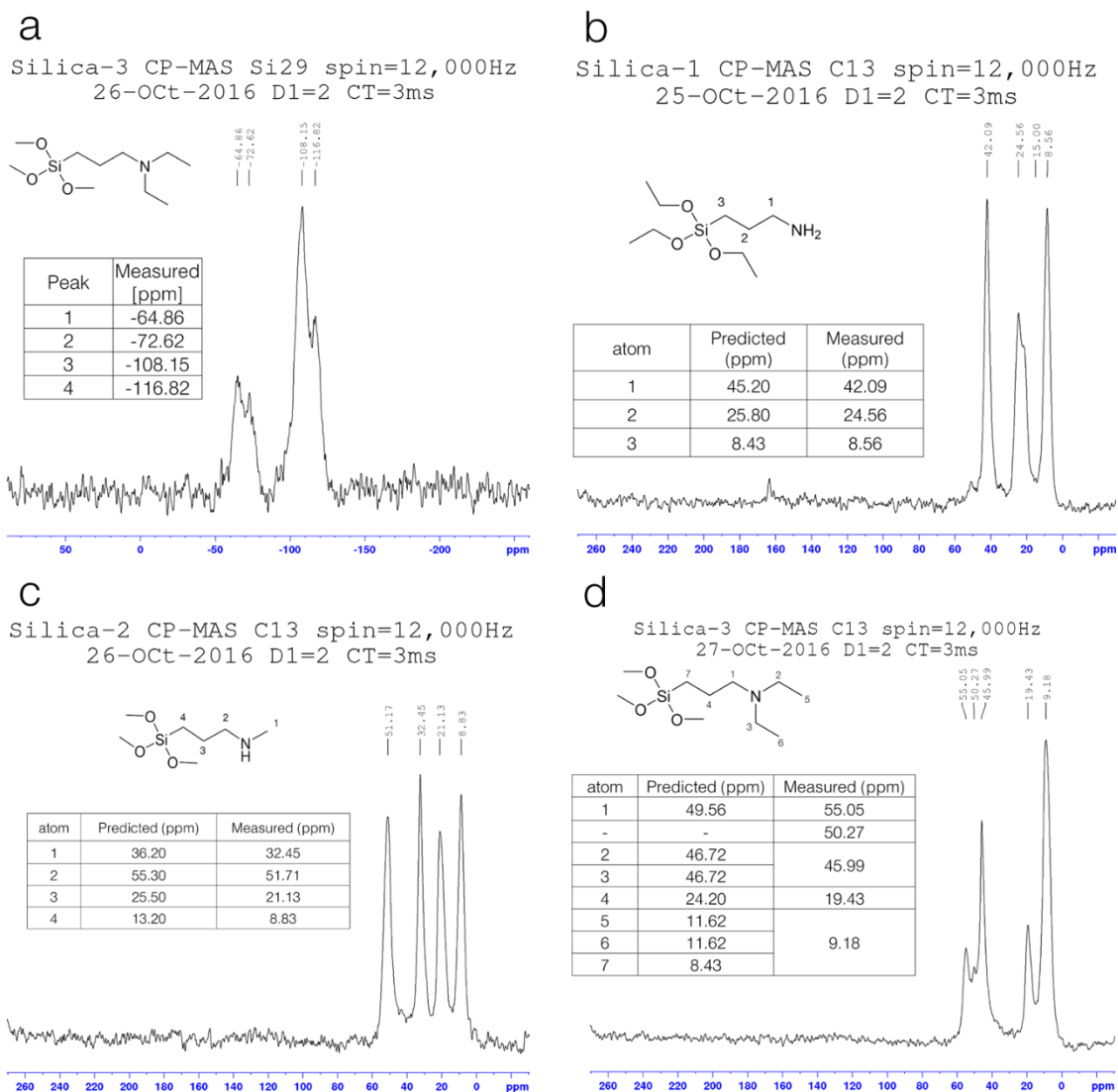


Figure 4.3 Solid-state NMR spectra and peak assignments. (a) ^{29}Si NMR spectrum of tertiary amine functionalized silica. (b) ^{13}C NMR spectrum of primary amine functionalized silica. (c) ^{13}C NMR spectrum of secondary amine functionalized silica. (d) ^{13}C NMR spectrum of tertiary amine functionalized silica.

4.3.2 Zeta potential of amine-functionalized silica

To characterize the surface charge of the amine-functionalized particles, the zeta potential was measured at different pH values (Figure 4.4). The bare silica particle showed a negative charge (~ -33 mV) from pH 9.0-5.1. A shift from -33 mV to -1.0 mV was

observed from pH 5.1 to pH 2.8, indicating the protonation of intrinsic silanol groups resulting from lower pH. NMR results mentioned earlier confirmed the presence of silanol groups. This protonation / deprotonation of silanol groups was also observed in previous studies²² and for similar substrates such as silica-based microfluidic channels.⁴⁰⁻⁴² The zeta potential measurement of primary, secondary and tertiary amine functionalized silica spheres showed a continuous surface charge increase from ~ -25 mV to $\sim +30$ mV from pH 9.0 to 2.8. The polarity switch from negative to positive with decreasing pH verifies the protonation of surface amine groups. Interestingly, the switch from a negative to a positive surface charge occurs for all three types of amine-functionalized particles. This indicates that the protonated amine groups are not the only ionizable groups because amine group may only present positive charge or no charge. It is considered that a significant number of silanol groups on the surface of the silica spheres contribute to the negative charge at higher pH. The surface charge of amine functionalized silica was also characterized when dispersed in carbonated water. After the sample was treated with CO₂ (100 mL min⁻¹) for 1 min, the zeta potential of amine-functionalized silica reached ≈ 25.0 mV. This value is almost as high as the surface charge (26.8 mV – 34.4 mV) of amine particles treated with glycolic acid (pH 2.8).³² This again confirms the protonation of amine groups caused by lower pH with the addition of CO₂.

4.3.3 Ion exchange equilibria

The dissociation of glycolic acid lowers the pH, thus causing the protonation of tertiary amines (Equation 4.1 and 4.2), but that isn't the only pH-dependent equilibrium in the system. Carboxylic acid containing analytes are protonated at lower pH, which can affect their retention time (Equation 4.3). Considering that the carboxylic acid analytes may

be deprotonated and negatively charged at higher pH, the positively charged stationary phase may separate the compounds through an ion exchange mechanism. Furthermore, the glycolic acid anion may act as a competing anion, while protonated amine groups are fixed cations participating in an ion exchange mechanism (Equation 4.4).

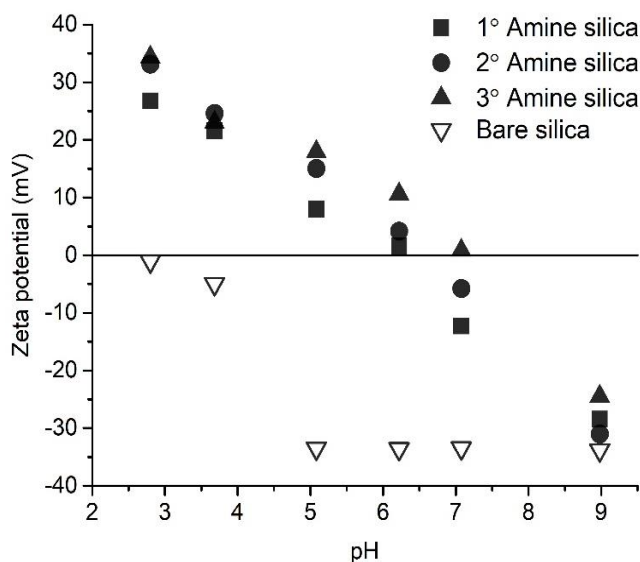
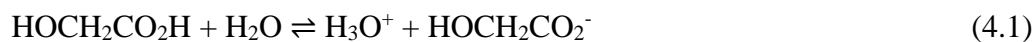


Figure 4.4 Zeta potential of bare silica (∇), primary (\blacksquare), secondary (\bullet) and tertiary (\blacktriangle) amine functionalized silica spheres at various pH's. The size of the error bars is less than the size of the symbols ($n \geq 3$).

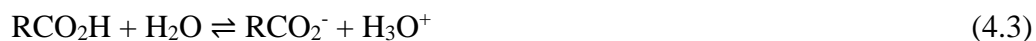
Dissociation of glycolic acid



Protonation of amine stationary phase by



Carboxylic acid analyte dissociation equilibrium



Ion exchange equilibrium with carboxylate analyte



4.3.4 Effect of pH

Previously, the interaction between dissolved CO_2 (aq) and tertiary amine groups has been well studied.^{26, 43, 44} Therefore, chromatographic tests were first performed on tertiary amine functionalized columns. As shown in Figure 4.5, the retention of the three carboxylic acid compounds showed a very characteristic dependency on pH. Naproxen, ibuprofen and ketoprofen have negligible retention ($t_R < 1.0$ min) on the tertiary amine column at pH 7.0. As the pH of the mobile phase is reduced, the retention is increased until the mobile phase pH is 4.6. A further decrease in pH of the mobile phase reverses the trend and decreases retention. It is hypothesized that this pH dependent retention is the joint action of the protonation/deprotonation of the stationary phase amine groups and the dissociation of carboxylic acid compounds.

To illustrate this further, the zeta potential of tertiary amine-functionalized silica spheres is plotted together with the dissociation of ibuprofen at various pH values (Figure 4.6 a). The tertiary amine functionalized silica spheres exhibit increasing positive charge as the pH increases from 2.8 until pH 7.0 (Figure 4.6 a, dotted). Additionally, the dissociation of carboxylic acid groups in ibuprofen (pK_a 4.9) also participates in the process. Ibuprofen undergoes dissociation at higher pH. The percentage of deprotonated ibuprofen is plotted as a dashed line in Figure 4.6 a. At pH 7.0, the majority of ibuprofen molecules are dissociated and thus negatively charged. The amine groups in the tertiary amine stationary phase are deprotonated and neutral. As a result, minimal electrostatic

interaction is expected and little retention is observed (ibuprofen, $t_R = 0.67$ min). At pH 5.0, $\approx 50\%$ of the ibuprofen molecules are deprotonated, whereas the amine functionalized stationary phase is protonated ($\zeta \approx 10\text{-}20$ mV). It is reasonable then, that in measurements at pH 4.6, ibuprofen exhibits stronger retention on the tertiary amine stationary phase ($t_R = 3.2$ min). At pH 3.0, the majority of ibuprofen exists in the neutral state and a shorter retention time ($t_R = 1.5$ min) was observed. The decreased retention is attributed to the reduced electrostatic attraction. The ion exchange retention behaviour at various pH's is shown schematically in Figure 4.6 b. At slightly acidic conditions (*e.g.* pH 5.0), retention of the carboxylic acid analyte was stronger because the electrostatic attraction between the positively charged amine and the negatively charged carboxylate favours retention.

The examination of this dynamic pH dependent retention is valuable because it corroborates the potential use of a CO₂ triggered retention switch. The pH region (pH 3.9 – 7.0) accessible with carbonated water is indicated by the blue shaded region in Figure 4.6 a. The CO₂ accessible region overlaps with protonation and deprotonation of the stationary phase and analytes. This pH-responsive behaviour provides a basis for investigating the potential of CO₂ as a weak acid modifier in ion exchange conditions.

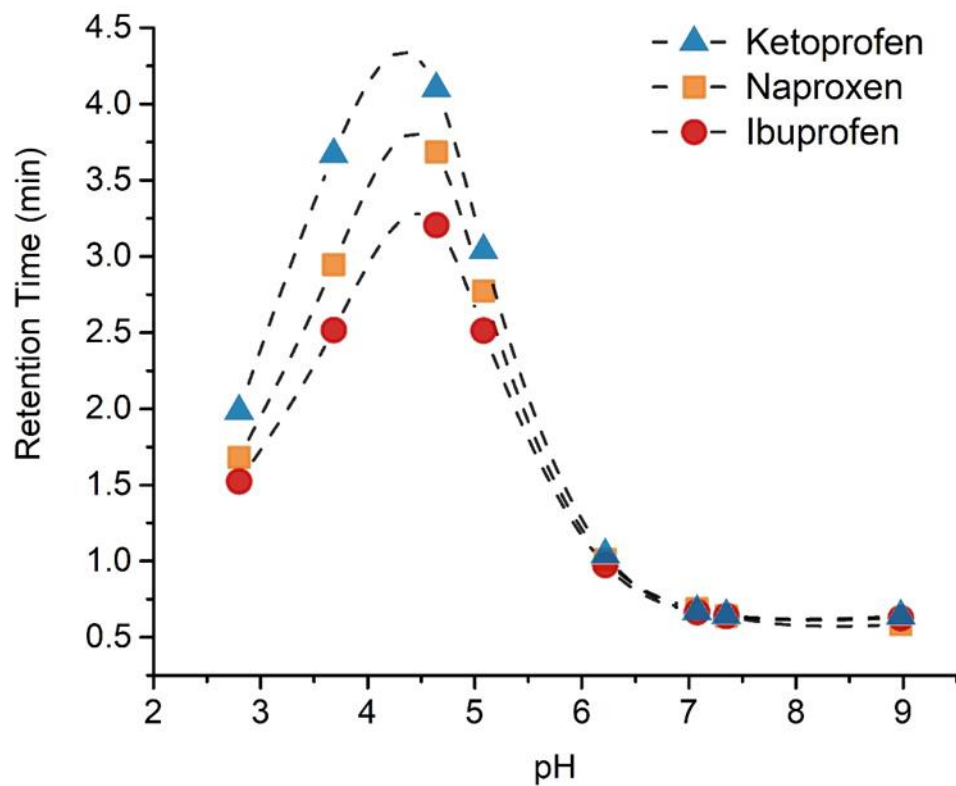


Figure 4.5 Retention time of naproxen (\square), ibuprofen (\circ) and ketoprofen (\triangle) at various mobile phase pH. Conditions: Tertiary amine functionalized column (2.1 mm \times 50 mm), flow rate 0.40 mL min^{-1} , UV 254 nm. Aqueous solutions at various pH's were generated by mixing 0.01 M glycolic acid and 0.001 M NaOH. The error bars are smaller than the symbols ($n \geq 3$).

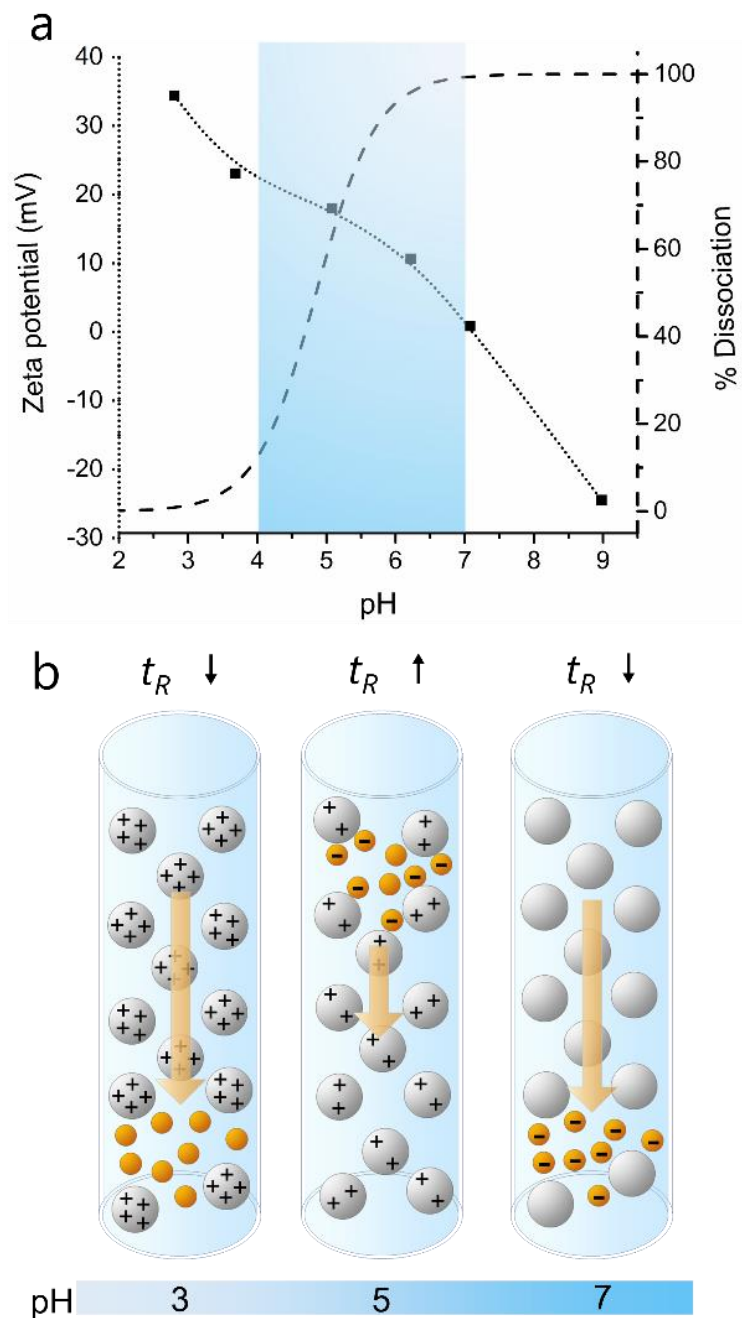


Figure 4.6 a) Overlaid figures containing the zeta potential of tertiary amine silica spheres vs pH (dotted line), and percentage fraction of deprotonated ibuprofen vs pH (dashed line). The blue shaded region shows the pH range that mixtures of water and carbonated water (1 bar) can access. The error bars are smaller than the symbols ($n \geq 3$). b) Schematic diagram showing the protonation of the stationary phase amine groups at lower pH (e.g. pH 3.0) and the dissociation of carboxylic acid compounds at higher pH (e.g. pH 7.0).

4.4 Separation of carboxylic compounds

4.4.1 Effect of CO₂

Similar to the addition of glycolic acid, the reduction in pH caused by the addition of CO₂ can also protonate the amine functionalized stationary phase (Equation 4.5). Moreover, dissociated bicarbonate ions may also participate as competing ions in the ion exchange equilibrium (Equation 4.6).

Protonation of amine stationary phase by CO₂



Ion exchange equilibrium with bicarbonate ion



Based upon those principles, a chromatographic separation of naproxen, ibuprofen and ketoprofen was attempted on the tertiary amine-functionalized column, using various mixtures of CO₂ saturated water (B) and non-carbonated water (A). As shown in Figure 4.7, the three compounds are not separated with 100% water at pH 7.0. The addition of 1% CO₂ saturated water changes the selectivity slightly, and 10% CO₂ saturated water as a mobile phase produced completely resolved chromatographic peaks (*resolution* > 1.5) for the individual compounds. A further increase in % CO₂ saturated water shows increased retention factors for the three compounds and improved separation selectivity (Table 4.2). Additionally, as indicated in higher tailing factor values, peak tailing becomes more apparent at higher concentrations of CO₂. The potential causes of peak tailing include mixed interactions among the solute, mobile phase, and stationary phase (column), rate of

secondary equilibria, *etc.* The peak shape / efficiency may be improved by packing longer columns and smaller particles, *etc.*⁴⁵ This example is a demonstration of the value of carbonated water as a solvent modifier in organic solvent-free chromatography.

Table 4.2 Chromatographic results on the tertiary amine column with 5%, 10%, 20% CO₂ saturated water as the mobile phase.

	Peaks	% CO ₂ saturated water		
		5%	10%	20%
Retention factor (<i>k</i>)	1	7.65	7.80	8.15
	2	9.85	10.44	11.29
	3	12.29	14.58	17.22
Selectivity (α)	$\alpha_{2/1}$	1.29	1.34	1.39
	$\alpha_{3/2}$	1.25	1.40	1.52
Tailing factor (<i>T_f</i>)	1	1.45	2.32	2.98
	2	1.68	2.25	3.22
	3	3.08	3.91	4.60

4.5 1°, 2°, 3° amines

4.5.1 Effect of pH

The retention time of ibuprofen on three amine columns at various pH's is shown in Figure 4.8 a. Primary and secondary amine columns showed a similar trend for retention time over the pH range from 2.8 to 9.0. The strongest retention appears when the aqueous mobile phase has a pH between 4.5 - 5.0. This indicates that the retention of ibuprofen on both primary and secondary amine columns likely participates through the ion exchange

mechanism described earlier. A stronger retention of ibuprofen was observed on the primary amine column ($t_R = 27.0$ min), than that on the secondary amine column ($t_R = 16.8$ min). The retention time of ibuprofen on the tertiary amine column is much shorter ($t_R = 3.2$ min). The retention time behaviour can be attributed to the electron donating effect of the substituents on the nitrogen, tertiary (2x ethyl) and secondary (methyl). The positive charge of the protonated amine is more dispersed because of the presence of the alkyl groups. Therefore, the anionic analyte (ibuprofen) has a stronger interaction with the primary amine compared to secondary and tertiary amines. It indicates the utility of primary and secondary amine functionalized materials for applications requiring a strong retention, such as solid phase extraction.

This data also suggests that hydrophobic interaction is not the dominant force in these retention processes, because a tertiary amine column should have stronger retention for ibuprofen if the hydrophobic effect is the principal interaction involved in the separation.

4.5.2 Effect of CO₂

Tertiary amine groups have been shown to be amongst the most promising CO₂ switchable functional groups,^{23, 26, 46, 47} but additional literature regarding CO₂ switchable hydrophilicity solvents and CO₂ capture agents have reported that secondary amine compounds may uptake CO₂ at a faster rate than tertiary amine compounds.^{25, 48} It is valuable to investigate the behaviour of secondary and tertiary amine-functionalized silica as CO₂ responsive stationary phase particles.

The separation of ibuprofen, naproxen, and ketoprofen on the secondary amine column was performed using 20% CO₂ saturated water as the mobile phase (Figure 4.8 b). The retention of all three compounds is significantly stronger on the secondary amine column ($k \geq 35$) than those observed on tertiary amine column ($k \leq 18$).

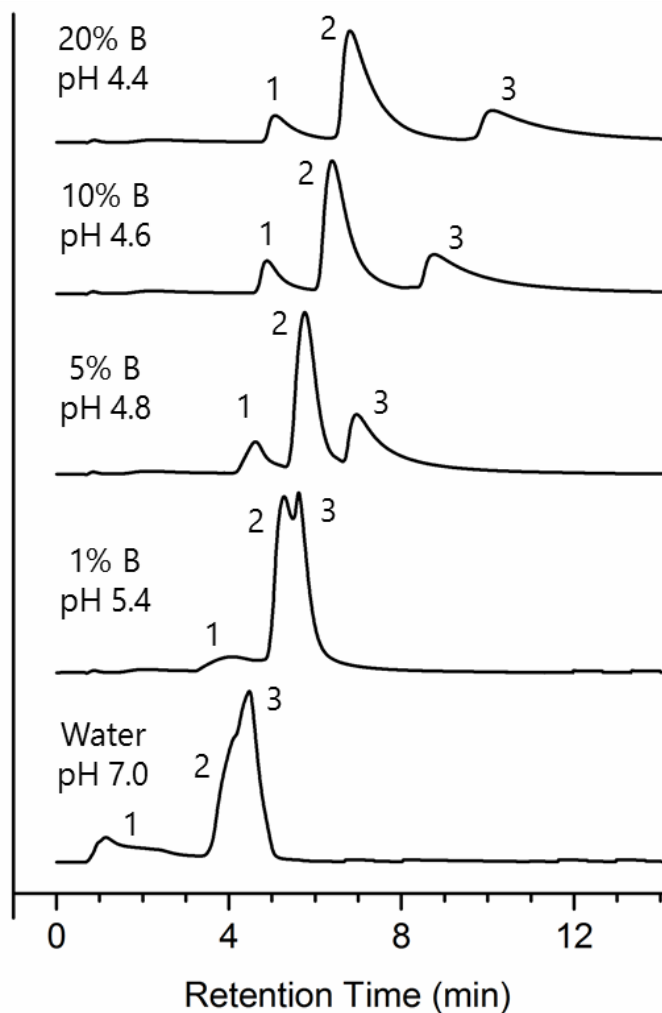


Figure 4.7 Chromatograms of ibuprofen (1), naproxen (2), and ketoprofen (3) on a tertiary amine column with various percentages of CO₂ saturated water (Solvent B) and non-carbonated water (Solvent A) as mobile phase. Conditions: tertiary amine-functionalized column (2.1 mm × 50 mm), flow rate 0.40 mL min⁻¹, UV 254 nm.

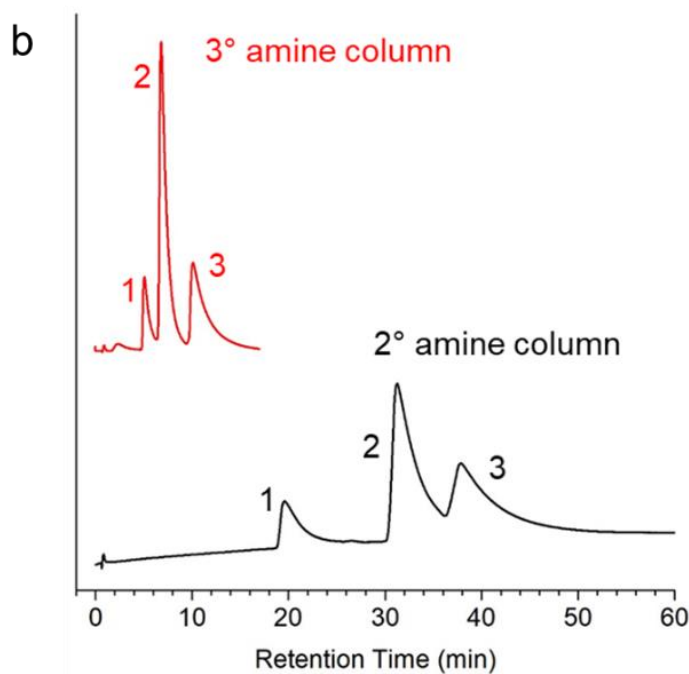
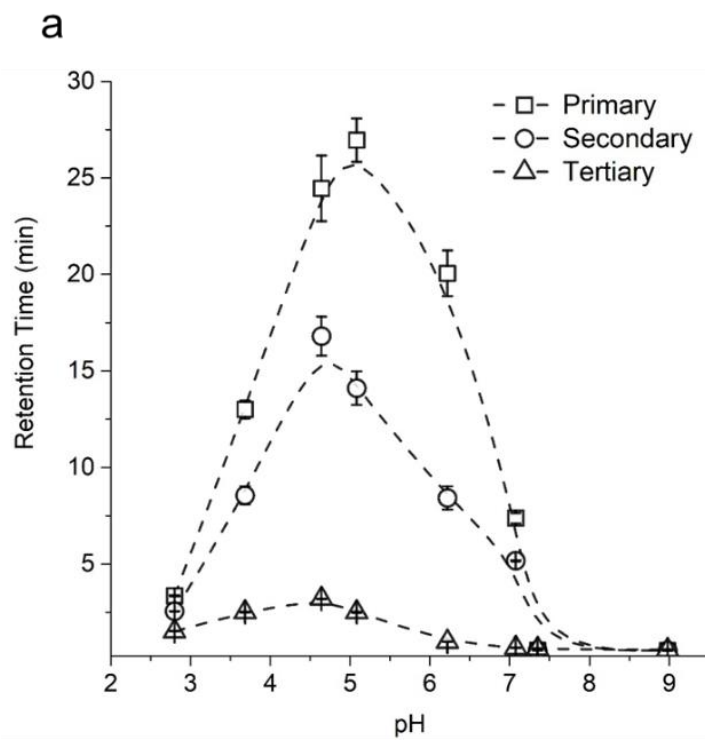


Figure 4.8 a) Retention time of ibuprofen on primary (\square), secondary (\circ), and tertiary (\triangle) amine columns at various pH's of the mobile phase. b) Chromatograms of ibuprofen (1), naproxen (2), and ketoprofen (3) on tertiary amine column and secondary amine column with 20% CO_2 saturated water as mobile phase. Conditions: secondary amine-functionalized column (2.1 mm \times 50 mm), flow rate 0.40 mL min^{-1} , UV 254 nm.

The selectivity $\alpha_{2/1}$ on the secondary amine column is improved over that on the tertiary amine column, although the selectivity $\alpha_{3/2}$ remains similar (shown in Table 4.2 and 4.3). This selectivity change implies the possibility of using different types of amine groups to adjust the chromatographic selectivity. Comparably, the tertiary amine column is more advantageous in this demonstration, because it achieves the complete separation of the three test compounds faster and more efficiently (Figure. 4.8 b). Secondary amine column shows longer retention time for all the compounds and it could be used for separations requiring stronger retention capability (e.g. purification, extraction).

Table 4.3 Chromatographic result for a secondary amine column with 20% CO₂ saturated water as the mobile phase.

	Peaks		
	1	2	3
Retention factor (k)	34.64	55.73	67.73
Selectivity (α)	$\alpha_{2/1} = 1.61$		$\alpha_{3/2} = 1.22$
Tailing factor (T_f)	5.97	3.16	5.07

4.6 Conclusions

Primary, secondary and tertiary amine functionalized silica spheres were prepared to evaluate their separation capability with CO₂-modified water as an environmentally friendly mobile phase. Measurement of surface charge of amine-functionalized silica confirms the protonation of surface amine groups at a lower pH. Dissociation of carboxylic acid analytes also participates in the ion exchange equilibrium, which showed a dynamic retention behaviour from pH 2.8 to 9.0. Tertiary amine columns have been used to separate

naproxen, ibuprofen, and ketoprofen, and are considered the most useful for this novel analytical separation. The separation is only achieved when CO₂-modified water is used as the eluent. Unmodified water is insufficient. Primary and secondary amine columns showed stronger retention of carboxylic acid analytes and may find potential applications that require relatively stronger retention such as solid phase extraction. This development holds significant potential for application in environmentally friendly chemical analysis and preparative processes.

4.7 References

1. C. J. Welch, N. J. Wu, M. Biba, R. Hartman, T. Brkovic, X. Y. Gong, R. Helmy, W. Schafer, J. Cuff, Z. Pirzada and L. L. Zhou, *Trac-Trend Anal Chem*, 2010, **29**, 667-680.
2. M. Koel, *Green Chem*, 2016, **18**, 923-931.
3. L. H. Keith, L. U. Gron and J. L. Young, *Chem Rev*, 2007, **107**, 2695-2708.
4. A. I. Olives, V. Gonzalez-Ruiz and M. A. Martin, *Acs Sustain Chem Eng*, 2017, **5**, 5618-5634.
5. A. Spietelun, L. Marcinkowski, M. de la Guardia and J. Namiesnik, *J Chromatogr A*, 2013, **1321**, 1-13.
6. C.-Y. Lu, in *Handbook of Green Analytical Chemistry*, John Wiley & Sons, Ltd, 2012, p. 175-198.
7. J. Plotka, M. Tobiszewski, A. M. Sulej, M. Kupska, T. Gorecki and J. Namiesnik, *J Chromatogr A*, 2013, **1307**, 1-20.
8. R. E. Majors, *LCGC North Am*, 2009, **27**, 458-471.
9. R. Sepehrifar, R. I. Boysen, B. Danylec, Y. Yang, K. Saito and M. T. Hearn, *Anal Chim Acta*, 2017, **963**, 153-163.
10. H. Shaaban and T. Gorecki, *Talanta*, 2015, **132**, 739-752.
11. P. Maharjan, E. M. Campi, K. De Silva, B. W. Woonton, W. R. Jackson and M. T. Hearn, *J Chromatogr A*, 2016, **1438**, 113-122.
12. R. Sepehrifar, R. I. Boysen, B. Danylec, Y. Yang, K. Saito and M. T. Hearn, *Anal Chim Acta*, 2016, **917**, 117-125.
13. Y. Shen, L. Qi, X. Y. Wei, R. Y. Zhang and L. Q. Mao, *Polymer*, 2011, **52**, 3725-3731.
14. N. Li, L. Qi, Y. Shen, Y. Li and Y. Chen, *ACS Appl Mater Interfaces*, 2013, **5**, 12441-12448.
15. K. Nagase, M. Kumazaki, H. Kanazawa, J. Kobayashi, A. Kikuchi, Y. Akiyama, M. Annaka and T. Okano, *ACS Appl Mater Interfaces*, 2010, **2**, 1247-1253.
16. A. F. Scott and K. B. Thurbide, *J Chromatogr Sci*, 2017, **55**, 82-89.

17. E. Darko and K. B. Thurbide, *Chromatographia*, 2017, **80**, 1225-1232.
18. S. T. Lee, S. V. Olesik and S. M. Fields, *J Microcolumn Sep*, 1995, **7**, 477-483.
19. M. C. Beilke, M. J. Beres and S. V. Olesik, *J Chromatogr A*, 2016, **1436**, 84-90.
20. Y. Cui and S. V. Olesik, *J Chromatogr A*, 1995, **691**, 151-162.
21. X. Yuan, E. G. Kim, C. A. Sanders, B. E. Richter, M. F. Cunningham, P. G. Jessop and R. D. Oleschuk, *Green Chem*, 2017, **19**, 1757-1765.
22. K. J. Boniface, R. R. Dykeman, A. Cormier, H. B. Wang, S. M. Mercer, G. J. Liu, M. F. Cunningham and P. G. Jessop, *Green Chem*, 2016, **18**, 208-213.
23. Y. Liu, P. G. Jessop, M. Cunningham, C. A. Eckert and C. L. Liotta, *Science*, 2006, **313**, 958-960.
24. S. Kumar, X. Tong, Y. L. Dory, M. Lepage and Y. Zhao, *Chem Commun*, 2013, **49**, 90-92.
25. J. R. Vanderveen, J. Durelle and P. G. Jessop, *Green Chem*, 2014, **16**, 1187-1197.
26. P. G. Jessop, L. Kozycz, Z. G. Rahami, D. Schoenmakers, A. R. Boyd, D. Wechsler and A. M. Holland, *Green Chem*, 2011, **13**, 619-623.
27. Y. Li, J. Yang, J. Jin, X. Sun, L. Wang and J. Chen, *J Chromatogr A*, 2014, **1337**, 133-139.
28. S. Bocian, S. Studzinska and B. Buszewski, *Talanta*, 2014, **127**, 133-139.
29. B. Buszewski, S. Bocian and E. Dziubakiewicz, *J Sep Sci*, 2010, **33**, 1529-1537.
30. B. Buszewski, M. Jackowska, S. Bocian and E. Dziubakiewicz, *J Sep Sci*, 2013, **36**, 156-163.
31. S. Bocian, E. Dziubakiewicz and B. Buszewski, *J Sep Sci*, 2015, **38**, 2625-2629.
32. J. Durelle, J. R. Vanderveen and P. G. Jessop, *Physical chemistry chemical physics : PCCP*, 2014, **16**, 5270-5275.
33. R. Sander, *Atmos Chem Phys*, 2015, **15**, 4399-4981.
34. L. Irving, *J Biol Chem*, 1925, **63**, 767-778.
35. J. B. Levy, F. M. Hornack and M. A. Levy, *J Chem Educ*, 1987, **64**, 260-261.

36. Chemicalize - Instant Cheminformatics Solutions., <http://chemicalize.com/#/calculation> (accessed April 17th, 2017).
37. J. W. Dolan, *LCGC North Am*, 2003, **21**, 612-616.
38. CAPCELL PAK C18 MGIII Type., http://hplc.shiseido.co.jp/e/column/html/mg3_index.htm (accessed April 17th, 2017).
39. P. R. Haddad and P. E. Jackson, *Ion Chromatography Principles and Applications*, Elsevier, 1990.
40. J. K. Beattie, *Lab Chip*, 2006, **6**, 1409-1411.
41. M. R. Monton, M. Tomita, T. Soga and Y. Ishihama, *Anal Chem*, 2007, **79**, 7838-7844.
42. B. J. Kirby and E. F. Hasselbrink, Jr., *Electrophoresis*, 2004, **25**, 203-213.
43. L. A. Fielding, S. Edmondson and S. P. Armes, *J Mater Chem B*, 2011, **21**, 11773-11780.
44. C. I. Fowler, P. G. Jessop and M. F. Cunningham, *Macromolecules*, 2012, **45**, 2955-2962.
45. L. R. Snyder, J. J. Kirkland and J. W. Dolan, *Introduction to Modern Liquid Chromatography*, A John Wiley & Sons Inc., Hoboken, NJ, 3rd ed., 2009.
46. S. M. Mercer and P. G. Jessop, *ChemSusChem*, 2010, **3**, 467-470.
47. P. G. Jessop, S. M. Mercer and D. J. Heldebrant, *Energ Environ Sci*, 2012, **5**, 7240-7253.
48. M. E. Boot-Handford, J. C. Abanades, E. J. Anthony, M. J. Blunt, S. Brandani, N. Mac Dowell, J. R. Fernandez, M. C. Ferrari, R. Gross, J. P. Hallett, R. S. Haszeldine, P. Heptonstall, A. Lyngfelt, Z. Makuch, E. Mangano, R. T. J. Porter, M. Pourkashanian, G. T. Rochelle, N. Shah, J. G. Yao and P. S. Fennell, *Energ Environ Sci*, 2014, **7**, 130-189.

Chapter 5 Towards the development of pH/CO₂-switchable polymer monolith surfaces with tunable surface wettability and adhesion

5.1 Literature review

5.1.1 Superhydrophobic surfaces

Research on the wettability of solid surfaces is attracting renewed interest. According to both the ability of the surface being wetted and the type of liquid in contact with a solid, several possible extreme states of superwettability have been proposed, including superhydrophilic, superhydrophobic, superoleophilic, and superoleophobic. In 1997, Barthlott and Neinhuis revealed that the self-cleaning property of lotus leaves was caused by the microscale papillae and the epicuticular wax, which suggested a microscale model for superhydrophobicity.¹ Jiang *et al.* demonstrated that the branch-like nanostructures on top of the microscale papillae of lotus leaves are responsible for the observed superhydrophobicity.² Since then, both the microscale and nanoscale roughness (hierarchical structures) are considered essential in contributing to superhydrophobicity. Following these original studies on the lotus leaf, a wide range of studies were performed which examined fundamental theory, surface chemistry, nanofabrication and biomimetic developments, *etc.* Furthermore, the surface superwettability of various materials has found valuable applications in self-cleaning surfaces, anti-biofouling, anti-icing, anti-fogging, oil-water separation, microfluidic devices, and biological assays, *etc.*³

5.1.2 Measurements of Surfaces with Superwettability

Water contact angle (WCA) is used to characterize the degree of surface wetting of a sessile droplet on a solid surface. The angle between the tangent planes of liquid-vapor

interface and the liquid-solid interface is usually measured using an imaging system. Hydrophobic surfaces are defined as having a water contact angle greater than 90° , while hydrophilic surfaces have a water contact angle less than 90° . Superhydrophobic surfaces refer to surfaces with a static water contact angle larger than 150° , but include the additional requirement of a “roll-off angle” (also called sliding angle, SA) of less than 10° .³ Conversely, superhydrophilic surfaces are characterized as having high surface energy and water completely wets the surface (WCA = 0°).

In addition, contact angle hysteresis is used to characterize surface adhesion. Contact angle hysteresis (CAH) is defined as the difference between the advancing and receding angle ($\theta_{\text{Rec}} - \theta_{\text{Adv}}$) of a water droplet. It should be noted that, superhydrophobic surfaces typically have a high water contact angle ($> 150^\circ$), but may have different adhesive behaviour (low or high hysteresis), described as a lotus state or rose petal state in the following section.

5.1.3 Different superhydrophobic states

Since the original description of surface wettability by Thomas Young in the 1800s⁴, a variety of physical states and theories have been proposed to understand the properties of surfaces with hydrophobic and superhydrophobic properties, including the Wenzel model and the Cassie-Baxter model. Several different superhydrophobic states are briefly presented in Figure 5.1.

In general, the Wenzel state is used to describe a wetting-contact state of water with all the topological features of the surface, which is characterized by a high WCA hysteresis. Therefore, although the droplet in Wenzel state may exhibit a high WCA ($>150^\circ$), the

droplet may still be pinned on the surface and does not easily roll off. In some cases, a droplet may bounce or roll off the surface very easily, which is typically explained in a Cassie-Baxter state (or Cassie state). Air is trapped between the topological features of the surface and the liquid resting on the solid surface. An ideal surface in a Cassie state is characterized by a low roll off angle (*e.g.* $< 2^\circ$) and low WCA hysteresis ($< 2^\circ$). Lotus leaves are considered a classic example of a Cassie state. Both microscale and nanoscale features on the lotus leaf are considered essential for its superhydrophobic and self-cleaning properties.

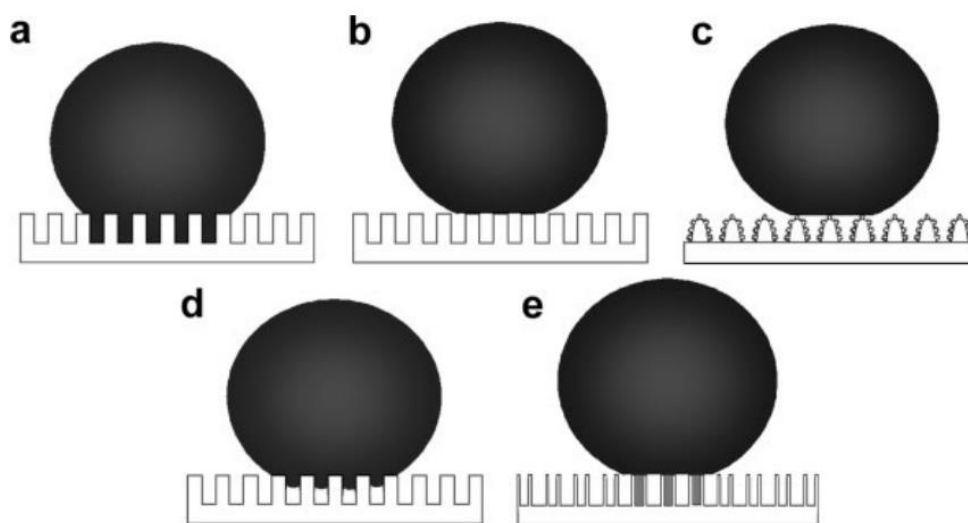


Figure 5.1 Different states of superhydrophobic surfaces: a) Wenzel state, b) Cassie's superhydrophobic state, c) the "Lotus" state (a special case of Cassie's superhydrophobic state), d) the transitional superhydrophobic state between Wenzel's and Cassie's states, and e) the "Gecko" state of the PS nanotube surface. The gray shaded area represents the sealed air, whereas the other air pockets are continuous with the atmosphere (open state). Reproduced from reference⁵ with permission. Copyright © (2007) John Wiley and Sons Inc.

Over the last decade, additional superhydrophobic states have been proposed and studied. In practical samples, there often exists a transitional, or metastable state between

the Wenzel state and the Cassie state. The WCA hysteresis in a transitional state is usually higher than those in Cassie state but lower than a Wenzel state. For example, in a transitional state a water droplet may roll off the surface at a higher angle ($10^\circ < SA < 60^\circ$). In addition, there is a high-adhesive case of the “gecko” state (Figure 5.1 e) that is different from the Cassie state. The origin of the “Gecko” state comes from the superhydrophobic surface of the PS nanotube reported by Jin *et al.*⁶ The negative pressure from the sealed air pocket is considered responsible for the high adhesion of the gecko state.

5.1.4 Fabrication of superhydrophobic and superhydrophilic surfaces

With inspiration from nature, a variety of methods have been adopted to generate superhydrophobic materials. Because surface roughness and surface chemistry are the two factors that govern the surface wettability, the strategies employed for the fabrication of superhydrophobic surfaces look to either roughen the surface of a pre-formed low-surface-energy surface, or to modify a rough surface with low-surface-energy materials. According to a recent review article, a wide variety of physical methods, chemical methods and combined methods have been developed to meet the requirement of certain applications.³ Physical methods include plasma treatment, phase separation, templating, spin-coating, spray application, electrohydrodynamics and electrospinning, ion-assisted deposition method. Chemical methods commonly employed include sol-gel, solvothermal, electrochemical, layer-by-layer and self-assembly methods as well as bottom-up fabrication of micro-/nanostructure and one-step synthesis. Combined methods include both vapor deposition and etching (*e.g.* photolithography, wet chemical etching, and plasma etching). However, from the perspective of a polymer chemist or analytical

chemist, porous polymer monolith materials are less explored for the generation of superhydrophobic and superhydrophilic surfaces.

As presented in Chapter 1, porous polymer monoliths (PPM) emerged in the 1990s as a novel kind of packing material for liquid chromatography and capillary electrochromatography. A very important advantage of PPM packing material in chromatography comes from simplified column preparation. This approach has allowed for the *in situ* fabrication of a chromatographic column, proved to be significantly simpler than the conventional slurry packing method. However, it was not until 2009 that the utilization of PPMs as superhydrophobic materials emerged. Levkin *et al.* introduced the “sandwich” template to prepare a fluorinated PPM surface based on UV-initiated free radical polymerization.⁷ A mixture containing photoinitiator, monomer(s), crosslinker, and porogenic solvent(s) was injected into a mold formed by two glass slides and a spacer, followed by polymerization with UV initiation. By introducing different types of monomer(s) and/or crosslinker and performing post-polymerization modification, the surface chemistry can be selectively manipulated. For example, fluorinated monomers are used to generate a low-surface-energy PPM. Furthermore, changing the composition of the porogenic solvent can be used to tailor the surface roughness. Therefore, PPM materials have the intrinsic ability to produce robust customized surfaces with specific properties, including transparent, conductive, superhydrophobic surfaces and superhydrophilic surfaces. For example, Zahner *et al.* reported the photografting of a superhydrophobic surface in order to create a superhydrophilic pattern (Figure 5.2).⁸ The method allows for precise control of the size and geometry of photografted superhydrophilic features, as well

as the thickness, morphology, and transparency of the superhydrophobic and hydrophobic porous polymer films.

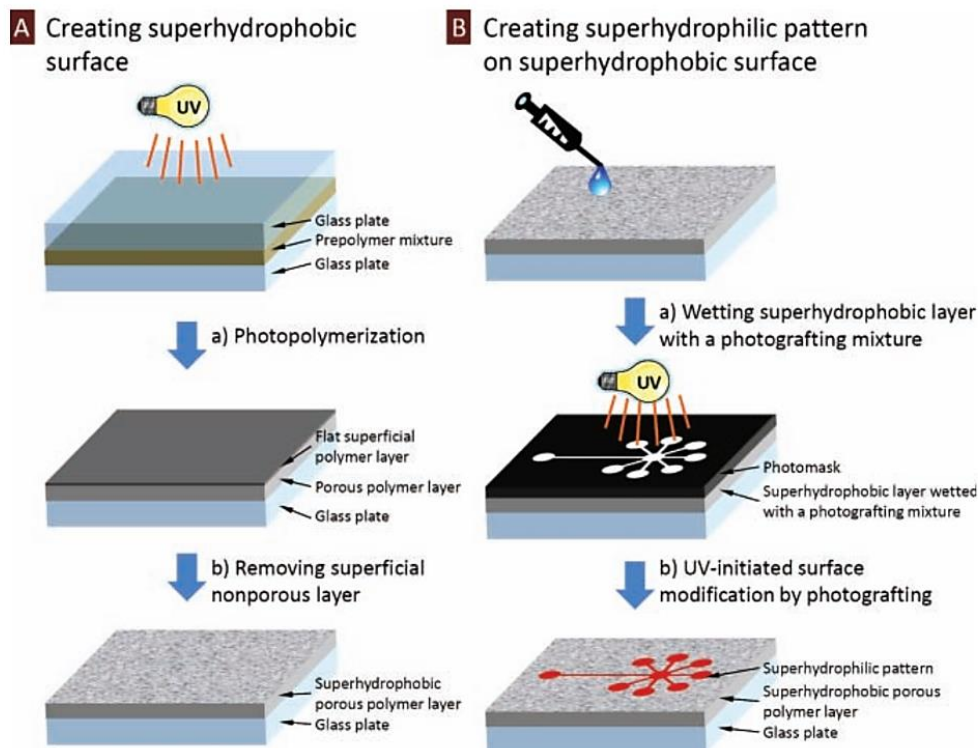


Figure 5.2 Schematic representation of the method for A) making superhydrophobic porous polymer films on a glass support and for B) creating superhydrophilic micropatterns by UV-initiated photografting. Reproduced from reference⁸ with permission. Copyright © (2011) John Wiley and Sons Inc.

5.1.5 Stimuli-responsive surfaces with switchable wettability and adhesion

Superhydrophobic and superhydrophilic surfaces have been found to be useful in various applications such as anticorrosion, antifogging, self-cleaning, water harvesting, oil-water separation, *etc.* However, the development of “smart” surfaces with the capability of reversible switching between superhydrophobic and superhydrophilic states has also attracted more interest in the last decade.³ A variety of stimuli-responsive materials have been developed via the incorporation of “smart” chemical moieties that respond to external

stimuli, such as temperature, light, pH, salt, sugar, solvent, stress, and electricity, as shown in Figure 5.3.

First, external stimuli have been successfully used to switch the wettability of surfaces. Lopez *et al.* reported the fast and reversible switching between superhydrophilic and superhydrophobic states across the lower critical solution temperature (LCST) on a poly(N-isopropylacrylamide) (PNIPAAm)-grafted porous anodic aluminum oxide (AAO) membranes.⁹ Fujishima *et al.* reported UV-generated superamphiphilicity on titanium dioxide surfaces.¹⁰ Water droplets and oil can both quickly spread out on these surfaces after UV irradiation, and hydrophobicity will recover after storage in the dark. Besides TiO₂, other photosensitive semiconductor materials, such as ZnO, WO₃, V₂O₅, SnO₂, and Ga₂O₃, have also been developed to exhibit light-switchable properties.³ In recent years, pH-responsive surfaces have also attracted attention for their potential application in drug delivery, separation and biosensors.³ For example, Zhu *et al.* reported the pH-reversible conversion of an electrospun fiber film between superhydrophobic and superhydrophilic states based on a coaxial polyaniline-polyacrylonitrile.¹¹

External stimuli have been effectively used to switch the wettability of surfaces. However, the development of switchable adhesion has also attracted research interest. Surfaces with the same water contact angle can vary significantly in the adhesion with liquids. For example, a surface with high WCA can have either a low or high sliding angle.¹² It should be noted that the different adhesion properties of surfaces are related with different superhydrophobic states as presented in section 5.1.3. Because of the great potential in many applications such as droplet microfluidics, printing, bioassay, stimuli-

responsive surface adhesion has encouraged significant research interest, in addition to the study of switchable surface wettability.

A transitional state between Cassie and Wenzel states is considered a practical case because a water droplet may partially wet the top of a superhydrophobic surface, leaving partial air gap in the grooves of the substrate. External stimuli, such as lighting, thermal treatment and pressure can realize the adhesion changes between the Cassie and Wenzel states. For example, Liu *et al.* reported a TiO₂ nanotube film modified with a perfluorosilane monolayer where the adhesion switched between sliding superhydrophobicity and sticky superhydrophobicity by selective illumination through a mask and heat annealing.¹³ The formation of hydrophilic regions containing hydroxyl groups still surrounded by superhydrophobic regions results in the dramatic adhesion change from easy sliding to highly sticky without sacrificing the superhydrophobicity.¹⁴

Grafting stimuli-sensitive polymers is a common approach to building stimuli-responsive surfaces. For example, pH-responsive polymers are typically used based upon their acidic or basic moieties including poly(acrylic acid) (PAA) and poly(2-(dimethylaminoethyl methacrylate) (PDMAEMA). Liu *et al.* grafted pH-responsive PDMAEMA brushes on a rough anodized alumina surface.¹⁵ The droplets with a pH from 1 to 6 show pinning behavior, due to a hydrophilic interaction between the acidic droplets and the amine groups of PDMAEMA. Conversely, SAs of the basic droplets (pH > 7.0) are smaller than 25° and the droplets can easily slide off the surface.¹⁵ In summary, those switchable adhesion surfaces can be valuable for various applications, in particular for microfluidics in microarrays/micropatterns.

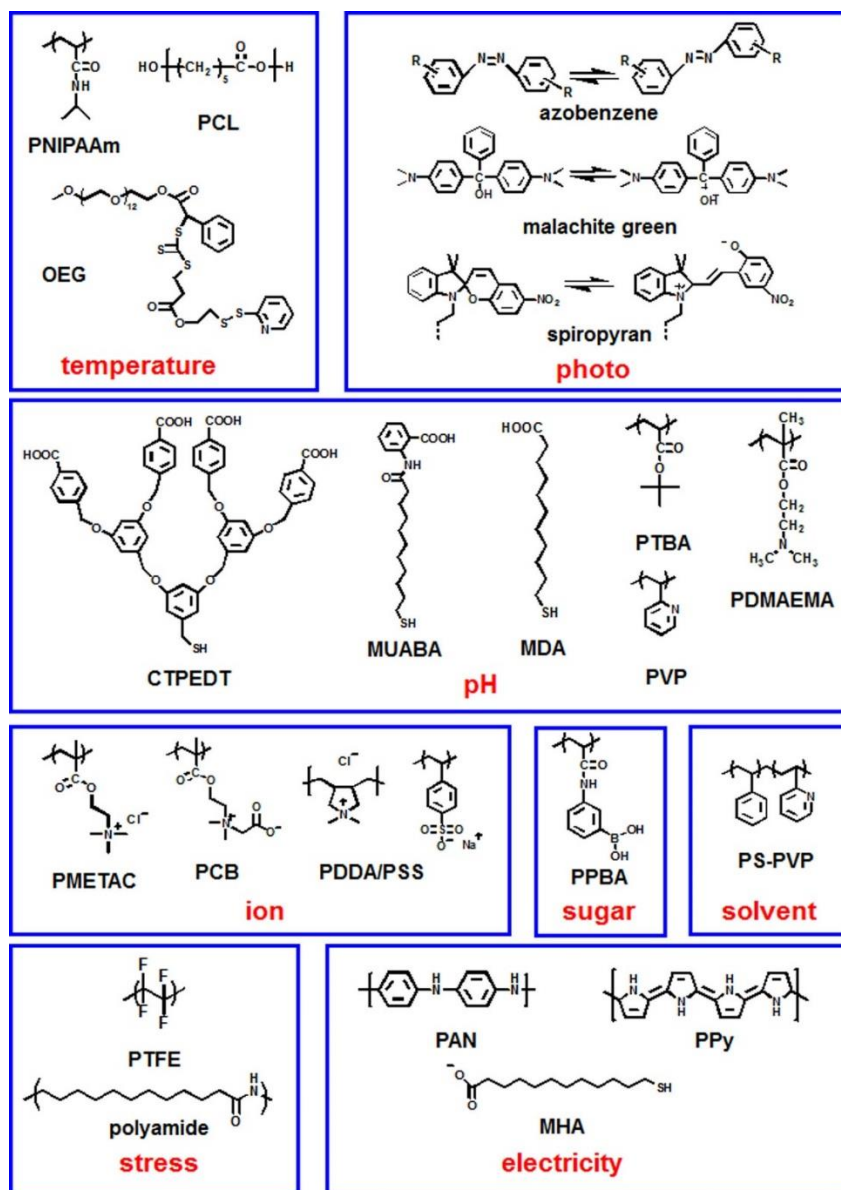


Figure 5.3 A summary of typical smart molecules and moieties that are sensitive to external stimuli including temperature, light, pH, ion (salt), sugar, solvent, stress, and electricity, and can respond in the way of wettability change. Reprinted with permission from reference.³ Copyright © (2015) American Chemical Society.

5.1.6 Superhydrophilic-Superhydrophobic Micropatterns / Microarrays

Superhydrophilic-superhydrophobic microarrays and micropatterns provide a new approach to the generation and manipulation of microdroplets on a substrate. For example,

Hancock *et al.* used customized hydrophilic-hydrophobic patterns to shape liquids into complex geometries, at both the macro- and microscale, to control the deposition of microparticles and cells or to create shaped hydrogels.¹⁶ Addition of a surfactant was needed to lower the surface tension of the liquid in order for it to completely fill the complex geometric patterns at the microscale. At the same time, Ueda *et al.* reported the formation of arrays of microdroplets on hydrogel micropads with defined geometry and volume (picoliter to microliter). By moving liquid along a superhydrophilic-superhydrophobic patterned surface, arrays of droplets are instantly formed, as shown in Figure 5.4. Bioactive compounds, nonadherent cells, or microorganisms can be trapped in fully isolated microdroplets/micropads for high-throughput screening applications.¹⁷

Patterned microchannels have been used as separation media in a similar fashion for thin layer chromatography. Because polymeric materials may be customized and *in situ* patterned on a substrate, a wide selection of functional groups may be utilized. Han *et al.* reported the application of a superhydrophilic channel photopatterned in a superhydrophobic porous polymer layer for the separation of peptides of different hydrophobicity and isoelectric point by two-dimensional thin layer chromatography.¹⁸ A 50 μm thick layer of poly(BMA-co-EDMA) was first formed onto a 4.0×3.3 cm glass plate using UV initiated polymerization. Afterwards, ionizable groups were grafted to form a 600 μm -wide superhydrophilic channel using a photomask, allowing for ion exchange separation in the first dimension. The second dimension of the separation was performed according to the hydrophobicity of the peptides along the unmodified part of the channel. Detection was performed by desorption electrospray ionization (DESI) mass spectroscopy

directly on the polymer surface, which was possible because of the open nature of the system.

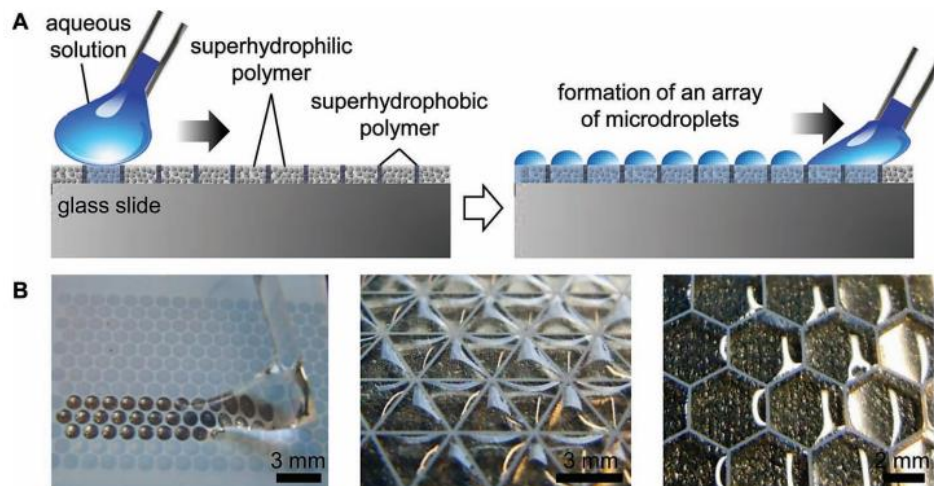


Figure 5.4 A) Schematic of a superhydrophilic, nanoporous polymer layer grafted with superhydrophobic moieties. When an aqueous solution is rolled along the surface, the extreme wettability contrast of superhydrophilic spots on a superhydrophobic background leads to the spontaneous formation of a high-density array of separated microdroplets. B) Snapshot of water being rolled along a superhydrophilic-superhydrophobic patterned surface (1.0 mm diameter circles, 100 μm barriers) to form droplets only in the superhydrophilic spots. Droplets formed in square and hexagonal superhydrophilic patterns. Reproduced from reference¹⁷ by permission of The Royal Society of Chemistry.

Cell assays are widely used for high-throughput screening in pharmaceutical development to identify the bioactivities of drug-like compounds. Conventional screening assays are typically performed in microwell plates that feature a grid of small, open reservoirs (*e.g.* 384 wells, 1536 wells). However, the handling of microliter and nanoliter fluids is usually tedious and requires a very complicated automated system (*e.g.* robot arms). In comparison, droplet microarrays seem to be a very promising alternative considering the facile deposition of droplets on a superhydrophilic-superhydrophobic

microarray that uses discontinuous dewetting.¹⁹ Based on this principle, Geyer *et al.* reported the formation of highly density cell microarrays on superhydrophilic-superhydrophobic micropatterns, using a hydrophilic poly(HEMA-co-EDMA) surface photografted with superhydrophobic poly(PFPMA-co-EDMA) regions.²⁰ Micropatterns consisting of $335 \times 335 \mu\text{m}$ superhydrophilic squares separated by $60 \mu\text{m}$ -wide superhydrophobic barriers were used, resulting in a density of $\sim 50,000$ patches in an area equivalent to that of a microwell plate ($8.5 \times 12.8 \text{ cm}$). Aqueous solutions spotted in the superhydrophilic squares completely wetted the squares and were completely contained by the “watertight” superhydrophobic barriers. Adhesive cells were cultured on the patterned superhydrophilic patches, while the superhydrophobic barriers prevent contamination and migration across superhydrophilic patches. Although the application of those microarrays as high-throughput and high-content screening tools has not been well explored, current progress has demonstrated promising advantages. Transparent superhydrophilic spots with contrasting opaque superhydrophobic barriers allowed for optical detection such as fluorescence spectroscopy and inverted microscopy. Moreover, it should be noted that adding modifications or functionalities to the polymer substrates, such as stimuli-responsive groups, could allow for new and interesting experiments such as selective cell harvesting or controlled release of substances from a surface.^{19, 21}

5.2 Overview

As presented in the literature review, the development of superhydrophobic surfaces was undoubtedly inspired by nature. Lotus leaves, butterfly wings and legs of water striders are the examples of natural surfaces exhibiting superhydrophobicity. Conversely, the study on the beetle in Namib Desert indicates the great benefit of

alternating hydrophilic and hydrophobic regimes, which is essential for the beetle to collect water and thrive in an extreme dry area. The combination of superhydrophobic and superhydrophilic surfaces in two-dimensional micropatterns (a.k.a. droplet microarray, superhydrophilic-superhydrophobic array) opens exciting opportunities for the manipulation of small amounts of liquid, which may find valuable applications in digital microfluidics²², drug screening^{23, 24}, and cell culture,²⁵ *etc.*

Creating superhydrophilic-superhydrophobic patterned surfaces is comprised of three general steps, namely, designing surface chemistry, building surface morphology, and creating alternating patterns. Of all the fabrication methods established for making superhydrophilic-superhydrophobic patterns, photografted polymer monoliths have been the least explored. The photografted polymer monoliths approach offers the following advantages: 1) intrinsic formation of porous structures using free radical polymerization, 2) robust covalent bonding of functionality on the monolithic backbone, 3) versatile grafting using a photomask.

In this chapter, we created a stimuli-responsive surface based upon the photografting of generic polymer monolith surfaces. BMA, HEMA and EDMA were selected as the generic substrate monomers based on previous studies.^{7, 20} DEAEMA and DIPAEMA are selected as the functional monomers because of their previously reported pH/CO₂-responsiveness.^{26, 27}

In particular, BMA-co-EDMA and HEMA-co-EDMA porous polymer monoliths were first made and photografted. Zeta potential measurements were used to characterize the materials produced. The CO₂-switchable wetting of PPM surfaces was first

characterized by submerging the prepared surfaces in carbonated water, and then measuring the water contact angle and contact angle hysteresis. Additionally, droplets (5 μL) with different pH values were dispensed on the prepared surfaces to observe their wetting of the surfaces over time. Following that, stimuli-responsive patterns are proposed and will be presented in future reports.

5.3 Experimental

5.3.1 Materials and instruments

Butyl methacrylate (BMA), ethylene dimethacrylate (EDMA), hydroxyethyl methacrylate (HEMA), diethylaminoethyl methacrylate (DEAE), 2-(diisopropylamino)ethyl methacrylate (DIPAE) were all acquired from Sigma-Aldrich (Milwaukee, WI, USA) and purified by passing them through an aluminum oxide column for removal of inhibitor. 3-(trimethoxysilyl) propyl methacrylate (γ -MAPS), 2, 2-dimethyl-2-phenylacetophenone (DMPAP) and benzophenone were also acquired from Sigma-Aldrich (Milwaukee, WI, USA). Cyclohexanol and 1-decanol were acquired from Fisher Scientific (Nepean, ON, Canada) and were used as solvents in polymerization mixture. Glass microscope slides were purchased from Fisher Scientific (Economy Plain Glass Micro Slides; $76 \times 25 \times 1.0$ mm) and were used as substrates. Water was prepared from a Milli-Q water purification system.

Photopolymerization and photografting of monolithic layers were carried out using a hand-held UV Lamp (ENF-280C with 254 nm tube) from Spectroline (Westbury, NY, USA). A Zetasizer Nano ZS (Malvern Instruments Ltd., Worcestershire, UK) was used to measure the zeta potential values of the prepared polymer materials. Contact angle

measurements were conducted with an OCA20 contact angle system (Dataphysics Instruments GmbH, Germany).

5.3.2 Preparation of generic polymer monolith substrate

Monolithic materials were prepared using modified procedures reported previously as shown in Figure 5.2.^{7,8} Prior to the polymerization, clean glass slides were activated by submerging in 1 M NaOH for 30 minutes followed by submerging in 1 M HCl for 30 minutes at room temperature. Afterwards, the glass plates were pretreated with a solution of 3-(trimethoxysilyl) propyl methacrylate (γ -MAPS), water, and glacial acetic acid (20:50:30; volume percentage) for 60 minutes to functionalize them with vinyl groups (facilitating monolith polymer attachment). After pretreatment, the slides were thoroughly rinsed with both methanol and acetone and dried under nitrogen. All glass slides were kept in a desiccator and used within a 4-day period.

For the preparation of porous monolithic layers, a pre-polymer mixture containing monomer, crosslinker, initiator and porogenic solvents was used (Table 5.1). The polymerization mixture was homogenized by sonication for 10 minutes and degassed by purging with nitrogen for 5 min. Teflon film strips with a thickness of 50 μm were placed along the longer sides of a glass plate, then covered with another glass plate, and clamped together to form a mold. The assembly forms the template and the thin strips define the thickness of the eventual material.

Two kinds of generic polymer monolithic substrates were prepared, including BMA-co-EDMA and HEMA-co-EDMA. The assembly was then filled with the degassed polymerization mixture described in Table 5.1, and irradiated with UV light for 15 minutes.

After completion of the polymerization, the sandwich assembly is taken apart so that a top plate and a bottom plate were acquired. The plates were rinsed with acetone first and immersed in methanol overnight, and left overnight to remove unreacted chemicals and porogens. Finally, the plates were dried in a vacuum at room temperature for further use.

Table 5.1 Composition of polymerization and photografting mixtures.

	Polymerization mixtures		Photografting mixture	
	1	2	A	B
	Poly(BMA-co-EDMA)	Poly(HEMA-co-EDMA)	Poly(DEAEMA)	Poly(DIPAEMA)
Initiator	DMPAP (1% wt.)		Benzophenone (0.25% wt.)	
Monomer	BMA (24% wt.)	HEMA (24% wt.)	DEAEMA (15% wt.)	DIPAEMA (15% wt.)
Crosslinker	EDMA (16% wt.)		-	
Solvents	1-Decanol (40% wt.), Cyclohexanol (20% wt.)		4:1 (v/v) tert-Butanol : water (85% wt.)	

5.3.3 Photografting

Photografting of the polymer monolith surfaces is based on the process reported previously.^{7, 28, 29} Briefly, a mixture of functional monomer, initiator and solvents was used to photograft the PPM substrates prepared above (Table 5.1). The porous layers (both top plates and bottom plates) prepared using mixtures 1 and 2 in Table 5.1 were wetted with the photografting mixture and covered with a fluorinated top plate and exposed to UV light at 254 nm for 60 minutes. A fluorinated top plate is used because it facilitates the disassembly of the top plate and the bottom plate. After this reaction, the monolithic layer was washed with methanol and acetone to remove unreacted components.

5.3.4 Material characterization

Zeta potential measurements were performed according to a method developed by Buszewski *et al.*³⁰⁻³² In order to characterize the effectiveness of photografting and the charge states of the functional groups, the non-grafted and grafted polymers were suspended in solutions with different pH values. In brief, a small area (1.0×2.5 cm) of the PPM substrate was scraped off from the top glass plate and suspended in different solutions. Glycolic acid and sodium hydroxide were used to prepare suspensions with pH 2.8, 4.0, 6.7 and 11.0. Zeta potential values were then determined ($n = 3$) by measuring the electrophoretic mobility of the particle suspension in a cuvette.

5.3.5 Contact angle measurement

In order to compare the surface wettability and adhesion before and after CO₂, static contact angle and contact angle hysteresis (CAH) were first measured on the polymer monolith surfaces. After-CO₂ measurements were performed following the submerging of the polymer coated slides in carbonated water for 20 minutes. Contact angle hysteresis (CAH) was measured using the advancing and receding contact angle (ARCA) program in the goniometer software. The difference of advancing contact angle and receding contact angle ($\theta_{\text{Rec}} - \theta_{\text{Adv}}$) was calculated as CAH. Droplets of 5.0 μL were dispensed at a rate of 2.0 $\mu\text{L/s}$.

5.3.6 Droplets with different pH

In order to test the effect of pH of the droplets on their wetting with the polymer monolith surfaces, water contact angles of various pH solutions were monitored. An acidic solution (pH 2.8 ± 0.1) was prepared from 0.01 M glycolic acid. Carbonated solution (pH

4.0 ± 0.1) was prepared by bubbling gaseous CO₂ (room temperature, 1 bar) at 100 mL/min for 15 minutes in a 100 mL glass bottle. Ultrapure water (neutral, pH 7.0 ± 0.5) was collected from a Milli-Q purification system and sealed in a vial to minimize the fluctuation of pH. A basic solution (pH 13.0 ± 0.1) was prepared from 0.1 M NaOH.

5.4 Results and discussions

5.4.1 Material characterization

The pH/CO₂-switchable groups may change their charge states depending on the pH of the solutions. For example, in acidic solutions (pH < pK_{aH}), amine functional groups should be protonated and exhibit positive charge. At basic conditions (pH > pK_{aH}), amine functional groups should be deprotonated and exhibit no charge. Therefore, zeta potential measurements were performed with the non-grafted BMA-co-EDMA and DEAEMA, DIPAEMA grafted polymer monolith material. As it shows in Figure 5.5, a general negative zeta potential is observed for BMA-co-EDMA. It should be noted that, although the BMA-co-EDMA polymer is presumably neutrally charged, the adsorption of negative ions onto the polymer surface may contribute to an observable negative charge, and this negative charge was also observed in other polymer substrates such as PDMS.³³

In comparison with non-grafted BMA-co-EDMA, both DEAEMA and DIPAEMA grafted polymers exhibit a positive zeta potential in acidic solutions (pH 2.8 and 4.0). This confirms our hypothesis that amine groups on poly(DEAEMA) and poly(DIPAEMA) are significantly protonated, if the pH is lower than the pK_{aH} (7-9) of the amine groups.²⁷ In basic solution (pH 11.0), both DEAEMA and DIPAEMA functionalized polymer materials exhibit a similar zeta potential as BMA-co-EDMA, indicating the deprotonation of the

amine groups. In general, those results confirm the effective photografting of the both functional monomers and it allows us to further characterize the wetting behaviour of the surfaces.

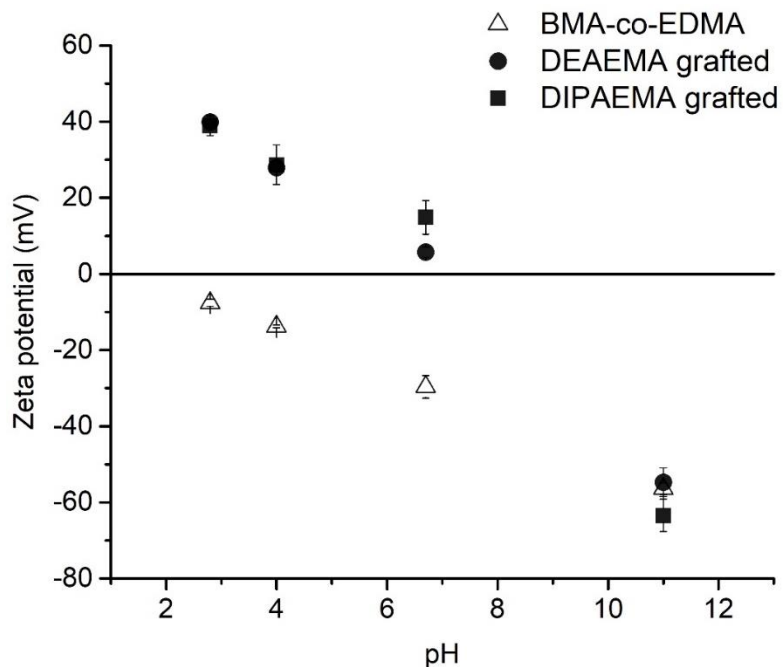


Figure 5.5 Zeta potential of non-grafted BMA-co-EDMA, DEAEMA and DIPAEMA grafted polymer at various pH conditions.

5.4.2 Characterization of surface wettability

The surface wettability of polymer monolithic surfaces was characterized by measuring static water contact angles. As it shows in Table 5.2, water contact angles of six types of polymer monoliths were measured, including non-grafted BMA-co-EDMA (sample 1) and HEMA-co-EDMA (sample 2), DEAEMA grafted BMA-co-EDMA (1A), DIPAEMA grafted BMA-co-EDMA (1B), DEAEMA grafted HEMA-co-EDMA (2A), DIPAEMA grafted HEMA-co-EDMA (2B).

5.4.2.1 Effect of generic polymer

The generic polymer monolith has an important effect on the surface wetting of the resulting photografted polymer monolith surface. As it shows in Table 5.2, BMA-co-EDMA and HEMA-co-EDMA show significantly different surface wettability. This shows the contribution from surface chemistry, because BMA (*Log P* 2.6) is a more hydrophobic monomer than HEMA (*Log P* 0.6). Additionally, surface roughness is responsible for an enhanced hydrophobicity or hydrophilicity compared to a flat surface. Therefore, the porous BMA-co-EDMA exhibits superhydrophobicity, while porous HEMA-co-EDMA exhibits superhydrophilicity. Furthermore, the water contact angles of DEAEMA and DIPAEMA grafted BMA-co-EDMA are generally higher than those of photografted HEMA-co-EDMA. It indicates that although photografting is supposed to cover all the surfaces of the generic polymer monolith surface, there still exists the “slight” contribution from the generic polymer, presumably caused by the inadequate coverage of grafted polymer.

5.4.2.2 Effect of top and bottom slides

In a previous study, it was found that pretreatment of both the top glass slide and the bottom glass slide is essential for the formation of required roughness for superhydrophobicity, because it allows the exposure of internal structures of the porous monolith upon the disassembly of the mold.¹⁸ It should also be noted that, since porous polymers are formed between two pretreated glass plates and UV radiation is applied from the top slide, a thicker material is usually formed on the top slide because of the vicinity of the top slide in relation to the UV light. A thinner material is formed on the bottom slide

because most of the polymer adheres to the top plate upon disassembly of the template. Preliminary results showed different wetting and adhesion behaviour for the top and bottom slides. Therefore, characterization was performed for both the top slides and the bottom slides of all the six surfaces.

Table 5.2 Water contact angles of non-grafted and grafted polymer monoliths before and after treatment with CO₂ (carbonated water).

Sample No.	Sample name	Side	Water contact angle (WCA, °)	
			Before CO ₂	After CO ₂
1	BMA-co-EDMA	Top	153.9 ± 1.7	157.4 ± 1.8
		Bottom	156.8 ± 0.5	148.4 ± 0.9
1A	DEAEMA grafted	Top	149.6 ± 2.9	154.6 ± 0.8
	BMA-co-EDMA	Bottom	153.2 ± 2.2	62.4 ± 3.3
1B	DIPAEMA grafted	Top	157.3 ± 1.2	153.9 ± 0.7
	BMA-co-EDMA	Bottom	154.3 ± 2.5	145.6 ± 3.0
2	HEMA-co-EDMA	Top	0	0
		Bottom	0	0
2A	DEAEMA grafted HEMA-co-EDMA	Top	145.5 ± 0.5	134.4 ± 1.1
		Bottom	117.1 ± 5.7	74.3 ± 4.0
2B	DIPAEMA grafted HEMA-co-EDMA	Top	148.2 ± 2.0	131.3 ± 6.3
		Bottom	145.3 ± 3.2	102.5 ± 10.1

Without the treatment of CO₂, the contact angles for all the top slides and bottom slides were very similar and they all exhibit a water contact angle about 150°, except for sample 2A. Sample 2A, the DEAEMA grafted HEMA-co-EDMA shows a much lower

water contact angle, which is supposed to be caused by the inadequate grafting and exposure of HEMA. Therefore, it is considered not ideal for our purpose of developing a photografted surface exhibiting superhydrophobicity in the absence of CO₂.

Additionally, the water contact angle change triggered by treatment with CO₂ shows a very interesting trend. After exposure to carbonated water, the grafted bottom plates (*e.g.* sample 1A, 1B, 2A, 2B) had lower contact angles than those for the grafted top plates. In particular, it was found that, DEAEMA grafted BMA-co-EDMA exhibits the most significant switch of surface wettability, indicating its potential for further development.

It is considered that the greater wettability switch on the bottom slides may result from more effective photografting of the bottom slides. Because the bottom slide has a thinner layer of polymer, after injecting the photografting mixture between the bottom plate and the cover glass plate, the assembly is transparent. Conversely, because a thicker coating is formed on the top plate, the assembly is not transparent and may obstruct the UV photografting through the thick layer of polymer on the top plate. That being said, only a thin layer of the generic polymer monolith on the top slide may be grafted and that caused a less effective switch of wettability. Nevertheless, scanning electron microscopy, X-ray photoelectron spectroscopy and profilometry measurements may be needed to confirm the hypothesis.

5.4.2.3 Effect of photografting monomer

Photografting is a valuable approach to the manipulation of surface chemistry and has been used to fabricate superhydrophobic patterns on a superhydrophilic film.²⁰ In this

study, pH/CO₂-switchable polymers were grafted to allow for the manipulation of surface wetting and adhesion with pH or CO₂. DEAEMA was initially selected as the functional monomer based on previous studies of its stimuli-responsive properties.^{26, 27}. Another monomer, DIPAEMA was also used as a comparison of their stimuli-responsive performance. As shown in Table 5.2, DEAEMA grafted polymer monoliths (sample 1A, 2A) exhibits a more significant switch of contact angles than those for DIPAEMA grafted samples (1B, 2B, bottom slides). In particular, the bottom slide of DEAEMA grafted BMA-co-EDMA surface has shown a contact angle change from 153.2° to 62.4° after treated with carbonated water (Figure 5.6).

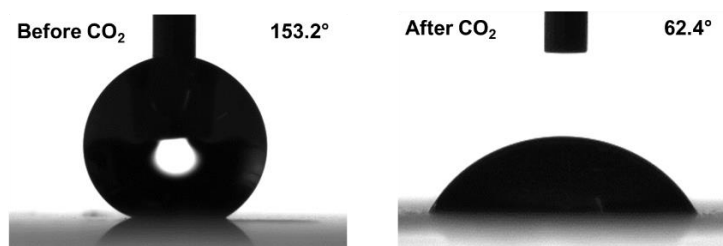


Figure 5.6 Water contact angles of DEAEMA grafted BMA-co-EDMA monolith surface (sample 1A, bottom slide), before and after treated with carbonated water.

The higher switching capability of DEAEMA grafted polymer is supposed to be a result of its slightly higher hydrophilicity and the easier protonation of DEAEMA (pK_{aH} 9.0, $\text{Log } P$ 2.0) than DIPAEMA (pK_{aH} 9.5, $\text{Log } P$ 2.9). The higher hydrophilicity (lower $\text{Log } P$) of DEAEMA may facilitate easier wetting following protonation of amine groups by the carbonated solution.

In general, non-grafted and grafted BMA-co-EDMA polymer monolith surfaces were further characterized for surface adhesion switching, because pH/CO₂-responsive surfaces with initial superhydrophobicity is considered as a primary goal of current project.

5.4.3 Characterization of surface adhesion by hysteresis

The switch of surface adhesion triggered by treatment with CO₂ (carbonated water) was characterized by contact angle hysteresis (CAH). Higher CAH indicates a more adhesive surface with higher surface energy, and lower CAH indicates a more slippery surface with low surface energy. As shown in Table 5.3, before treated with CO₂, the bottom slide of DEAEMA grafted BMA-co-EDMA shows a CAH 4.9°. After treatment with carbonated water, the CAH of the bottom slide of DEAEMA grafted BMA-co-EDMA is 68.5° and it behaves as a highly adhesive surface. In comparison, the bottom slide of DIPAEMA grafted BMA-co-EDMA shows a less noticeable switch of surface adhesion (25.8°).

Table 5.3 Water contact angle hysteresis of non-grafted and photografted BMA-co-EDMA monolith before and after treatment with carbonated water.

Sample No.	Sample name	Side	Contact angle hysteresis (CAH, °)	
			Before CO ₂	After CO ₂
1	BMA-co-EDMA	Top	11.1 ± 1.1	31.1 ± 1.9
		Bottom	3.2 ± 1.7	24.1 ± 3.8
1A	DEAEMA grafted BMA-co-EDMA	Top	52.4 ± 14.1	56.8 ± 1.7
		Bottom	4.9 ± 1.1	68.5 ± 12.5
1B	DIPAEMA grafted BMA-co-EDMA	Top	43.9 ± 0.3	56.8 ± 1.7
		Bottom	9.0 ± 4.3	25.8 ± 5.8

Furthermore, it should be noted that, the top slides of both samples 1A and 1B exhibit a high CAH value (52.4° and 56.8°) regardless if they are treated with CO₂ or not. This may be caused by a difference in the surface roughness between the top slide and the bottom slide. It is proposed that, the process of disassembling of glass slides may result in a bottom slide exhibiting narrower and sharper features on the surface, while the top slide should exhibit wider and shallower features on the surface. The difference in their surface roughness may contribute to the differential surface adhesion. Nevertheless, it remains to be confirmed by further investigation using atomic force microscopy, scanning electron microscopy and profilometry.

5.4.4 Surface wetting with different pH droplets

Another study of surface wettability was performed by introducing droplets with different pH. It was found that, all the droplets (pH 13, pH 7.0, pH 4.0, pH 2.8) did not show any change of contact angle on the non-grafted BMA-co-EDMA surface. Droplets

with pH 13.0, pH 7.0, and pH 4.0 did not show noticeable change of contact angle on the DEAEMA and DIPAEMA grafted polymer monolith surfaces. Interestingly, droplets with pH 2.8 showed a contact angle change over a short period of time for some of the photografted surfaces. As it shows in Figure 5.7, the water contact angle dropped from 132.2° to 108.3° in 3 minutes for the bottom slide of DIPAEMA grafted surface. The water contact angle dropped more significantly for the DEAEMA grafted surfaces, especially for the bottom slide (128.4° to 88.2° in 3 minutes). Consequently, the water contact angle dropped continuously until the droplet completely wetted the surface. It indicates that the contact angle change is attributed to the protonation of the amine groups on the polymer surface by the acidic droplet.

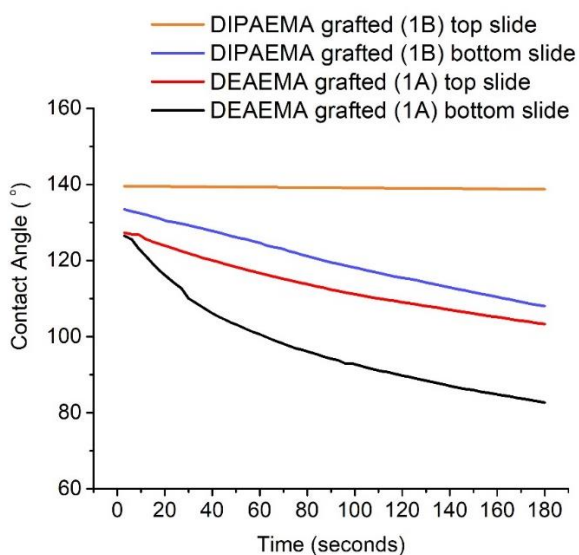


Figure 5.7 Contact angle change of a droplet of pH 2.8 on different surfaces.

It should also be noted that droplets with pH 4.0 (carbonated water) should theoretically also wet the surface. However, this was not observed in current conditions. It may be a result of the change of pH for the carbonated water droplets. The pH of carbonated water is significantly affected by the gaseous environment around the solution. When the

water contact angle is measured in air, the carbonated water droplet may quickly equilibrate with air and shift the pH to be higher than 4.0. To verify the proposed pH fluctuation affected by air, bromocresol green (BCG) was used to monitor the pH of carbonated water. As it shows in Figure 5.8 A, 5×10^{-5} M BCG in deionized water is a blue solution, the pH of which is measured to be 6.7 ± 0.2 . After bubbling CO_2 (100 mL min^{-1}) for 10 seconds, the solution turns to light green, pH of which is measured to be 3.9 ± 0.1 . N_2 (100 mL min^{-1}) was also used to purge away CO_2 and it was observed that, after 2 minutes purging, the solution turns back to blue (pH 6.5 ± 0.2). It indicates a significant impact of the vapor environment on the aqueous pH.

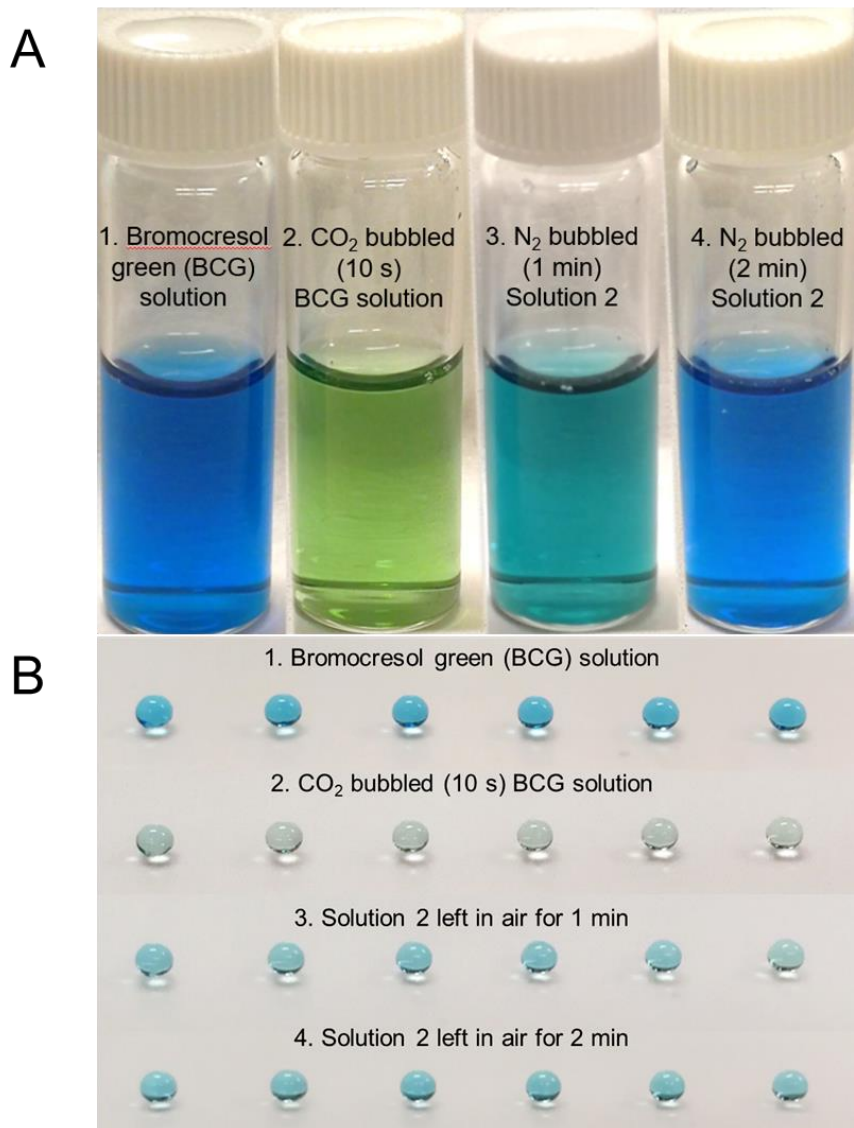


Figure 5.8 (A). Photographs of 1) aqueous solutions of bromocresol green (BCG, 5×10^{-5} M), 2) BCG solution treated with gaseous CO₂ for 10 seconds, 3) carbonated solution treated with N₂ for 1 minute, 4) Carbonated solution treated with N₂ for 2 minutes. Flow rate of CO₂ and N₂ are 100 mL min⁻¹, a gas dispersion tube (O.D. \times L 7.0 mm \times 135 mm, porosity 4.0 – 8.0 μ m) was used. (B). Photographs of 10 μ L droplets dispensed on a hydrophilic array. 1) Aqueous solutions of BCG (5×10^{-5} M), 2) BCG solution treated with gaseous CO₂ for 10 seconds, 3) carbonated solution exposed in air for 1 minute, 4) carbonated solution exposed in air for 2 minutes.

Droplets of CO₂ bubbled solution were also dispensed on a superhydrophilic array to observe the color change over time. As it shows in Figure 5.8 B, the droplets turn from

yellow to blue after being exposed to air for 1 minute, and even darker blue for 2 minutes. Although quantitative measurement of the pH of the droplet has not been performed, it proves the significant change of pH of droplets when the water contact angle is measured and they are exposed in air. Therefore, it may require a substitutive solution with pH 4.0 to perform a comparable measurement. Alternatively, a CO₂ purging chamber may be assembled on the goniometer to accurately measure the WCA for a carbonated water (1 bar) droplet.

5.5 Conclusions

This chapter has presented the characterization of stimuli-responsive surfaces created by photografting porous polymer monoliths. Generic porous polymer monolithic surfaces were prepared and grafted with DEAEMA and DIPAEMA to create pH/CO₂-responsive surfaces. Zeta potential measurement confirmed the protonation of the amine groups at acidic conditions. Water contact angle measurements indicate the higher switching ability of the DEAEMA grafted BMA-co-EDMA coating, especially the bottom slide. Contact angle hysteresis also showed that after treatment with CO₂, an increase in surface adhesion was observed for the DEAEMA grafted surfaces. Additionally, significant change of water contact angle was observed in a short time (3 minutes) when acidic droplets (pH 2.8) are dispensed on the DEAEMA grafted surfaces.

Further investigations may involve the characterization of top and bottom slides in terms of coating thickness using scanning electron microscope. Another study regarding the effect of carbonated water droplet may also be conducted by testing the water contact angle with a substitute solution (pH 4.0) or assembling a CO₂-saturated chamber while

measuring the contact angle. Characterization of grafting efficiency may be performed using X-ray photoelectron spectroscopy. Preparation of stimuli-responsive patterns and arrays may also be necessary to demonstrate the capability of the “smart” microarrays. It is believed that the stimuli-responsive microarrays may find various applications in droplet microarrays such as controllable chemical deposition and switchable cell adhesion.

5.6 References

1. W. Barthlott and C. Neinhuis, *Planta*, 1997, **202**, 1-8.
2. L. Feng, S. Li, Y. Li, H. Li, L. Zhang, J. Zhai, Y. Song, B. Liu, L. Jiang and D. Zhu, *Advanced materials*, 2002, **14**, 1857-1860.
3. S. Wang, K. Liu, X. Yao and L. Jiang, *Chem Rev*, 2015, **115**, 8230-8293.
4. T. Young, *Philos T R Soc Lond*, 1805, **95**, 65-87.
5. S. Wang and L. Jiang, *Adv Mater*, 2007, **19**, 3423-3424.
6. M. Jin, X. Feng, L. Feng, T. Sun, J. Zhai, T. Li and L. Jiang, *Adv Mater*, 2005, **17**, 1977-1981.
7. P. A. Levkin, F. Svec and J. M. Frechet, *Adv Funct Mater*, 2009, **19**, 1993-1998.
8. D. Zahner, J. Abagat, F. Svec, J. M. Frechet and P. A. Levkin, *Adv Mater*, 2011, **23**, 3030-3034.
9. Q. Fu, G. Rama Rao, S. B. Basame, D. J. Keller, K. Artyushkova, J. E. Fulghum and G. P. López, *J Am Chem Soc*, 2004, **126**, 8904-8905.
10. R. Wang, K. Hashimoto, A. Fujishima, M. Chikuni, E. Kojima, A. Kitamura, M. Shimohigoshi and T. Watanabe, *Nature*, 1997, **388**, 431-432.
11. Y. Zhu, L. Feng, F. Xia, J. Zhai, M. Wan and L. Jiang, *Macromol Rapid Comm*, 2007, **28**, 1135-1141.
12. L. Feng, S. Li, Y. Li, H. Li, L. Zhang, J. Zhai, Y. Song, B. Liu, L. Jiang and D. Zhu, *Adv Mater*, 2002, **14**, 1857-1860.
13. D. Wang, Y. Liu, X. Liu, F. Zhou, W. Liu and Q. Xue, *Chem Commun*, 2009, 7018-7020.
14. G. Caputo, B. Cortese, C. Nobile, M. Salerno, R. Cingolani, G. Gigli, P. D. Cozzoli and A. Athanassiou, *Adv Funct Mater*, 2009, **19**, 1149-1157.
15. X. Liu, Z. Liu, Y. Liang and F. Zhou, *Soft Matter*, 2012, **8**, 10370-10377.
16. M. J. Hancock, F. Yanagawa, Y. H. Jang, J. He, N. N. Kachouie, H. Kaji and A. Khademhosseini, *Small*, 2012, **8**, 393-403.

17. E. Ueda, F. L. Geyer, V. Nedashkivska and P. A. Levkin, *Lab Chip*, 2012, **12**, 5218-5224.
18. Y. Han, P. Levkin, I. Abarientos, H. Liu, F. Svec and J. M. Frechet, *Anal Chem*, 2010, **82**, 2520-2528.
19. E. Ueda and P. A. Levkin, *Adv Mater*, 2013, **25**, 1234-1247.
20. F. L. Geyer, E. Ueda, U. Liebel, N. Grau and P. A. Levkin, *Angew Chem Int Ed Engl*, 2011, **50**, 8424-8427.
21. H. Takahashi, M. Nakayama, K. Itoga, M. Yamato and T. Okano, *Biomacromolecules*, 2011, **12**, 1414-1418.
22. K. J. Bachus, L. Mats, H. W. Choi, G. T. T. Gibson and R. D. Oleschuk, *ACS Appl Mater Interfaces*, 2017, **9**, 7629-7636.
23. T. Tronser, A. A. Popova and P. A. Levkin, *Curr Opin Biotechnol*, 2017, **46**, 141-149.
24. A. A. Popova, S. M. Schillo, K. Demir, E. Ueda, A. Nesterov-Mueller and P. A. Levkin, *Adv Mater*, 2015, **27**, 5217-5222.
25. E. Ueda, W. Feng and P. A. Levkin, *Adv Healthc Mater*, 2016, **5**, 2646-2654.
26. J. Pinaud, E. Kowal, M. Cunningham and P. Jessop, *Acs Macro Lett*, 2012, **1**, 1103-1107.
27. A. Darabi, P. G. Jessop and M. F. Cunningham, *Chem Soc Rev*, 2016, **45**, 4391-4436.
28. T. B. Stachowiak, F. Svec and J. M. J. Fréchet, *Chem Mater*, 2006, **18**, 5950-5957.
29. S. Eeltink, E. F. Hilder, L. Geiser, F. Svec, J. M. J. Fréchet, G. P. Rozing, P. J. Schoenmakers and W. T. Kok, *J Sep Sci*, 2007, **30**, 407-413.
30. B. Buszewski, S. Bocian and E. Dziubakiewicz, *J Sep Sci*, 2010, **33**, 1529-1537.
31. B. Buszewski, M. Jackowska, S. Bocian and E. Dziubakiewicz, *J Sep Sci*, 2013, **36**, 156-163.
32. S. Bocian, E. Dziubakiewicz and B. Buszewski, *J Sep Sci*, 2015, **38**, 2625-2629.
33. B. Wang, R. D. Oleschuk and J. H. Horton, *Langmuir*, 2005, **21**, 1290-1298.

Chapter 6 Conclusions and recommendations

Throughout the thesis CO₂-switchable chemistry has been first applied in the development of environmentally friendly chromatography or green chromatography approaches.

Because DMAEMA was reported previously for its stimuli-responsive applications in switchable surfaces, switchable hydrogels, a copolymer monolith poly(DMAEMA-co-EDMA) was prepared and examined as a stimuli-responsive polymeric column support. By introducing acetic acid as a low pH modifier in mobile phase, a slight decrease of retention time (polycyclic aromatic hydrocarbon compounds) was observed. This indicates a slight decrease of hydrophobicity for the copolymer stationary phase. However, the experiments of introducing CO₂ in the mobile phase did not show reproducible chromatography presumably caused by the formation of bubbles and subsequently fluctuating flow rate. Therefore, a conventional HPLC was used in following experiments and the results were reproducible and reliable.

Regarding the problems experienced in the study of the copolymer monolith column, several approaches may be taken for further studies. A conventional analytical column (*e.g.* I.D. 2.0 mm or 4.6 mm) could be used with functional polymer monolith prepared *in situ*. In a proof of concept study, a larger column should provide more reliable control of the supply of CO₂ in a conventional analytical HPLC. It should be noted that, care should be taken in preparation of the analytical column, because the polymeric rod may swell or shrink more significantly depending on the solvation conditions. Another approach is to functionalize the polymer monolith column using photografting or surface-

initiated ATRP, instead of copolymerization. In comparison, photografting is usually performed on a well-studied generic polymer monolith and it does not require tedious optimization of polymerization conditions (*e.g.* composition of monomer, crosslinker, porogenic solvent). Additionally, ATRP may allow for the preparation of homogenous polymer brushes on PPM, which may provide a higher density of accessible functional groups and also the possibility of controlling hydrophobicity by changing the conformation of polymer brushes.

Nevertheless, the poly(DMAEMA-co-EDMA) column has also been examined for separation at different pH and temperature conditions. It shows the potential of manipulating retention time and selectivity by changing pH and temperature because of the pH and thermo-responsiveness of the column. Because of the presence of ionizable groups on the column, an ion exchange separation of proteins was performed and it demonstrated the flexibility of the column and its potential for mixed mode separations.

Because of the difficulty experienced with the custom polymer monolithic column, we proposed to examine the performance of commercially available columns because of the presence of CO₂-switchable groups in those columns. We demonstrated the decrease of hydrophobicity triggered by CO₂ on the diethylaminoethyl column and the polyethylenimine column. Although the carboxymethyl column did not show the retention time switch for most compounds tested, the retention time of 4-butylaniline (pK_a 4.9) was significantly affected by CO₂. Considering the ionization of this compound responding to CO₂, it indicates the significant contribution of electrostatic interactions in this

chromatographic process. Therefore, a follow-up study was performed to demonstrate this hypothesis.

Primary, secondary and tertiary amine functionalized silica particles were packed in columns and examined for their switchable separation to CO₂. It was firstly observed that, compounds containing carboxylic acid groups have a very strong retention using aqueous solution at pH 4.0 – 5.0. This is found to be a result of the ion exchange mechanism, based on the protonation of amine functional groups on the column, and the dissociation of the carboxylic group of the analytes. Additionally, three pharmaceutical compounds were successfully separated using carbonated water as the mobile phase. The retention time of carboxylic acid compounds on different columns follows the order: primary amine > secondary amine > tertiary amine.

Despite the results achieved, some ideas remain to be investigated to extend the applicability of the CO₂-switchable chromatography. Firstly, a gradient of CO₂ has not been attempted in the chromatographic experiments. It is considered that a gradient of CO₂ may provide a higher separation efficiency because of the dynamic control of solution pH. Also, a technical study of the equilibration time of CO₂ in columns may be necessary. This is important because the equilibration time of CO₂ has to be reasonably short (*e.g.* 10 minutes) to allow for the successive operation of HPLC without delay. Furthermore, although satisfactory chromatography has been performed with hydrophobic organic molecules (*Log P* 3 - 4) and carboxylic acid compounds (*pK_a* 3 - 5), more analytes should be tested to expand the potential application of this efficient and green chromatography methodology.

In addition to the chromatographic techniques developed in this thesis, polymer monolithic surfaces were also prepared and functionalized with pH/CO₂-switchable groups, allowing for a tunable surface wettability and adhesion. Preliminary results showed a significant change of wettability (water contact angle) on a DEAEMA grafted BMA-co-EDMA surface, triggered by CO₂. The switch of surface adhesion (contact angle hysteresis) was also observed on the same surface, indicating the great potential of this surface. Further studies will focus on the characterization of surfaces with different techniques such as X-ray photoelectron spectroscopy and optical profilometry. Preparation of pH/CO₂-responsive micropatterns and microarrays will be performed to demonstrate the application of the “smart” microarrays in controllable chemical adsorption and cell adhesion.